NWRI Contr.
00-126

Environment Canada
Water Science and Technology Directorate

Direction générale des sciences et de la technologie, eau
Environnement Canada

Analysis of Observed Hydrological and Meteorological Data to Identify and Model Trends Due to Climate Change

J.Y. Diiwu, A.G. Bobba and R.P. Rudra

NWRI Contribution No. 00-126

Management Perspective

Simple statistical tests for equality of means and variances, and Box-Jenkins univariates and input-output models are shown to be tools to detect hydrologic changes. The structural decomposition of daily runoff series into periodic and stochastic components and the step response function of daily runoff processes in relation to daily rainfall processes provide parameters that form a basis for evaluating the changes in the hydrologic environments due to climate change.

This report is first part on the study of "Stochastic Analysis and Modelling of Hydrologic and Climatologic Time Series" of Northern Canadian Environment due to climate change.

Sommaire à l'intention de la direction

On montre que de simples tests statistiques d'égalité des moyennes et des variances, ainsi que des modèles d'entrée-sortie Box-Jenkins à une variable, sont utiles pour détecter les changements hydrologiques. En utilisant la décomposition structurale de séries quotidiennes de données sur le ruissellement en éléments périodiques et stochastiques et la fonction de réponse graduelle des processus quotidiens de ruissellement par rapport aux processus quotidiens de précipitations, on obtient des paramètres qui peuvent servir à l'évaluation des changements causés par le changement climatique dans les milieux hydrologiques.

Ce rapport est la première partie de l'étude de l'environnement du nord canadien « Stochastic Analysis and Modelling of Hydrologic and Climatologic Time Series », qui porte sur les changements climatiques.

Abstract

Temperature, precipitation and streamflow data from the Northeast Pond River watershed were analyzed to identify any trends and estimate their magnitudes. Graphical trend detection was carried out using ten-year moving average and robust locally weighted regression modelling. Mann-Kendall trend test was also done, and the magnitude of detected trends was estimated using Kendall slope estimates. Trends were detected for each of the three variables, and their magnitudes and directions appear to be season-dependent. Temperature showed a downward trend in winter and an upward trend in spring, summer and fall seasons, with the change varying between 0.1 and 7 degrees per year. For each of the four seasons the change in precipitation varied between 0.6 and 13 mm per year, with the greatest upward trend being in October and the greatest downward trend in February. Over the period, monthly mean streamflow changed by less than 0.5 cm per year. Frequency analysis showed that the lognormal and Weibull probability models are equally good choices for precipitation and streamflow in the watershed. In the case of temperature, the normal model gives the best fit for late fall to early spring while the lognormal model is best for the rest of the months.

Résumé

On a analysé les données sur la température, les précipitations et l'écoulement des cours d'eau du bassin versant de la rivière Northeast Pond afin de déterminer les tendances existantes et d'en évaluer l'importance. On a détecté les tendances graphiques à l'aide d'une moyenne mobile de dix ans et d'une modélisation robuste par régression à pondération locale. On a également effectué des tests de tendances de Mann-Kendall et on a estimé l'ordre de grandeur des tendances décelées à l'aide d'estimations des pentes de Kendall. On a décelé des tendances pour chacune des trois variables, et il semble que leur ordre de grandeur et leur direction dépendent de la saison. Les températures présentaient des tendances à la baisse en hiver et à la hausse au printemps, en été et en automne, avec des changements compris entre 0,1 et 7 degrés par année. Pour chacune des saisons, le changement dans les précipitations était compris entre 0,6 et 13 mm par année; on observait la plus forte tendance à la hausse en octobre, et la plus forte tendance à la baisse en février. Au cours de cette période, les variations mensuelles moyennes de l'écoulement des cours d'eau étaient inférieures à 0,5 cm par année. Une analyse de fréquences indiquait que le modèle de probabilité lognormal et celui de Weibull sont également utiles pour l'évaluation des précipitations et de l'écoulement des cours d'eau dans le bassin versant. Dans le cas de la température, le modèle normal donne le meilleur ajustement pour la période comprise entre la fin de l'automne et le début du printemps, alors que le modèle lognormal est préférable pour les autres mois.

ANALYSIS OF OBSERVED HYDROLOGICAL AND METEOROLOGICAL DATA TO IDENTIFY AND MODEL TRENDS DUE TO CLIMATE CHANGE

J. Y. Diiwu[1], A. G. Bobba[2], R. P. Rudra[1]

INTRODUCTION

Concern over changes in climate caused by rising atmospheric concentrations of carbon dioxide and other trace gases has increased in recent years. Despite a better understanding of climatic processes, many of the effects of anthropogenic climate changes are still poorly understood. This not withstanding there are bound to be geophysical and socioeconomic impacts of the changes in climate (Manabe and Weatherald, 1987; Lettenmaier and Gan, 1990). These include major changes in water availability caused by alterations in temperature, precipitation and streamflow patterns. Such hydrologic changes will affect nearly every aspect of human well being, from agricultural productivity and energy use to flood control, municipal and industrial water supply, and fish and wildlife management at watershed and regional levels. Also, altering precipitation patterns may greatly affect the onset, duration and severity of extreme events such as floods and droughts (Nemec and Shaake, 1982). It is therefore extremely

[1] School of Engineering, University of Guelph, Guelph, Ontario, Canada N1G 2W1
[2] National Water Research Institute, Burlington, Ontario, Canada L7R 4A6

important to understand how changes in climate would affect water supply at the watershed and regional levels.

Historical trends in hydrologic variables are important for water resource planning purposes. Such trend information can be used to hypothesize future climatic scenarios for management decision-making (Bobba et al., 1997, 1999). Thus there is a need to identify hydrologic trends in Canadian watersheds that may be attributable to climate variability and change, and model such trends for future planning purposes. The study was therefore carried out to identify and model trends in observed time series of temperature, precipitation and streamflow.

The Northeast Pond River watershed was selected for the study. The study watershed, which has an area of 3.90 km^2 is located approximately 20 km west of St. John's in Newfoundland. The climate of the study area is dominated by the Labrador current, which consists primarily of arctic waters. The area has a marine climate, characterized by short but pleasant summers and mild winters (Environment Canada, 1995; Bobba et al., 1997). Monthly mean temperature, precipitation and stream flow were analyzed for the period 1952 to 1983. The monthly means were computed from daily observed data. Daily temperature and precipitation data were obtained from St. John's meteorological station, and daily streamflow data were obtained from the gauge at the watershed outlet at Portugal Cove (Bobba et al., 1997).

METHOD OF ANALYSIS

Summary Statistics

The trend analysis was preceded by computation of the descriptive statistics of the time series. The statistics obtained were the mean, median, standard deviation, and the range. The mean and median are intended as measures of central tendency of the time series, while the standard deviation and range give measures of how the series is spread about the central values (McCuen, 1993). The summary statistics obtained for the time series of temperature, precipitation and streamflow are presented in Tables 1, 2 and 3 respectively.

Frequency Analysis

Frequency analysis was carried out to determine appropriate probability models that may be used to make probability statements about the occurrence of the hydrologic variables. The probability models were identified by carrying out probability plots for some well known probability functions: normal, lognormal, Weibull and extreme value functions. For each variable the probability plot in which the sample points are closest to a straight line and within the 95% confidence limits was selected as the best fit plot. The probability function corresponding to the best fit probability plot was then selected as the most representative probability model for the variable (McCuen, 1993). The selected probability models are presented in Table 4. The corresponding best fit probability plots are presented in Figures 1 to 48. The first and third quantiles were then determined from the probability plots; these are presented in Tables 1 to 3 alongside the summary statistics. The second quantile is also the median, while the zeroth and fourth quantiles are the minimum and maximum values specified in the range. The quantiles are useful because, just like probability models, they can be used to make probability statements about future trends in the variable.

Seasonal Trend Analysis

Trend analysis was carried out for each of the twelve months January to December for the period 1952 to 1983. This was intended to minimize the effect of seasonal variations on the trends in the variables. The twelve months were then grouped into four seasons as follows: winter, December to February; spring, March to May; summer, June to August; and fall, September to November. The trend analysis was then carried out using two graphical trend detection methods, ten-year moving average and robust locally weighted regression (Cleveland, 1979), and the Mann-Kendall non-parametric trend test (Mann, 1955; Kendall, 1975).

Ten-Year Moving Average

For each of the twelve months the ten-year moving average was computed to identify trends in the time series. The ten-year moving average technique has the advantage of removing any periodicities in the data.

Robust Locally Weighted Regression (RLWR)

The RLWR technique combines locally weighted regression with polynomial smoothing. The major advantage of the RLWR technique is that it does not allow outliers to distort the smoothing. The technique involves determination of : the order of the polynomial to be locally fitted to each point of the scatter plot, the weighting functions to be used at each point, and the number of iterations to be performed in the fitting procedure. The closest neighbours of each point are assigned the largest weights, while the points which are furthest away from it are assigned the least weights. This minimizes the effects of outliers on the fitted curve. At each point the polynomial to be fitted is of the general form (Cleveland, 1979):

$$y_k = B_0 + B_1 x_k + B_2 x^2_k + ... + B_d x^d_k$$

where B_i are parameters to be determined by weighted least squares using weights $w_k(x_i)$ for (x_k, y_k). Following the recommendation of Cleveland (1979 the values d = 1 and f = 0.5 were taken for the smoothing parameters. The RLWR and ten-year moving average curves are presented alongside the time series plots in Figures 49 to 84.

Mann-Kendall test

A non-parametric test was chosen for the trend test to avoid the dependence of the test on the probability distribution of the population. The Mann-Kendall test is used because of its simplicity and the fact that the sample size is less than 40 (Hollander and Wolfe, 1973). The test is used to determine if a time series is moving upward, downward, or remaining relatively level over time. This is accomplished by computing a statistic based on all possible data pairs, that represents the net direction of movement of the time series. All possible differences $x_i - x_j$ are calculated, where x_j precedes x_i in time. This difference will either be positive ($x_i > x_j$), negative ($x_i < x_j$), or zero ($x_i = x_j$) for each of the pairs. The number of positive differences minus the number of negative differences is calculated; this becomes the test statistic, the Mann-Kendall statistic S. A positive value of S indicates an upward trend, a negative value indicates a downward trend and a value of zero indicates that there is no change over time. Significance of the test is assessed by comparing the values with those of the standard normal variate. The test statistic is defined as (McCuen, 1993):

$$S = \sum_{1}^{n-1} \sum_{j+1}^{N} Sgn(y_j - y_k)$$

where

$$Sgn(\theta) = \begin{cases} 1, & if\ \theta > 0 \\ 0, & if\ \theta = 0, \\ -1, & if\ \theta < 0. \end{cases}$$

$$E(S) = 0$$

$$Var(S) = n(n-1)(2n+5)/18$$

If S has an approximate normal distribution, then the test statistic z is (McCuen,1993):

$$z = \begin{cases} (S-1)/(Var(S))^{0.5} & if\ S > 0 \\ 0 & if\ S = 0 \\ (S+1)/(Var(S))^{0.5} & if\ S < 0 \end{cases}$$

where z is the value of the standard normal variate with zero mean and unit standard deviation.

In the case where a trend is detected, a non-parametric estimate of the magnitude of the trend is indicated by the Kendall slope estimate (Hollander and Wolfe, 1973). In this study the estimate is taken as the mean of the slope estimates for the lines connecting all possible pairs of data in the time series. The Kendall slope estimates Ks obtained in the study are presented alongside the corresponding Mann-Kendall statistics in Table 5.

RESULTS AND DISCUSSION

Summary Statistics

From Tables 1 to 3 the standard deviation of temperature is higher for the winter months, with the highest value being for February. The standard deviation then gradually decreased for spring months and into the summer and fall. The lowest standard deviation value is for October. This seems to indicate that the variation in temperature during the month was highest in winter and lowest in fall. The mean and median temperature values seem to indicate that between 1952 and 1983 July and August were the warmest months in the watershed.

In the case of precipitation, standard deviation is highest for fall months, decreases for winter and spring and attains its lowest for the summer months. From these values it may be deduced that the variation in precipitation during the month was highest in fall and lowest in summer. The mean and median precipitation values seem to indicate that most precipitation in the watershed occurred in winter and least in summer between 1952 and 1983.

The mean and median streamflow values seem to indicate that the most streamflow occurred in the watershed in early spring and the least in summer. The standard deviation values for streamflow seem to indicate that in the watershed the lowest variation in this variable occurred in summer while the highest variation occurred in early spring to late fall between 1952 and 1983.

The quantile values for precipitation seem to indicate that during the winter months the lowest 25% of precipitation that occurred were below 4.5 cm while the highest 25% were between 6.8 and 7.6 cm. The corresponding values for spring were 3.8 cm and between 4.6 and 6.6 cm respectively; for summer they were 1.9 cm and between 3.2 and 5.4 cm, while the values for fall were 4.3 cm and between 5.7 and 7.3 cm.

Probability Models

The probability plots presented in Figures 1 to 48 show that the probability model for monthly temperature in the watershed is season-dependent. The normal model appears to give the best fit for data for late fall to early spring, while the lognormal model appears to give the best fit for temperature data for the rest of the months. This is not surprising since some negative temperatures were recorded during late fall to early spring and so the lognormal model did not give a good fit.

For precipitation and streamflow both the lognormal and Weibull models appear to fit the data equally well for all the months. It may be worth noting that that the choice between lognormal and Weibull models as the representative probability model for precipitation and streamflow in the watershed should be determined by computational convenience.

Graphical Trend Detection

The RLWR and ten-year moving average plots are shown in Figures 49 to 84 alongside the times series plots. The RLWR and ten-year moving average trends are similar in direction for each variable in all the months.

In spring, summer and fall months temperature showed an upward trend except in August for which no trend was detected. Also, temperature showed a downward trend in the winter months except in December for which no trend was detected. In the case of precipitation there is no upward trend in spring, summer and fall months, except for July and November when downward trends were detected. For streamflow an upward trend was detected for late spring, part of summer and most of fall, while a downard trend was detected for the months of January, April and November and no trend for February, March and December. The precipitation trends in late spring to late fall are similar to the streamflow trends during that period of the year, as one would expect. However, the precipitation trends in winter and early spring did not translate into similar trends in streamflow in those months probably because of the effects of storage during that period.

Mann-Kendall Statistics

The computed Mann-Kendall statistics presented in Table 5 confirm the trends detected using RLWR and ten-year moving average techniques. However, the absolute values of the statistics seem to indicate that only a few of the detected trends are significant. The Kendall slope estimates (in Table 5) appear to indicate that from 1952 to 1983 monthly temperature in the watershed changed between 0.1 and 7 degrees per year, precipitation changed between 0.6 and 13 mm per year, while streamflow changed by less than 0.5 cm per year. Analysis of longer duration time series would be needed to confirm those trends that do not appear to be significant.

CONCLUSIONS

Time series of temperature, precipitation and streamflow for the period 1952 to 1983 for the Northeast Pond River watershed in Newfoundland were analyzed for trends on a seasonal basis. Both graphical methods and Mann-Kendall trend test detected trends in the time series for most winter, spring, summer and fall months. However, some of the trends did not appear to be significant probably because the time series was not long enough to show such trends as significant at the watershed level. The analysis also showed that both the lognormal and Weibull probability models are good choices for precipitation and streamflow. In the case of temperature the normal model gives the best fit for late fall to early spring, while the lognormal model is best for the rest of the months.

RECOMMENDATIONS FOR FURTHER WORK

In light of the foregoing results it is recommended that:

1. Similar analysis be carried out for other watersheds in the region to confirm or reject the detected trends due to climate change; for such regional analysis all available time series of temperature, precipitation and streamflow would need to be considered.

2. In view of the fact that some trends have been detected, autocorrelation analysis needs to be carried out with the objective of developing a stochastic model for each of temperature, precipitation and streamflow for forecasting and future trend detection.

REFERENCES

Bobba, A. G., V. P. Singh, D. S. Jeffries and L. Bengtsson. 1997. Application of a watershed runoff model to Northeast Pond River, Newfoundland: to study water balance and hydrological characterisitcs owing to atmospheric change. Hydrol. Proc., 11: 1573 – 1593

Bobba, A. G., D. S. Jeffries and V. P. Singh. 1999. Sensitivity of hydrological variables in the Northeast Pond River watershed, Newfoundland, Canada, due to climate change. Water Resour. Mngt., 13: 171 – 188

Cleveland, W. S. 1979. Robust locally weighted regression and smoothing scatter plots. J. Am. Statistical Assoc., 74(368): 829 – 836

Environment Canada. 1995. The state of Canada's climate: monitoring variability and change. SOE Report No. 95 – 152. Downsview, Ontario, Canada.

Hollander, M.and D. A. Wolfe. 1973. Non-parametric Statistical Methods. Wiley, New York. 503pp

Kendall, M. G. 1975. Rank Correlation Methods, 4th ed. Charles Griffin, London.

Lettenmaier, D. P.and T. Y. Gan. 1990. Hydrologic sensitivity of the Sacramento-San Joaquim River Basin, California, to global warming. Water Resour. Res. 26: 69 – 86

Manabe, S., R.and T. Weatherald. 1987. Large scale changes in soil wetness induced by an increase in carbon dioxide. J. Atmos. Sci. 44: 1211 – 1235.

Mann, H. B. 1945. Non-parametric tests against trend. Econometrica 13: 245 – 259.

McCuen, R. H. 1993. Microcomputer Applications in Statistical Hydrology, 1st ed. Englewood Cliffs, N. J.: Prentice Hall. 306pp

Nemec, J. and J. Schaake. 1982. Sensitivity of water resource systems to climate variation. Hydrol. Sci. 27(3): 327 – 343

Table 1. Summary Statistics for Temperature

Month	Mean	Median	Standard Deviation	Range	First Quantile	Third Quantile
January	-3.616	-3.661	2.353	-8.145, 0.321	-5.296	-2.100
February	-4.456	-4.378	2.385	-10.236, -0.882	-5.923	-3.183
March	-1.976	-2.323	1.750	-4.915, 1.694	-3.268	-0.522
April	1.651	1.355	1.318	-0.958, 4.658	0.858	2.386
May	5.923	5.427	1.505	3.484, 9.194	4.718	7.309
June	10.852	10.937	1.748	7.683, 14.830	9.353	11.838
July	15.444	15.403	1.514	11.979, 18.868	14.448	16.329
August	15.389	15.317	1.373	12.087, 19.100	14.594	16.187
September	11.654	11.567	0.941	10.133, 13.640	10.863	12.210
October	7.153	7.023	0.888	5.758, 9.315	6.524	7.622
November	3.564	3.850	1.429	1.198, 6.230	2.381	4.708
December	-1.280	-1.202	1.912	-6.190, 2.840	-2.395	0.100

Table 2. Summary Statistics for Precipitation

Month	Mean	Median	Standard Deviation	Range	First Quantile	Third Quantile
January	6.045	5.648	2.098	3.258, 11.491	4.412	7.518
February	5.855	5.511	2.085	2.921, 10.979	4.310	6.979
March	5.217	5.337	1.740	1.932, 8.745	3.794	6.538
April	4.435	4.268	1.898	1.660, 10.063	2.952	5.582
May	3.474	3.437	1.451	1.326, 6.271	2.136	4.617
June	2.807	2.497	1.466	0.620, 6.727	1.854	3.596
July	2.459	2.294	1.268	0.526, 5.777	1.660	3.273
August	3.699	2.876	2.272	0.800, 9.971	1.725	5.344
September	4.064	3.785	2.016	0.743, 9.183	2.414	5.790
October	4.858	4.479	2.201	1.313, 9.155	2.885	7.023
November	5.624	5.123	2.252	2.377, 11.083	4.272	7.292
December	5.395	5.019	1.774	2.829, 9.574	4.252	6.823

Table 3. Summary Statistics for Streamflow

Month	Mean	Median	Standard Deviation	Range	First Quantile	Third Quantile
January	0.1512	0.1216	0.1004	0.0187, 0.4217	0.0747	0.2064
February	0.1336	0.1024	0.0986	0.0184, 0.3598	0.0581	0.1757
March	0.1628	0.1719	0.0774	0.0390, 0.3170	0.0923	0.2199
April	0.2358	0.2214	0.1025	0.0658, 0.5077	0.1607	0.3064
May	0.1701	0.1644	0.0942	0.0399, 0.4288	0.0836	0.2264
June	0.08827	0.07453	0.05574	0.01507, 0.26467	0.04512	0.12088
July	0.04545	0.03403	0.03517	0.00432, 0.13393	0.01593	0.07461
August	0.0768	0.0514	0.0740	0.0012, 0.3008	0.0261	0.1189
September	0.0905	0.0739	0.0648	0.0023, 0.2258	0.0307	0.1528
October	0.1424	0.1240	0.0806	0.0234, 0.3555	0.0735	0.2020
November	0.2119	0.1516	0.1979	0.0452, 1.1834	0.1233	0.2310
December	0.1606	0.1420	0.0790	0.0754, 0.3861	0.0965	0.2043

Table 4. Best Fit Probability Model

Months	Temperature	Precipitation	Streamflow
November to April	Normal	Lognormal	Lognormal
May to October	Lognormal	Lognormal, Weibull	Lognormal, Weibull

Table 5. Mann-Kendall Statistics (S) and Kendall Slope Estimates (Ks)

Month		Temperature	Precipitation	Streamflow
January	S	-5	1	-3
	Ks	-0.0423	0.0411	-0.00129
February	S	-1	-1	-3
	Ks	-0.0216	-0.0634	-0.000391
March	S	1	5	3
	Ks	0.0687	0.0418	0.000857
April	S	3	1	-1
	Ks	0.0298	0.0219	-0.000717
May	S	1	5	-1
	Ks	0.0462	0.00661	-0.000361
June	S	3	3	1
	Ks	0.0610	0.0415	0.000324
July	S	3	-3	-1
	Ks	0.0540	-0.00877	-0.0000795
August	S	-5	1	1
	Ks	-0.00671	0.0436	0.000713
September	S	1	3	1
	Ks	0.0194	0.0678	0.00178
October	S	1	3	9
	Ks	0.0113	0.12745	0.00399
November	S	1	-1	-3
	Ks	0.00895	-0.0432	-0.00342
December	S	7	7	-5
	Ks	0.00105	0.00605	-0.000137

Figure 1

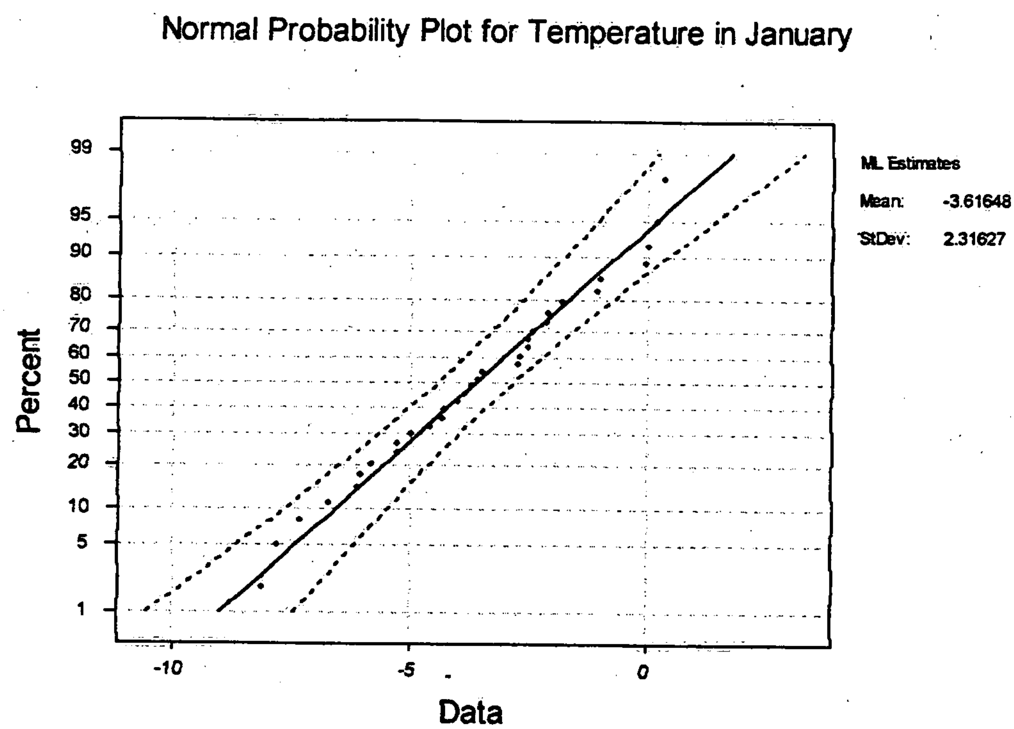

Figure 2

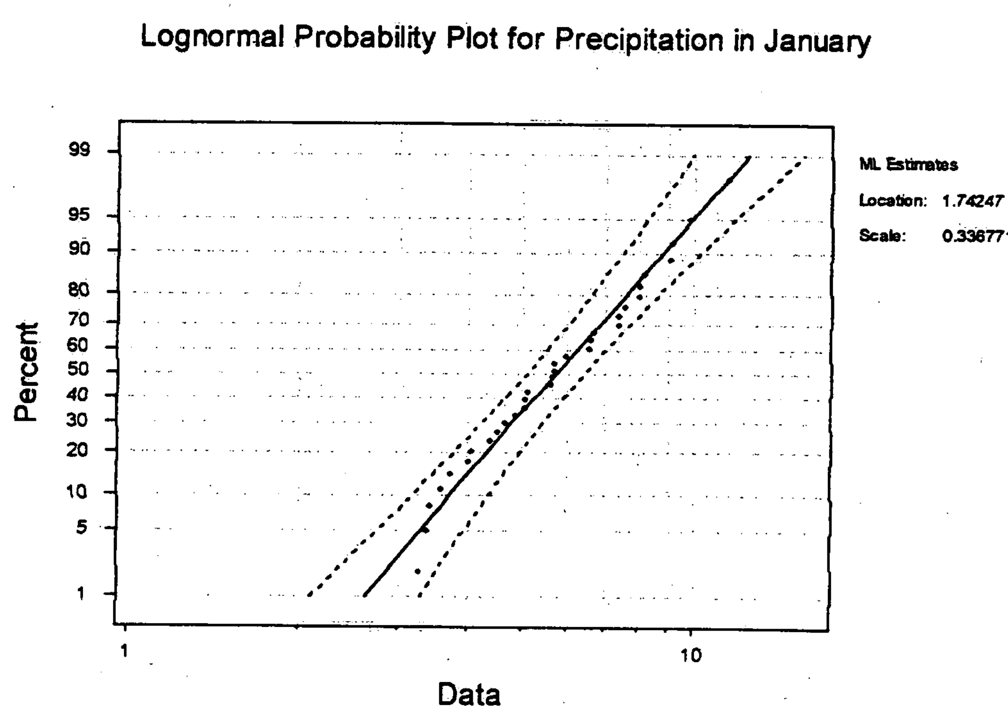

Figure 3

Lognormal Probability Plot for Flow in January

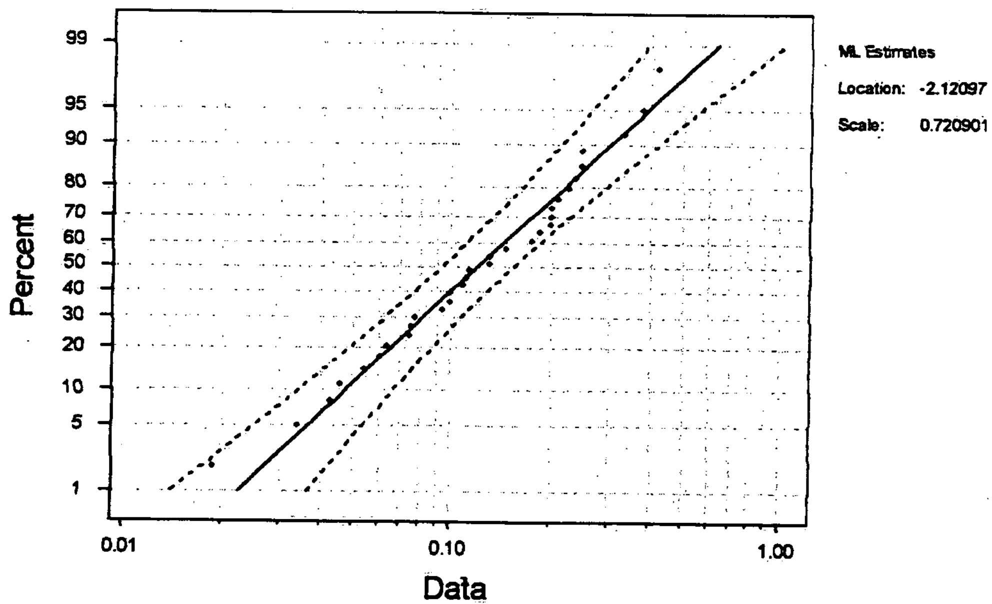

Figure 4

Normal Probability Plot for Temperature in February

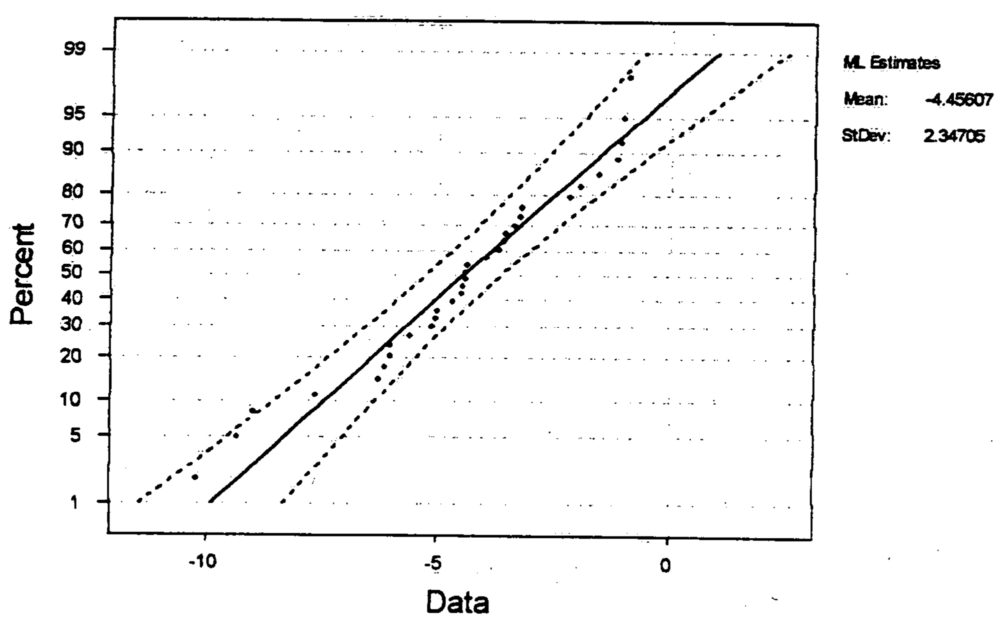

Figure 5

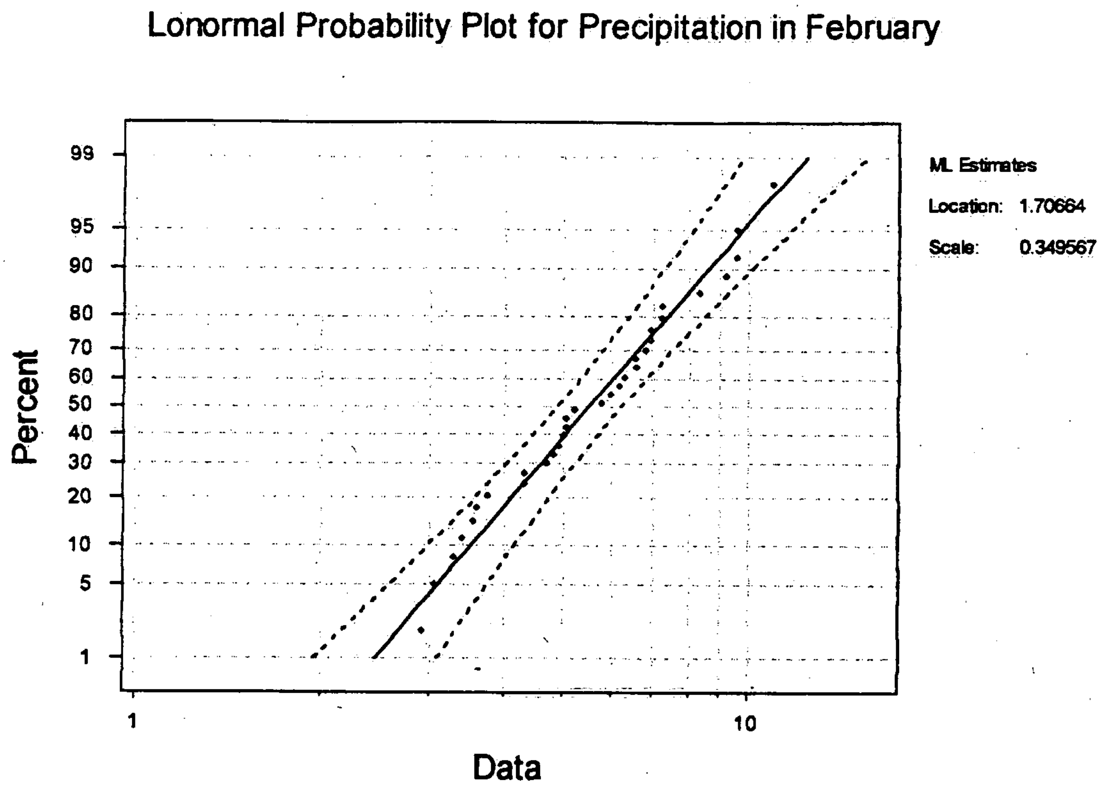

Figure 6

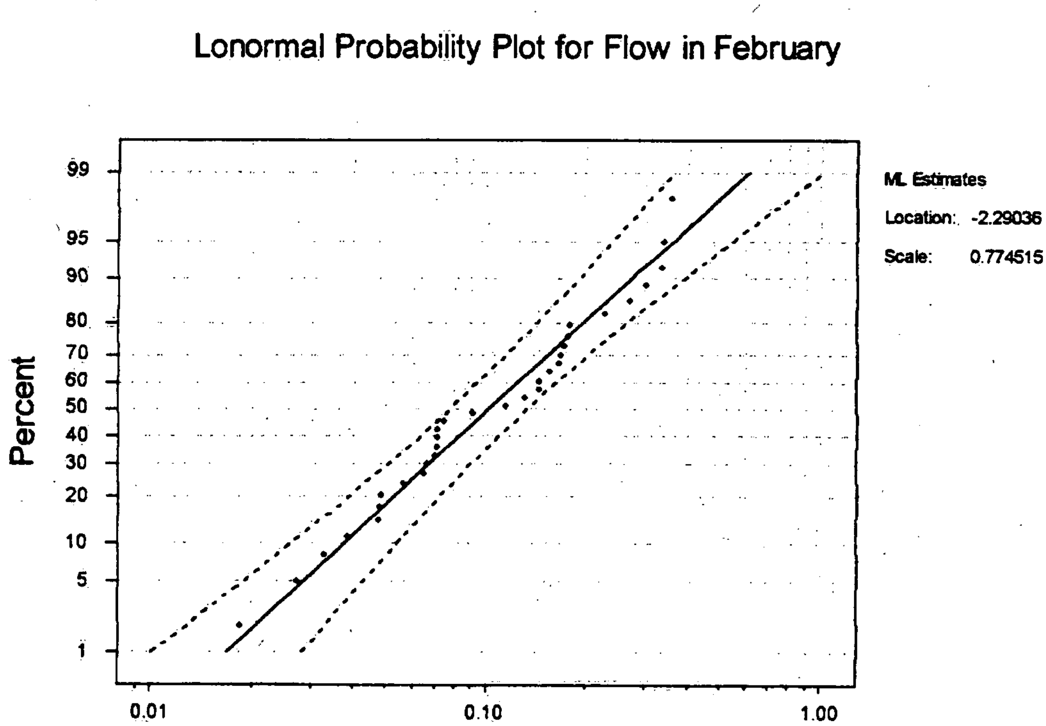

Figure 7

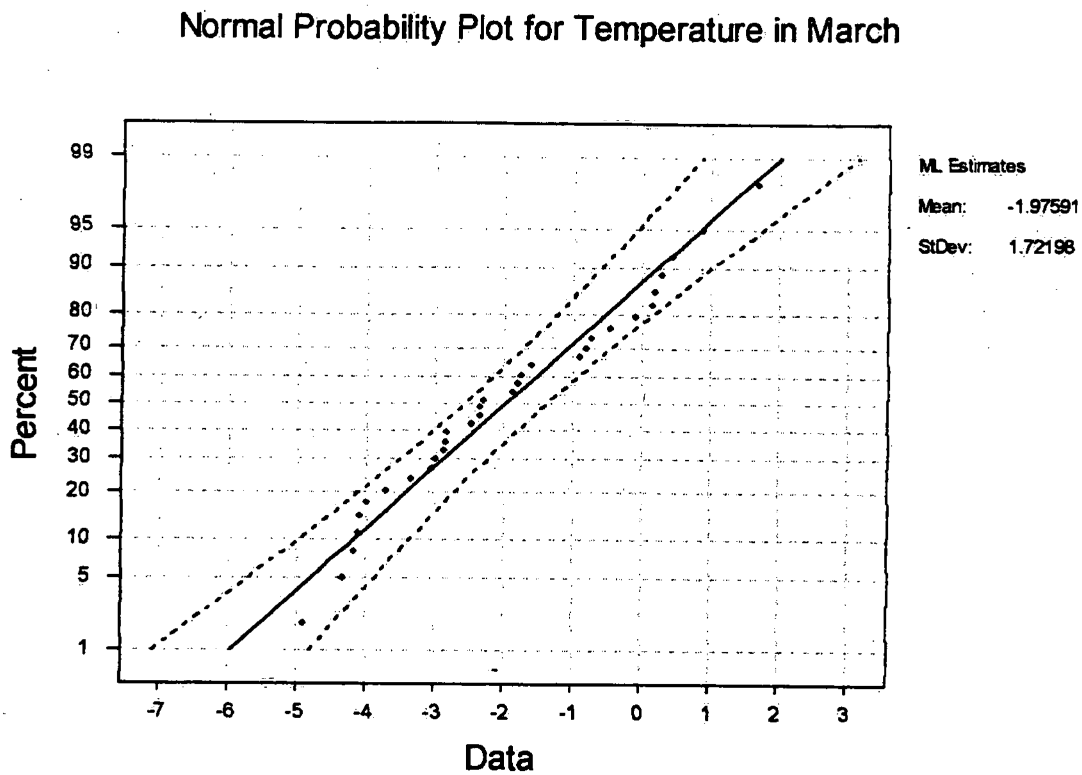

Figure 8

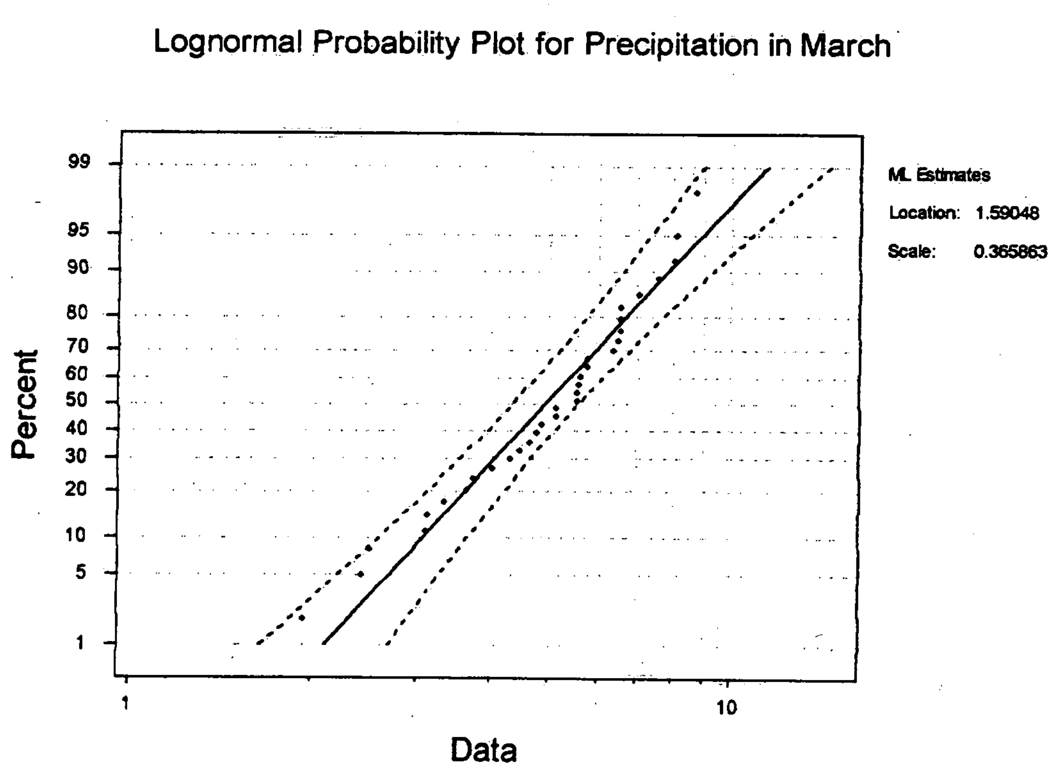

Figure 9

Lognormal Probability Plot for Flow in March

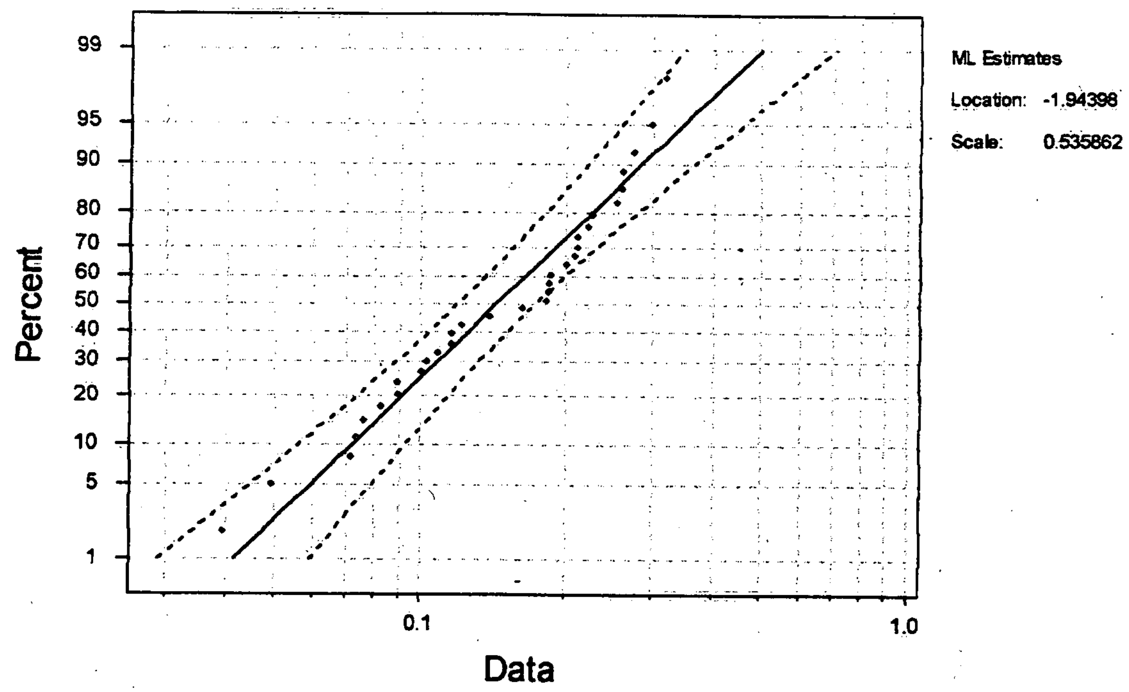

Figure 10

Normal Probability Plot for Temperature in April

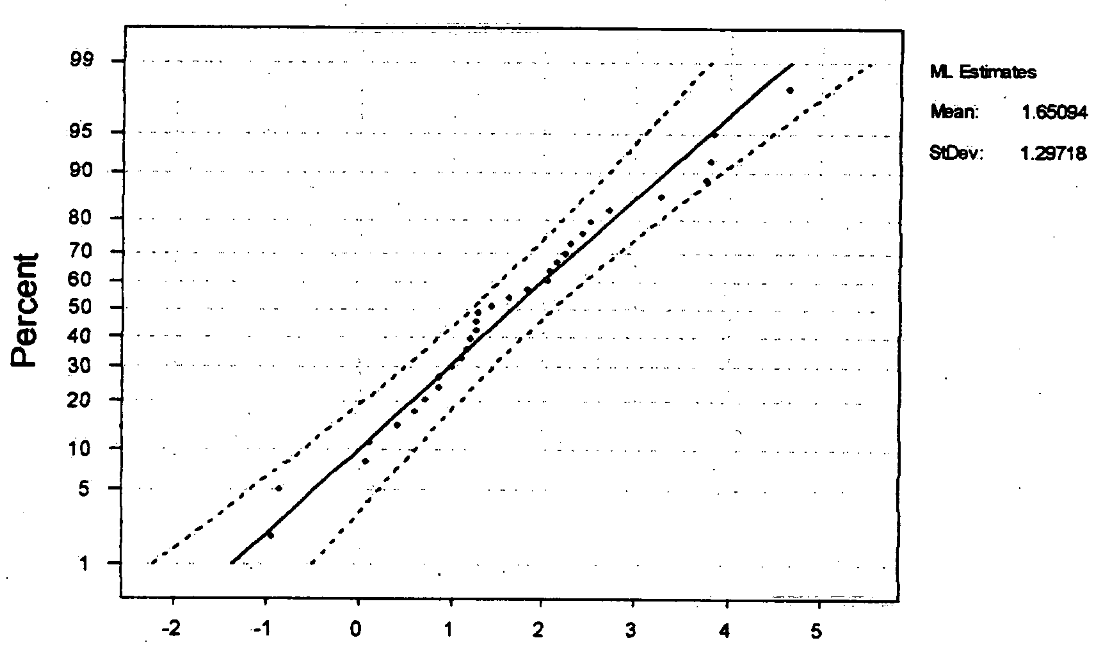

Figure 11

Lognormal Probability Plot for Precipitation in April

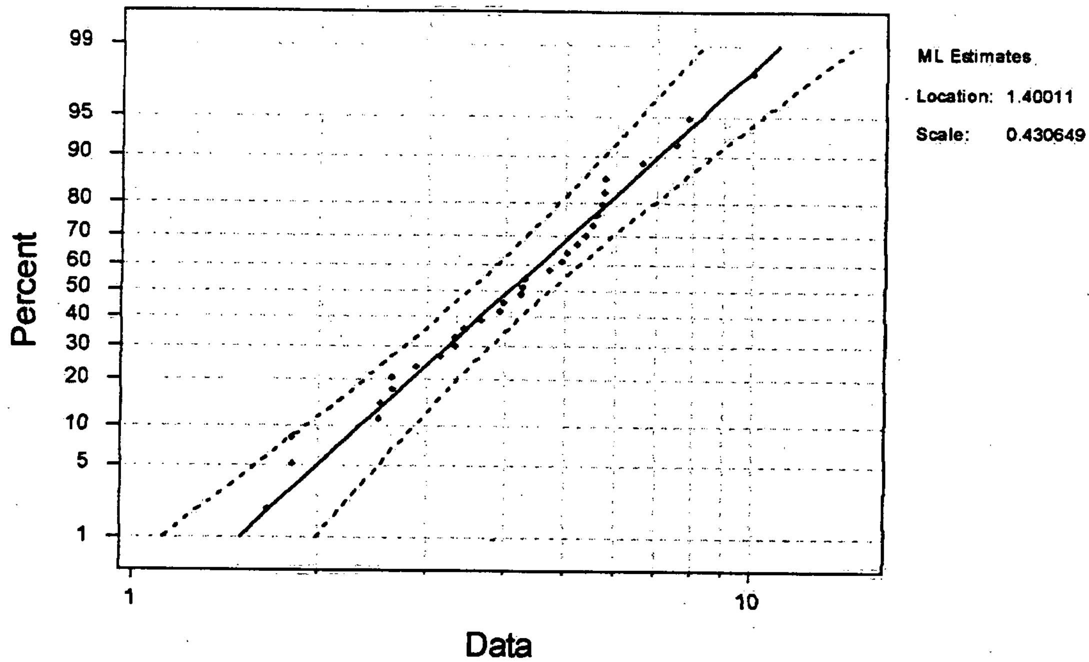

Figure 12

Lognormal Probability Plot for Flow in April

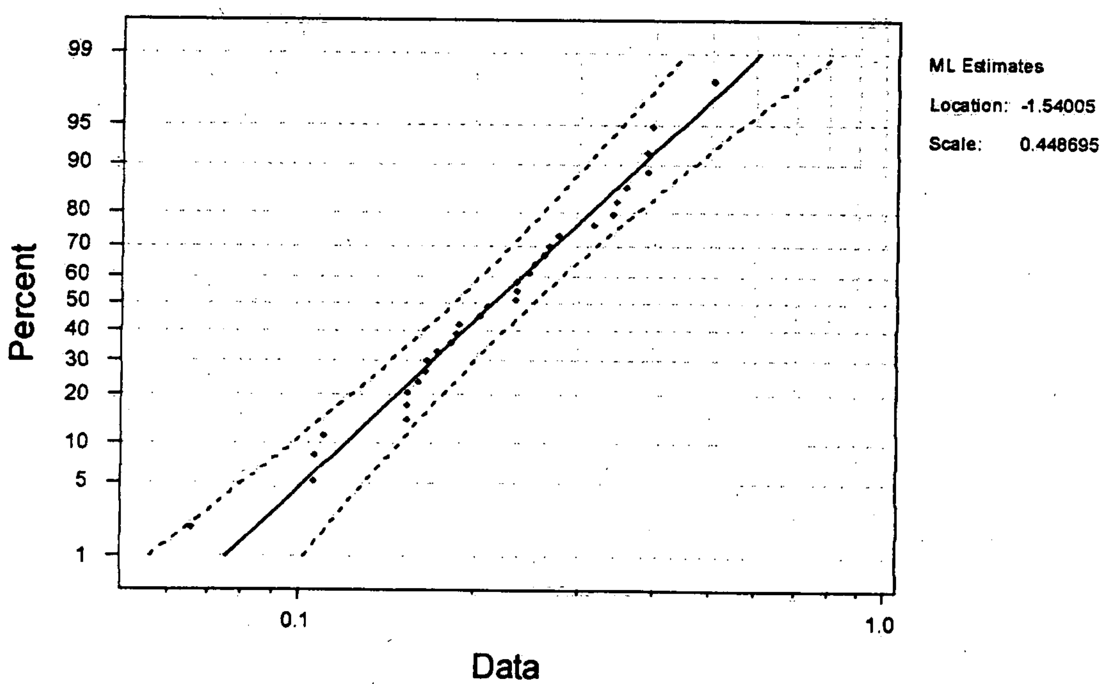

Figure 13

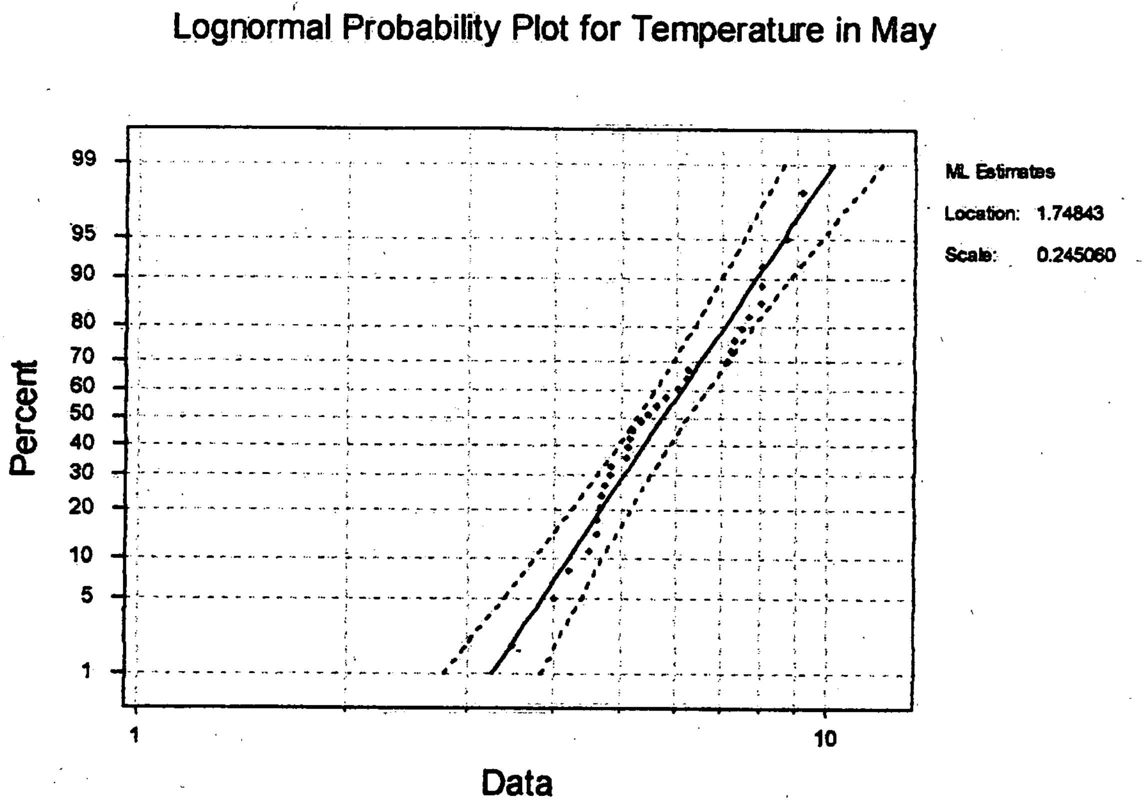

Figure 14

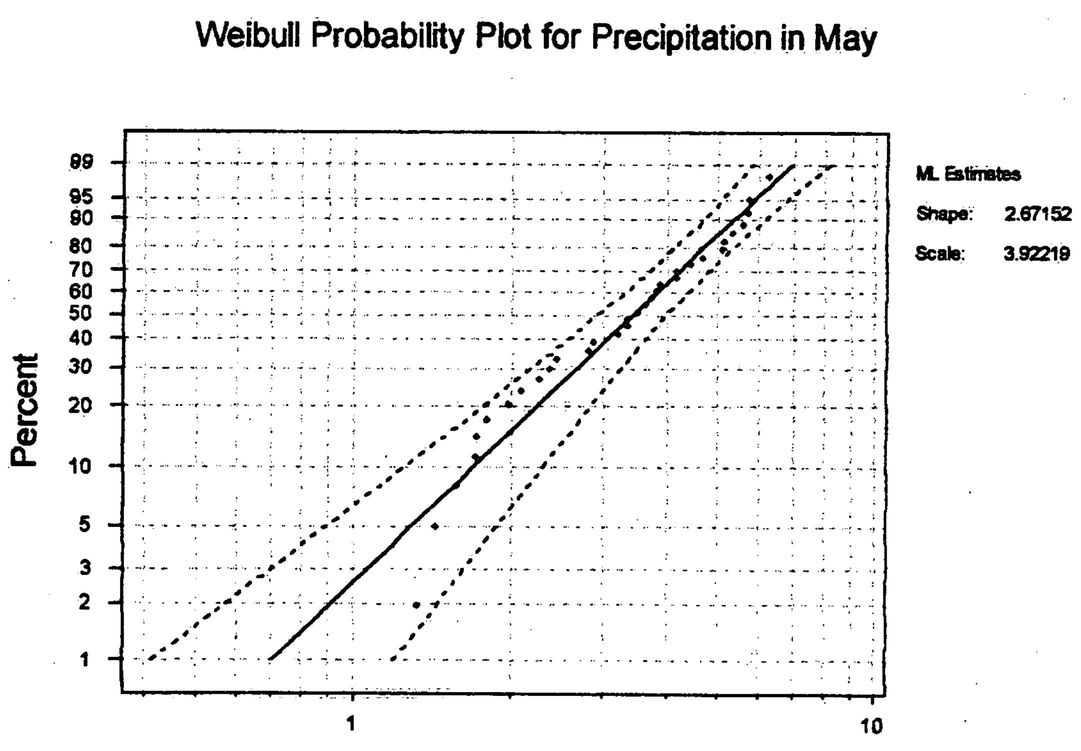

Figure 15

Weibull Probability Plot for Precipitation in May

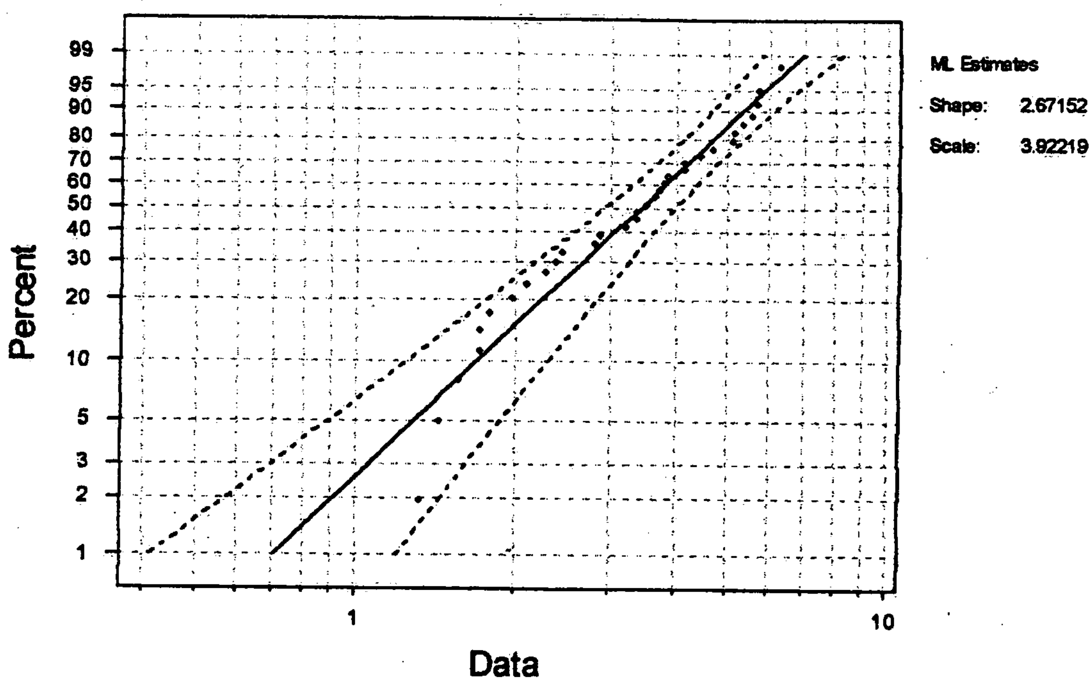

Figure 16

Lognormal Probability Plot for Flow in May

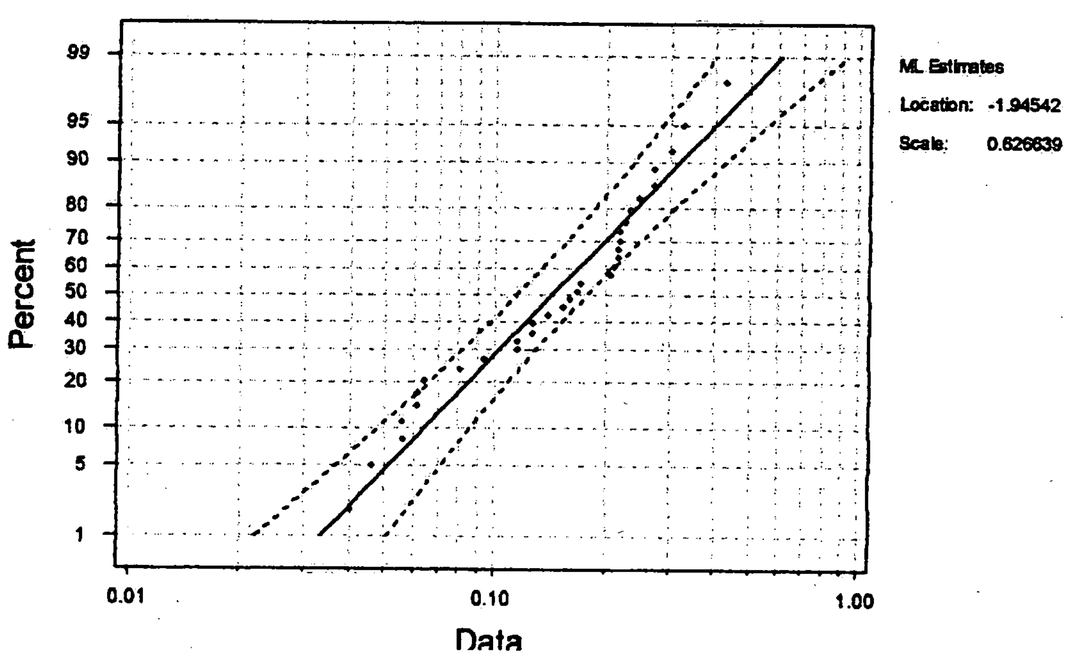

Figure 17

Weibull Probability Plot for Flow in May

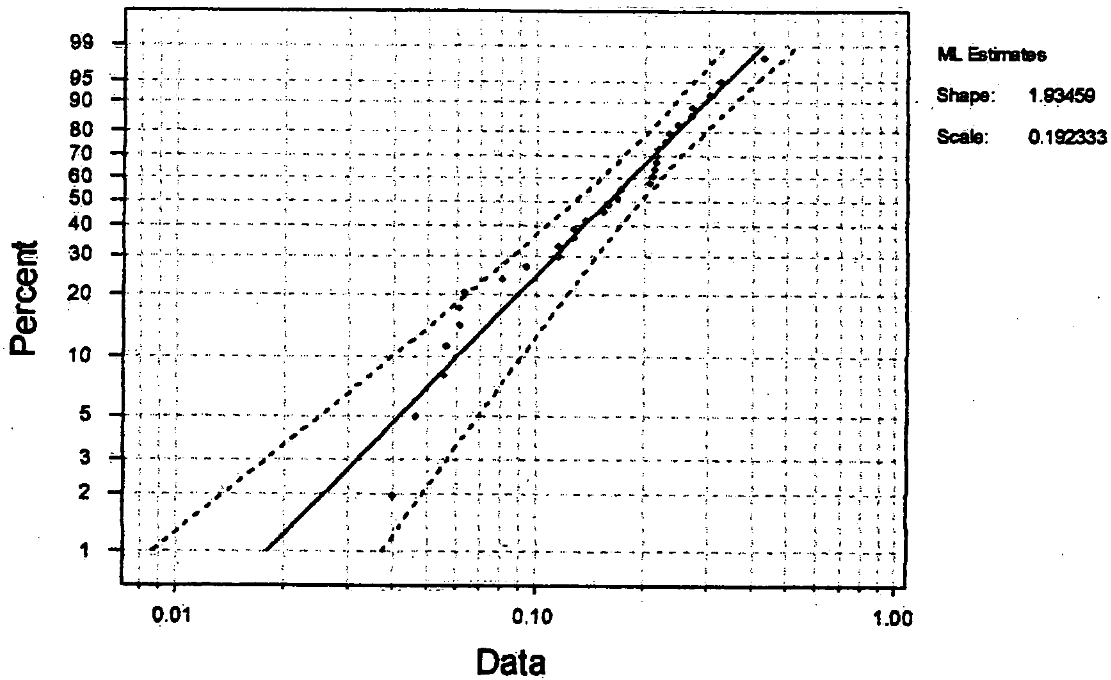

Figure 18

Lognormal Probability Plot for Temperature in June

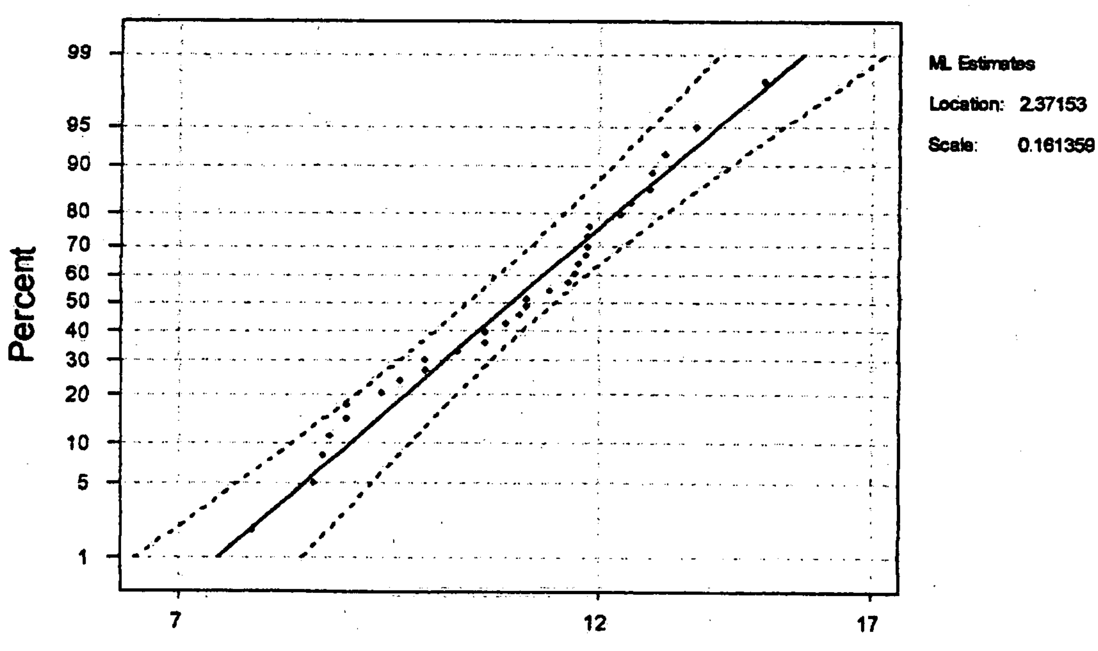

Figure 19

Lognormal Probability Plot for Precipitation in June

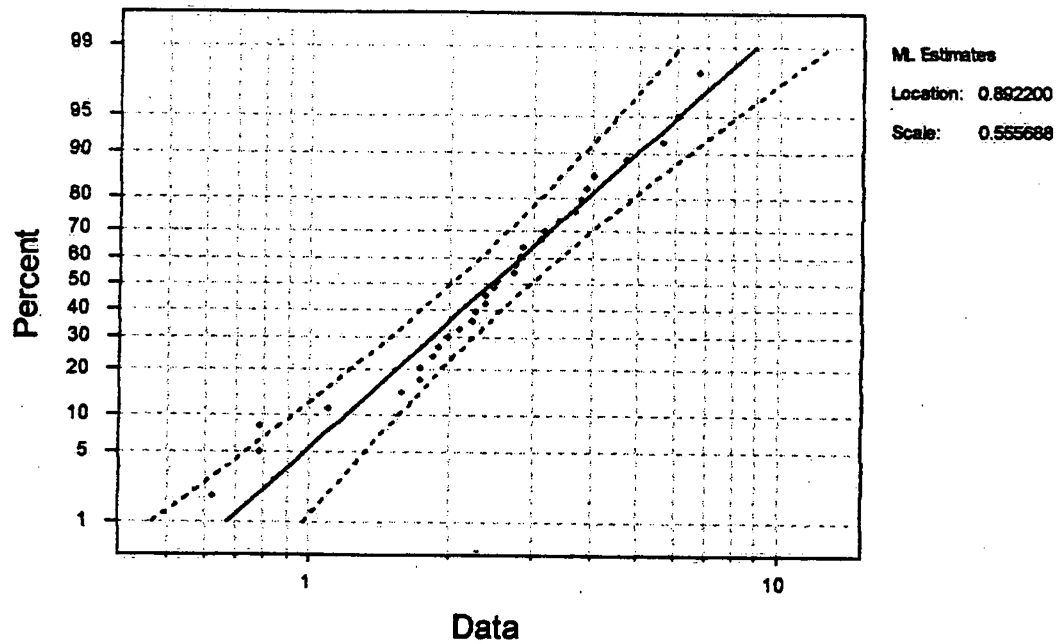

Figure 20

Weibull Probability Plot for Precipitation in June

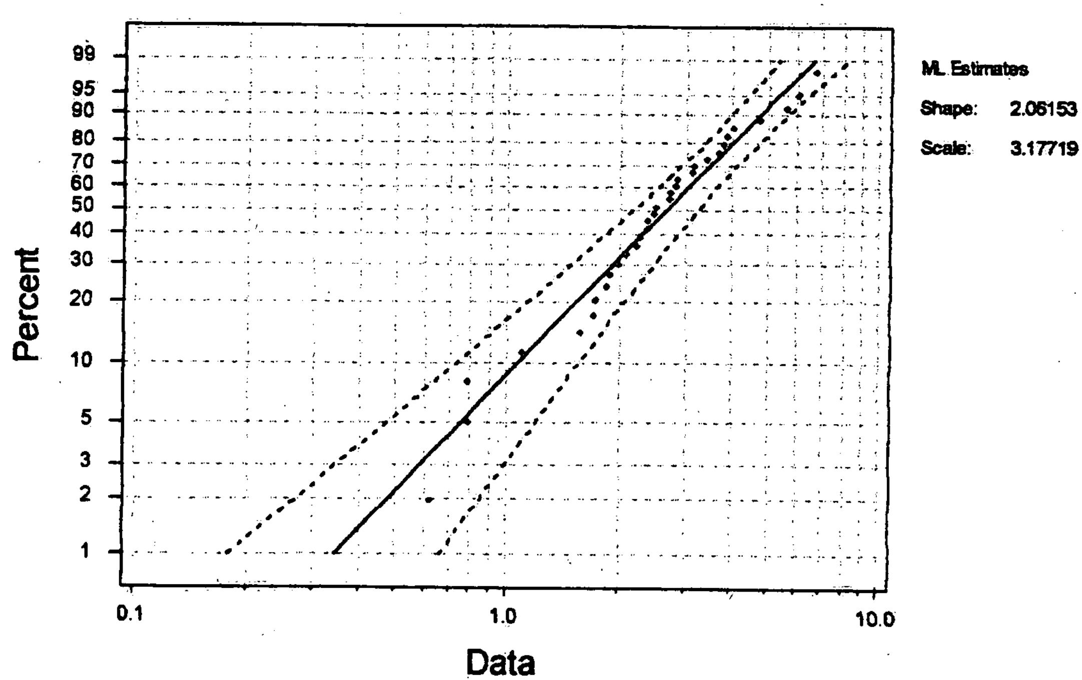

Figure 21

Lognormal Probability Plot for Flow in June

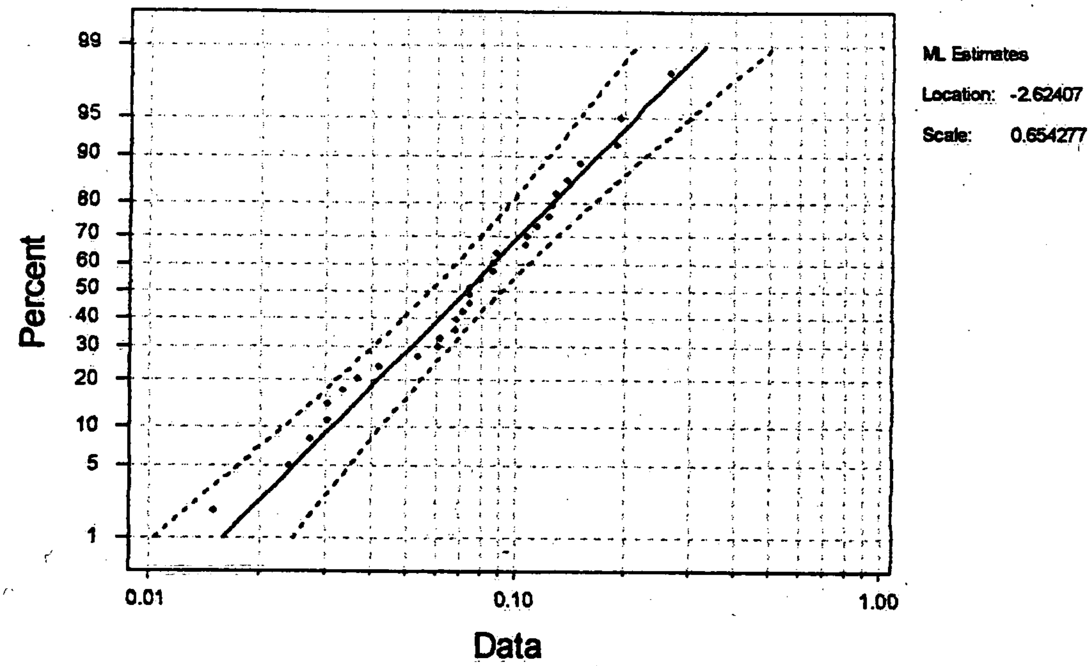

Figure 22

Weibull Probability Plot for Flow in June

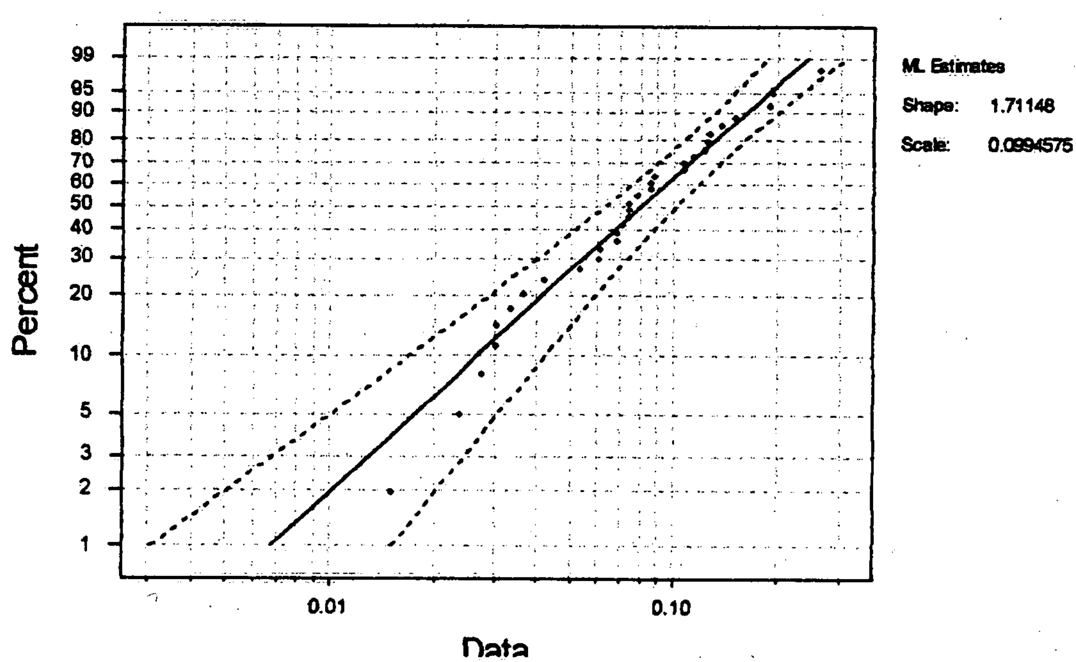

Figure 23

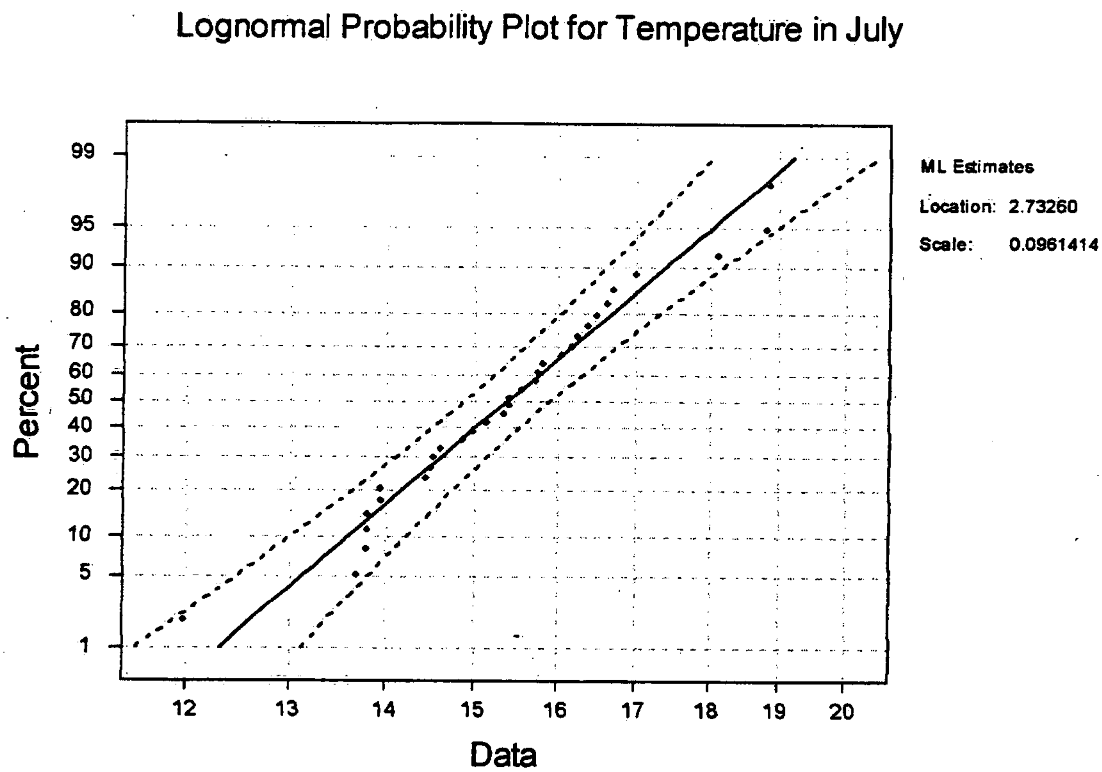

Figure 24

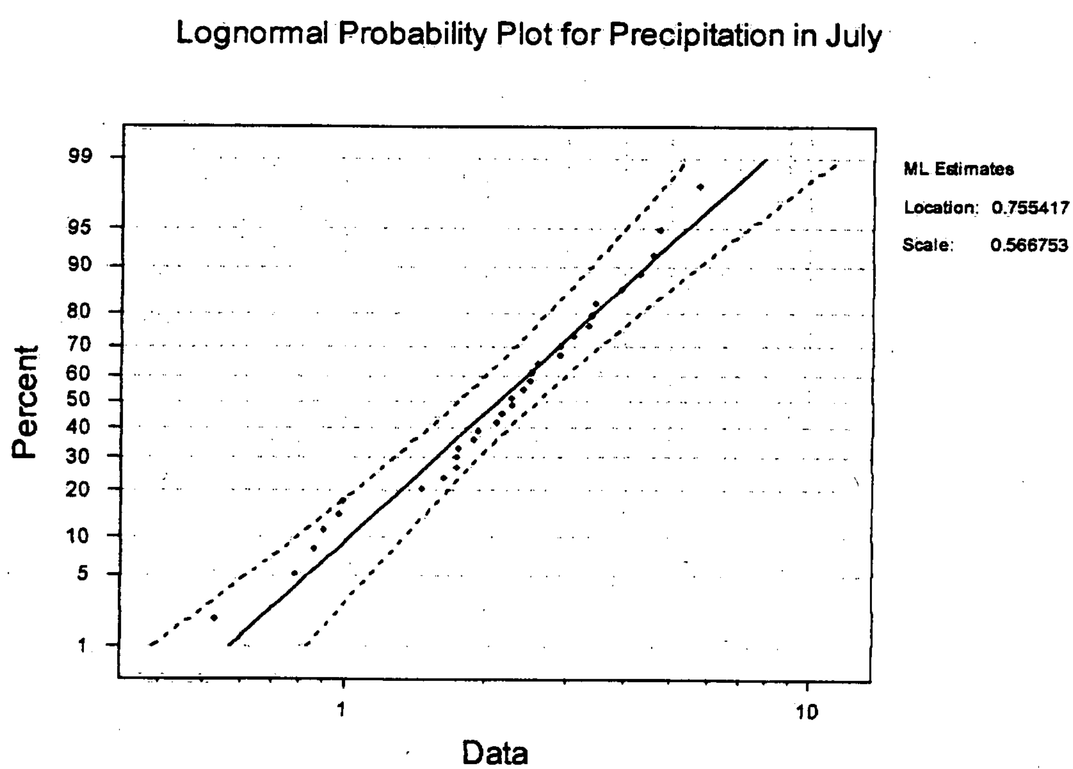

Figure 25

Weibull Probability Plot for Precipitation in July

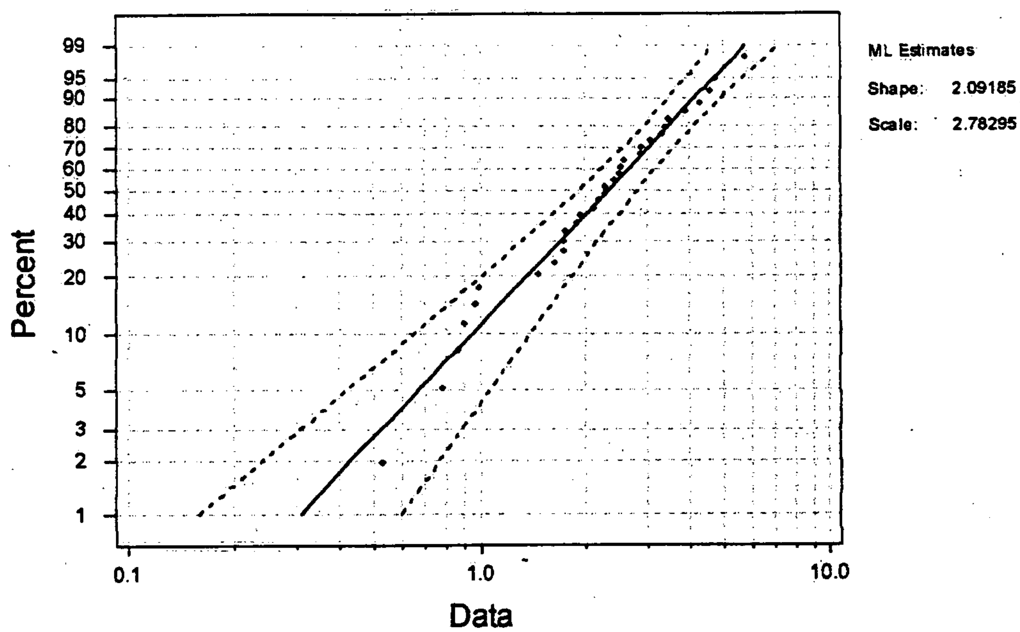

Figure 26

Lognormal Probability Plot for Flow in July

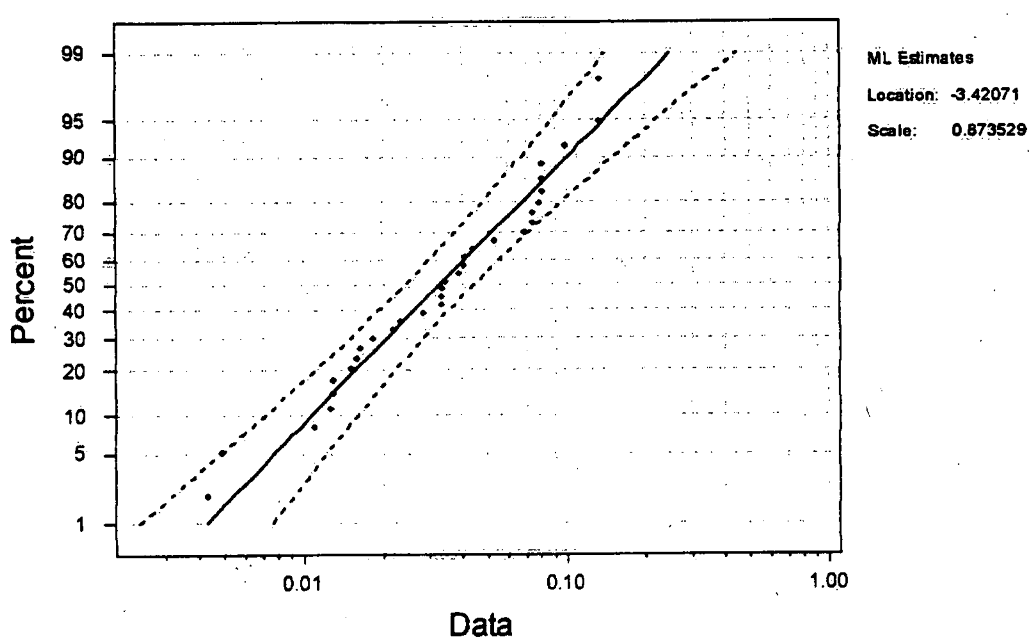

Figure 27

Weibull Probability Plot for Flow in July

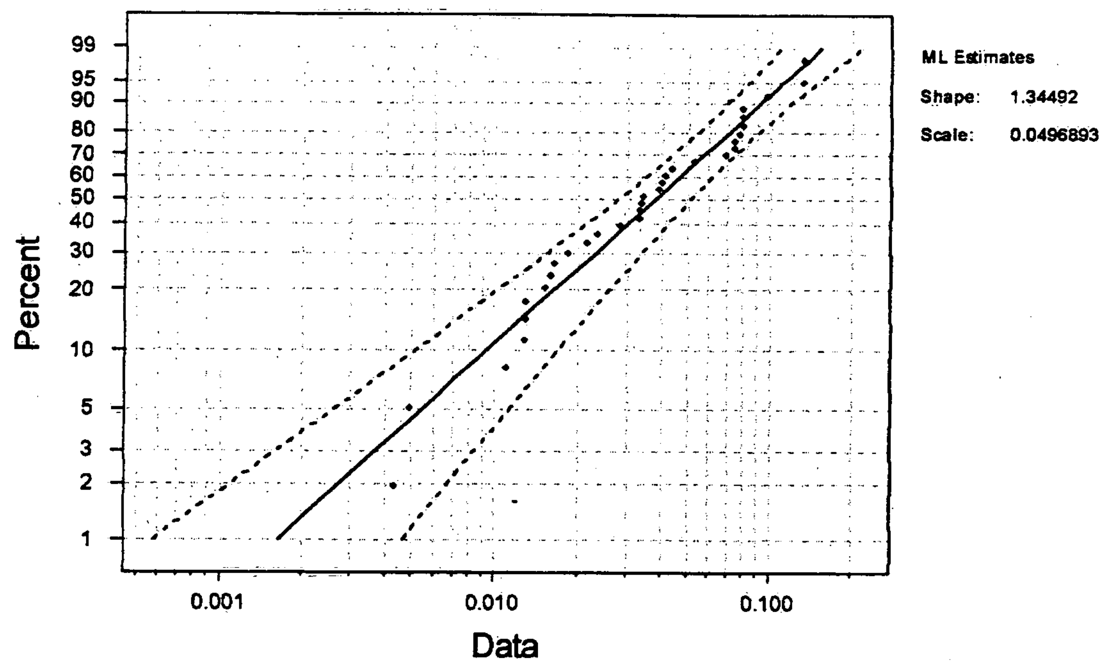

Figure 28

Lognormal Probability Plot for Temperature in August

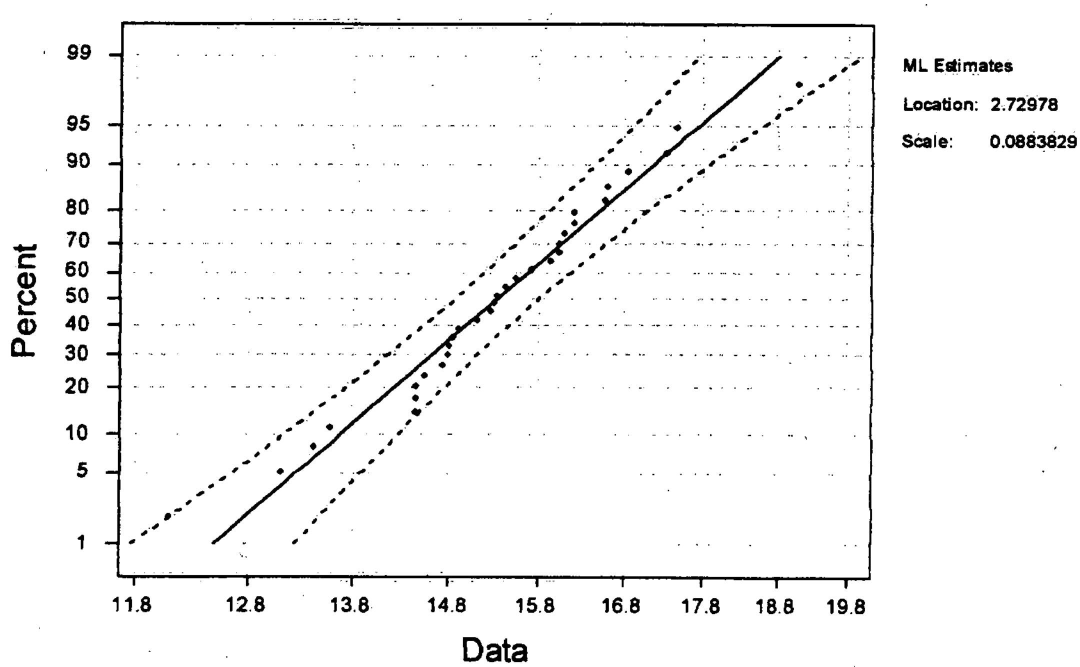

Figure 29

Lognormal Probability Plot for Precipitation in August

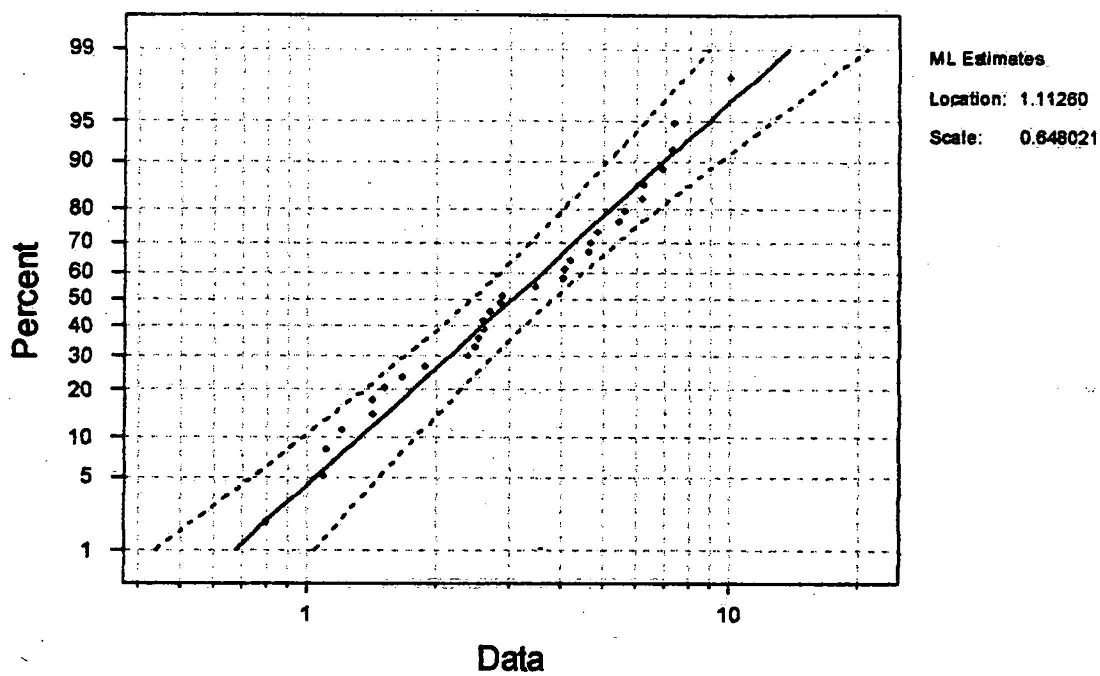

Figure 30

Weibull Probability Plot for Precipitation in August

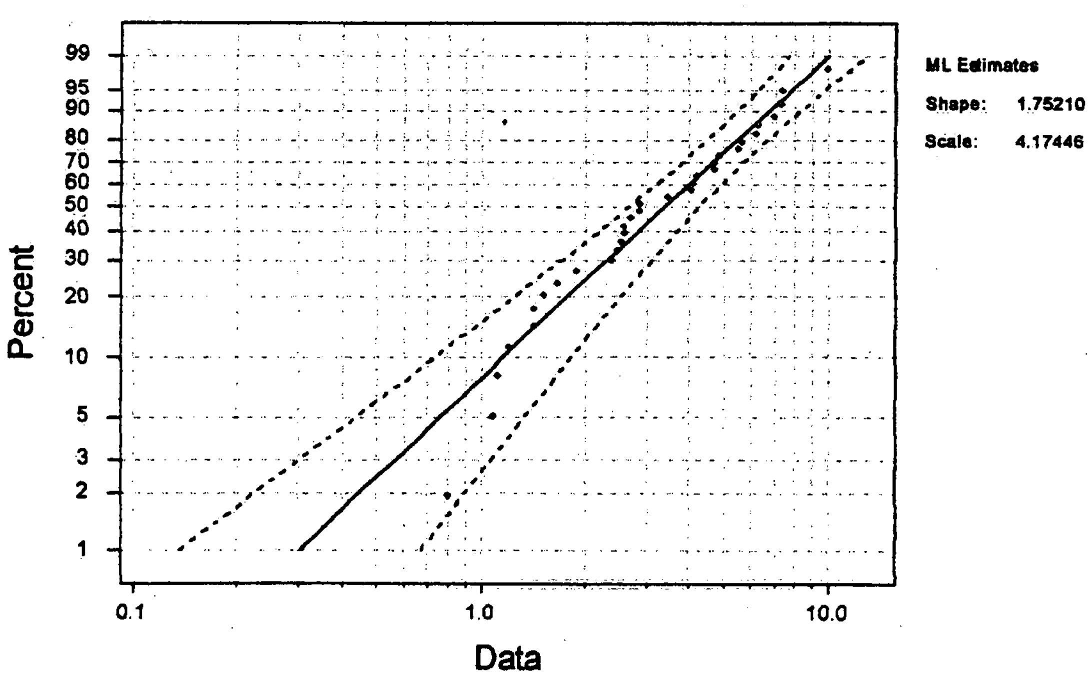

Figure 31

Lognormal Probability Plot for Flow in August

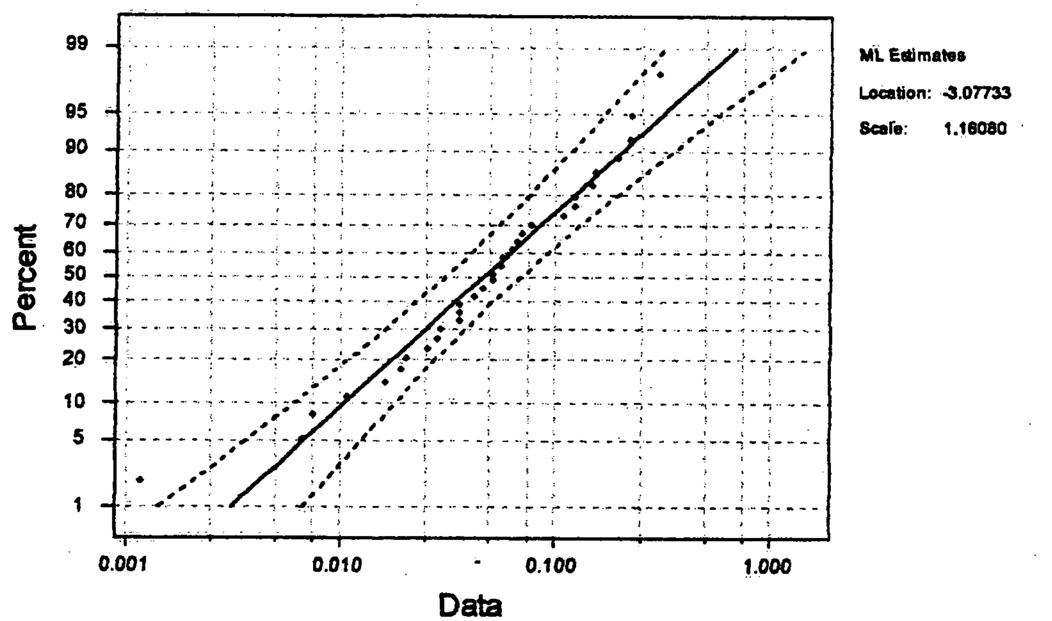

Figure 32

Weibull Probability Plot for Flow in August

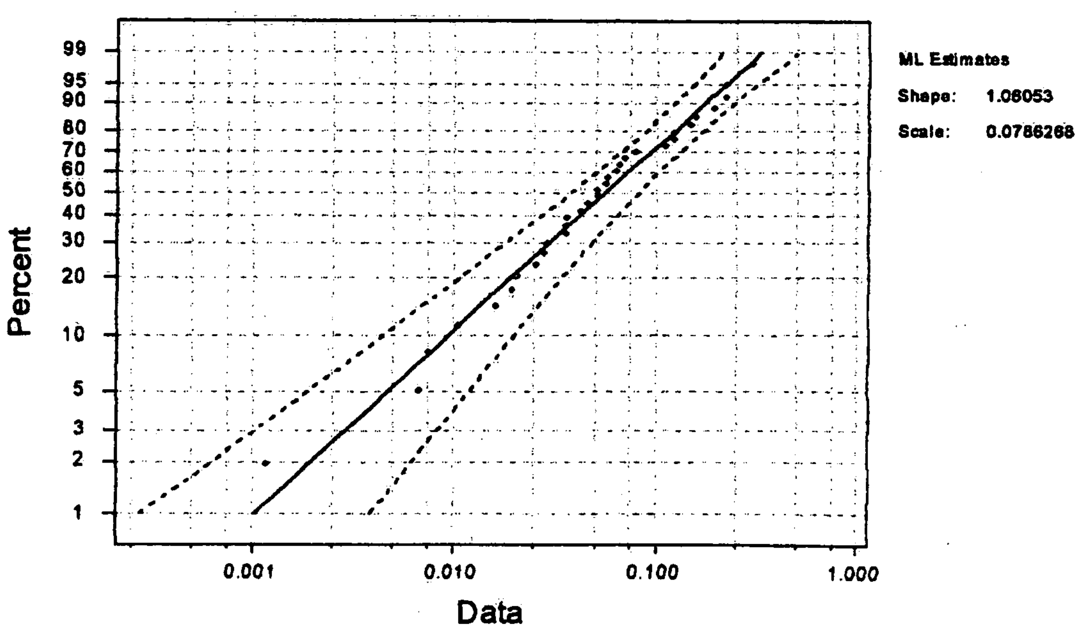

Figure 33

Lognormal Probability Plot for Temperature in September

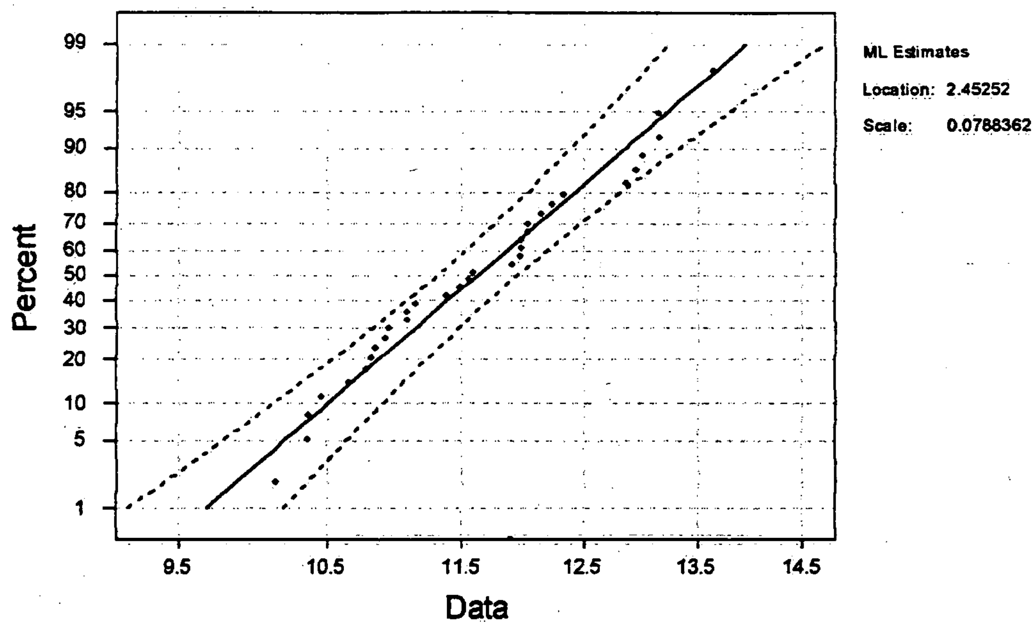

Figure 34

Lognormal Probability Plot for Precipitation in September

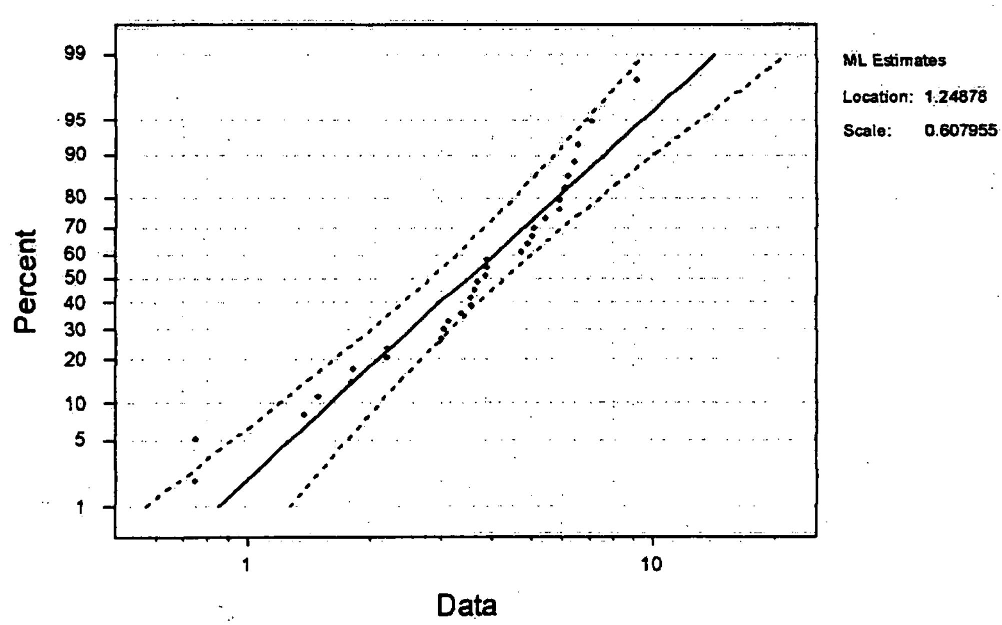

Figure 35

Weibull Probability Plot for Precipitation in September

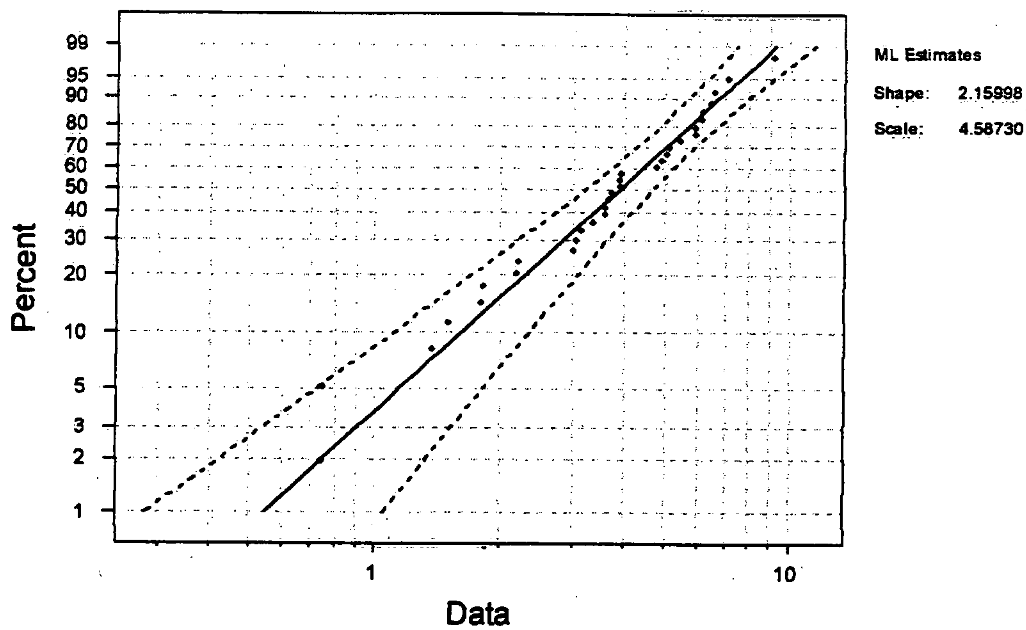

Figure 36

Lognormal Probability Plot for Flow in September

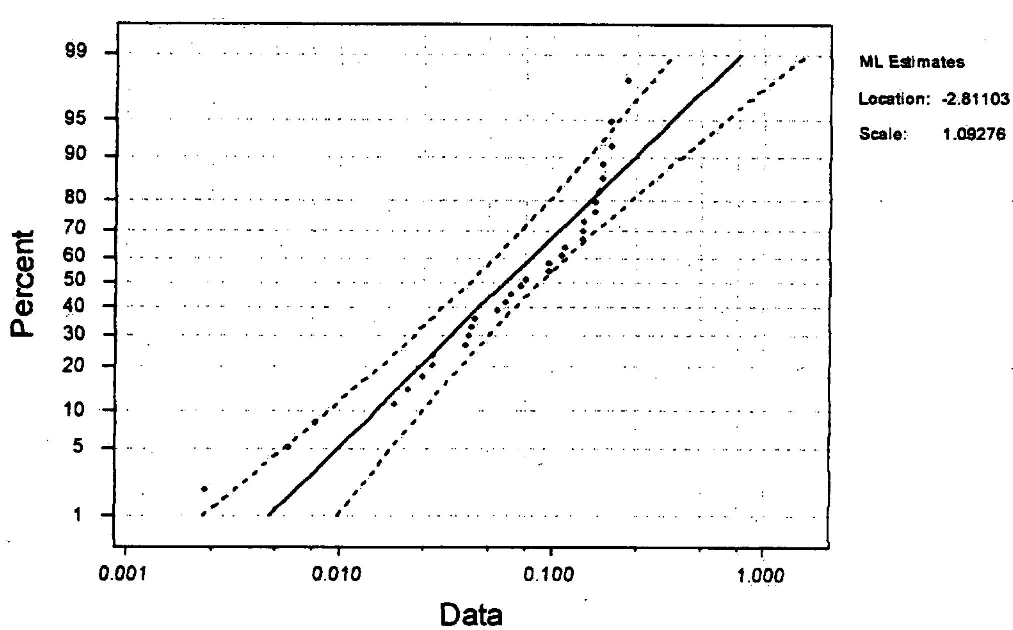

Figure 37

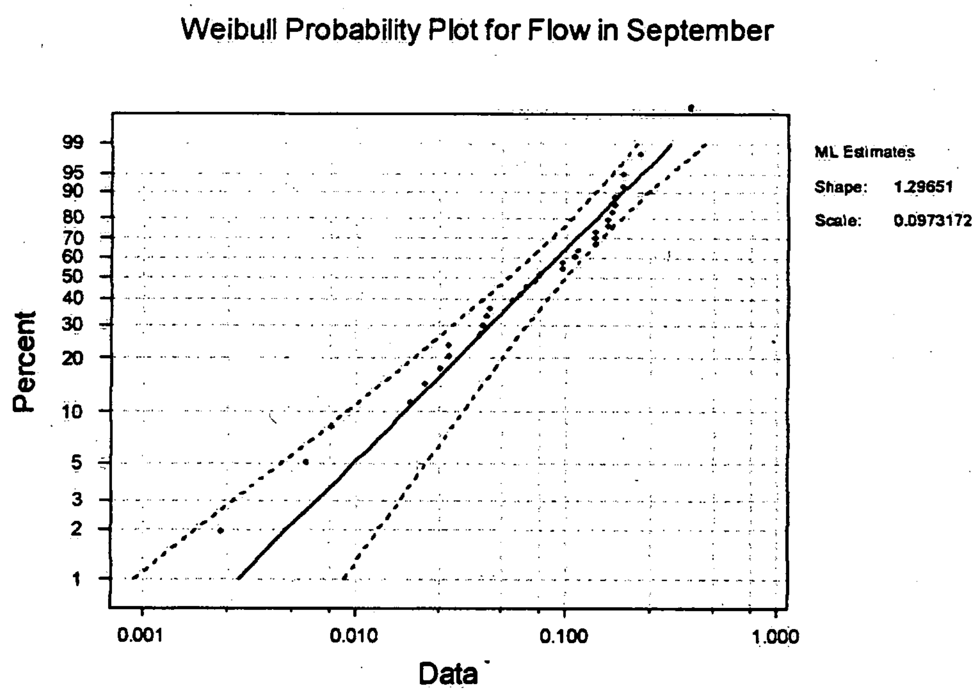

Figure 38

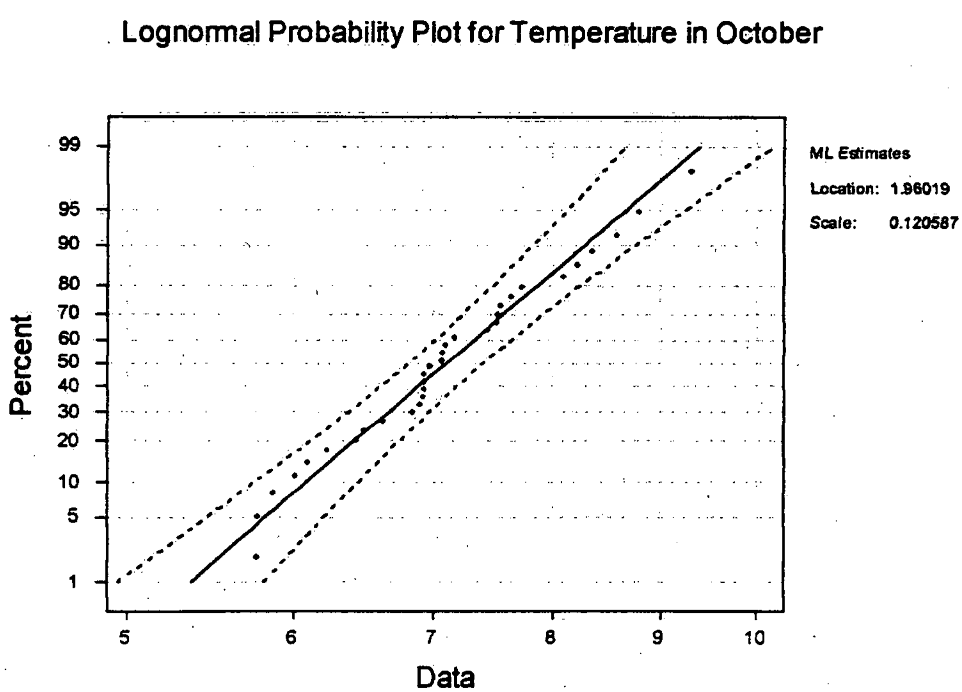

Figure 39

Lognormal Probability Plot for Precipitation in October

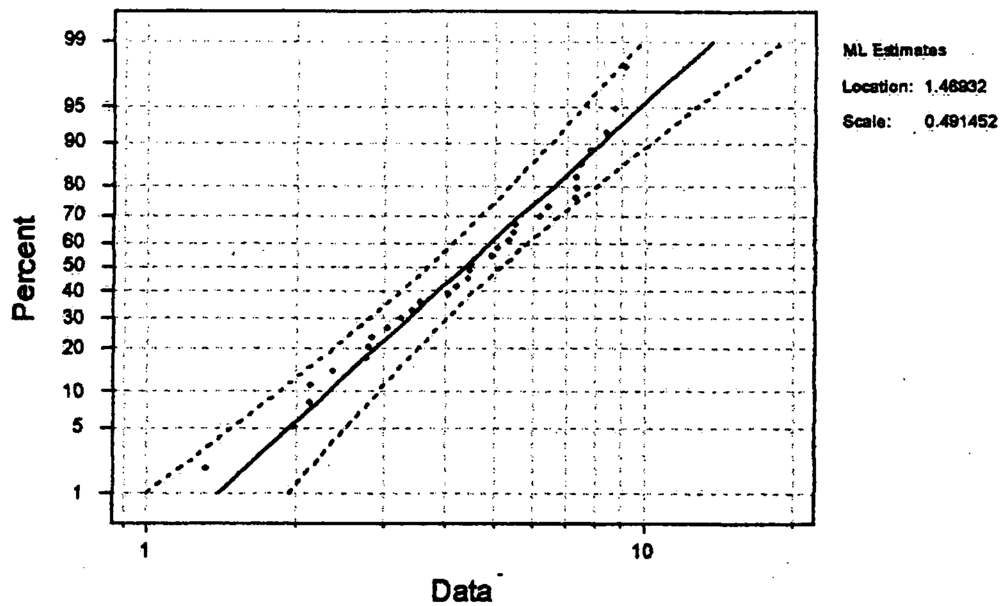

Figure 40

Weibull Probability Plot for Precipitation in October

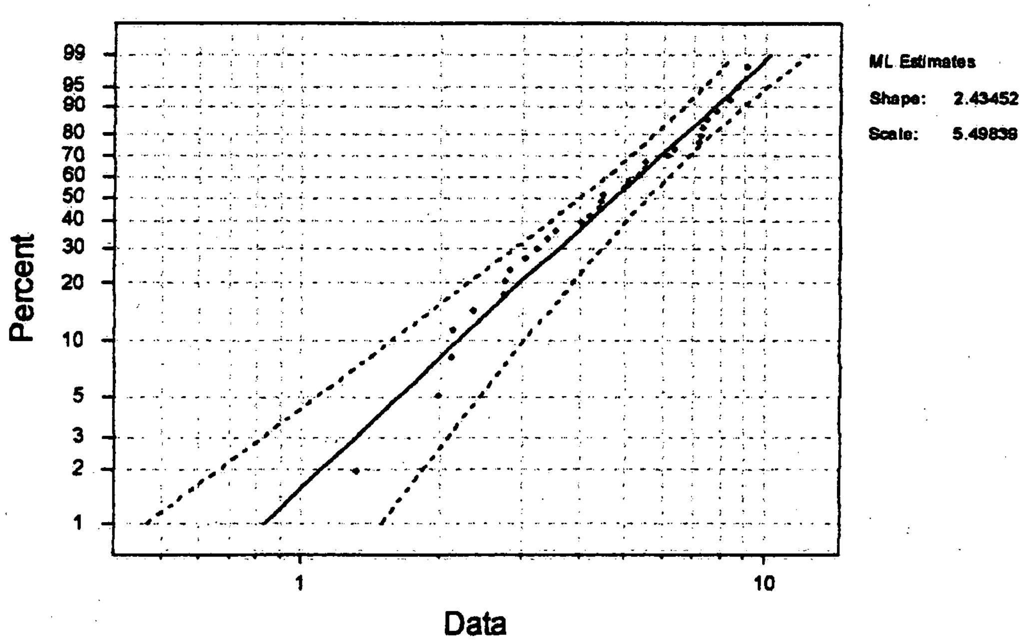

Figure 41

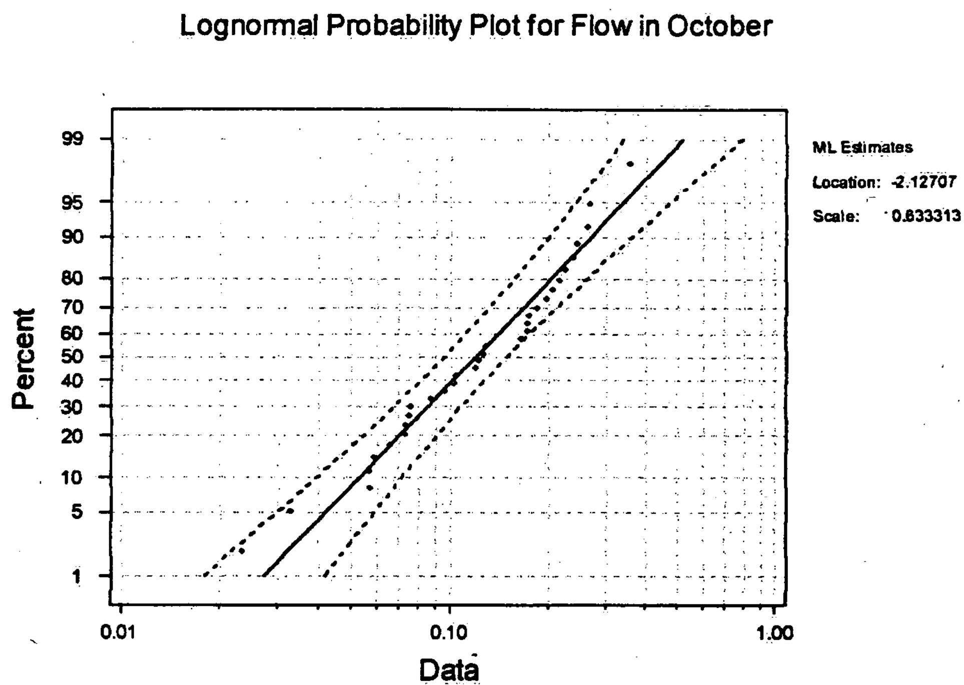

Figure 42

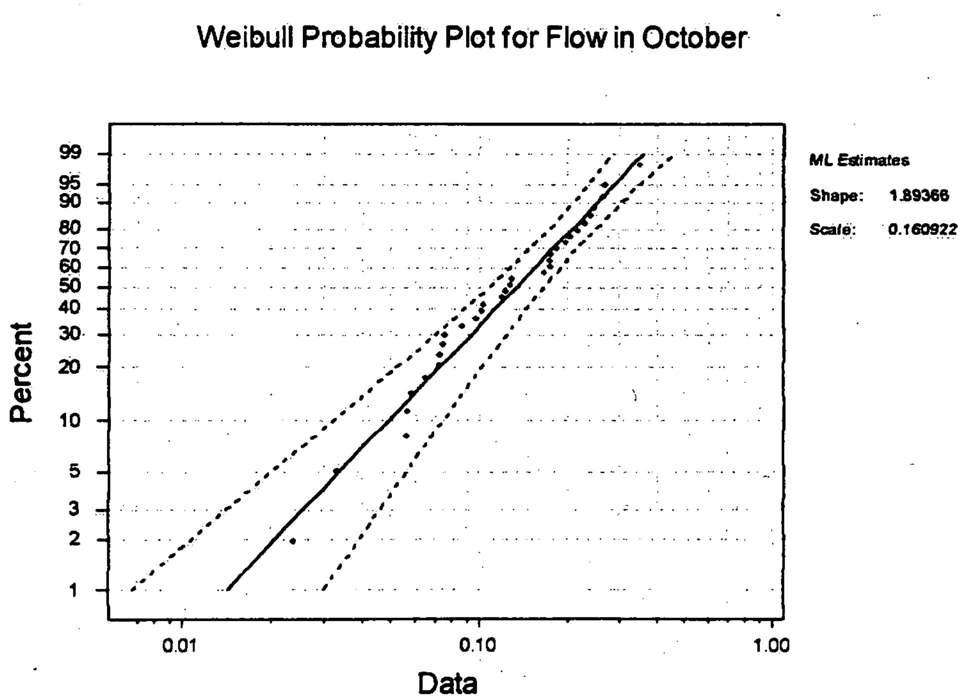

Figure 43

Normal Probability Plot for Temperature in November

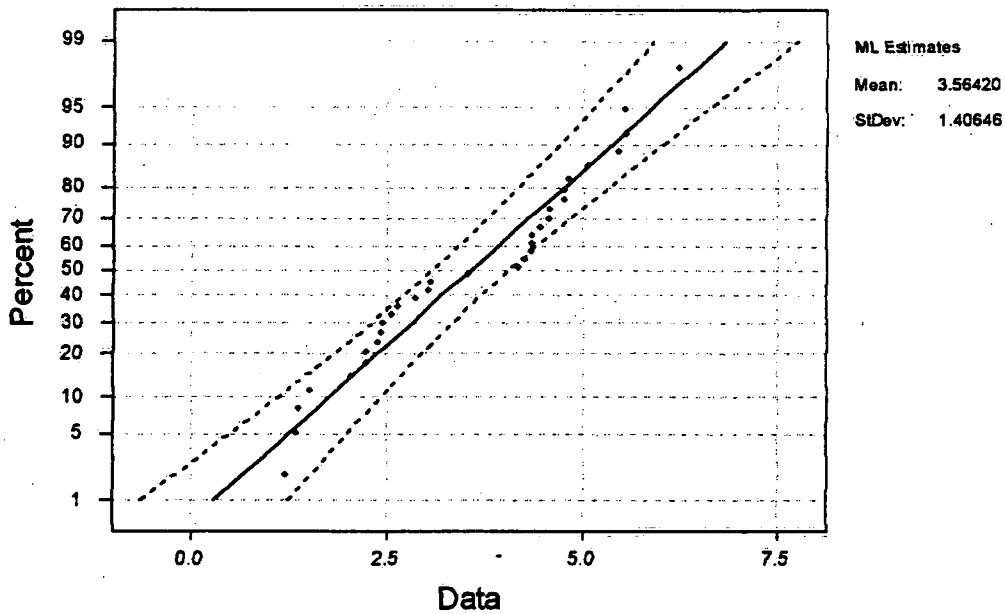

Figure 44

Lognormal Probability Plot for Precipitation in November

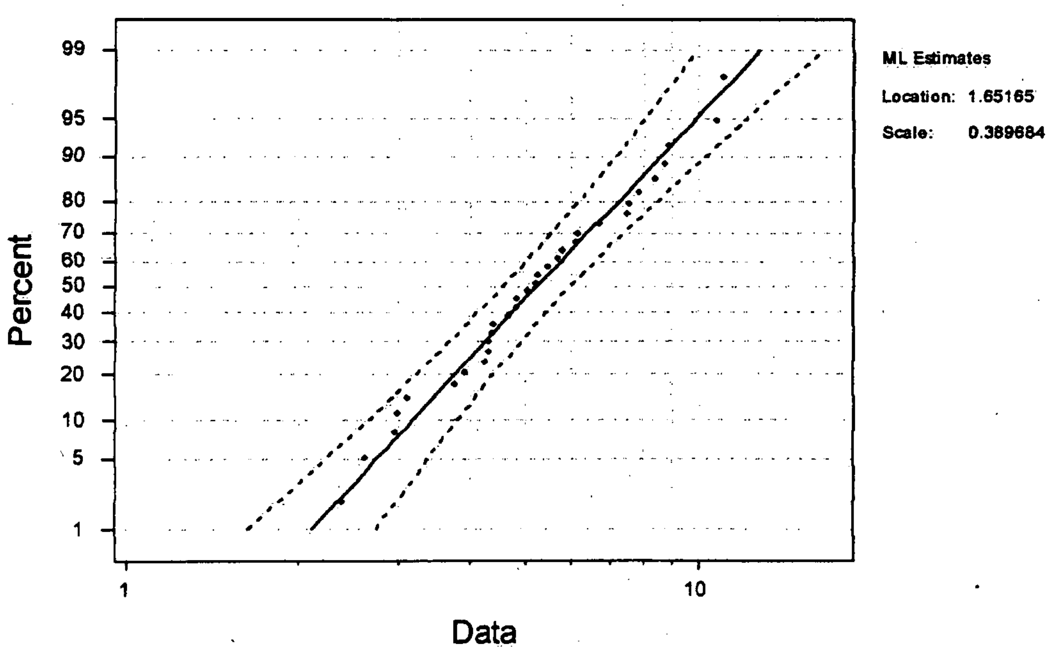

Figure 45

Lognormal Probability Plot for Flow in November

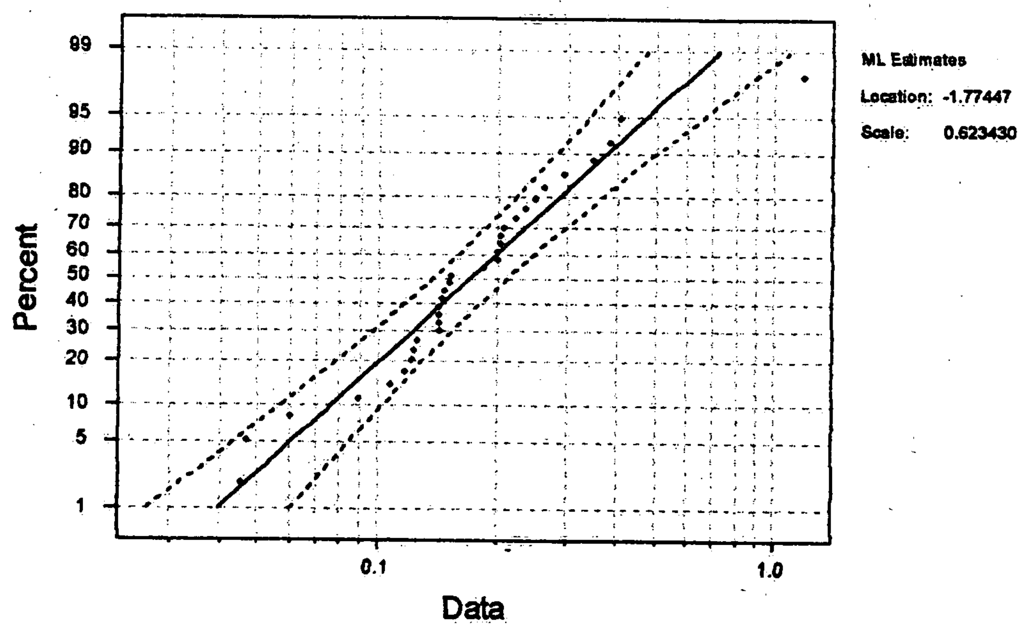

Figure 46

Normal Probability Plot for Temperature in December

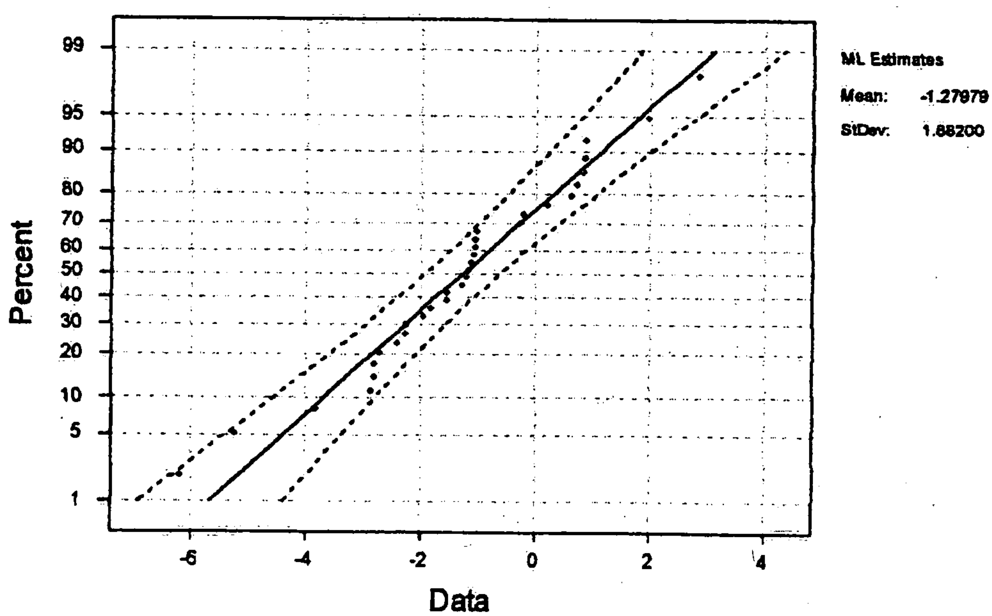

Figure 47

Lognormal Probability Plot for Precipitation in December

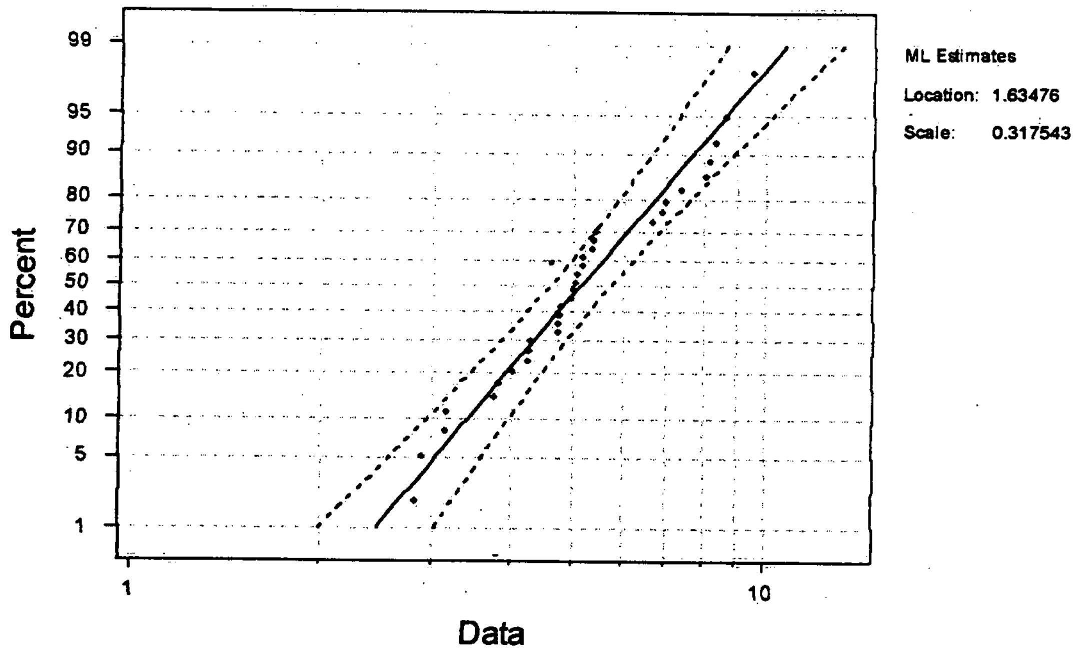

Figure 48

Lognormal Probability Plot for Flow in December

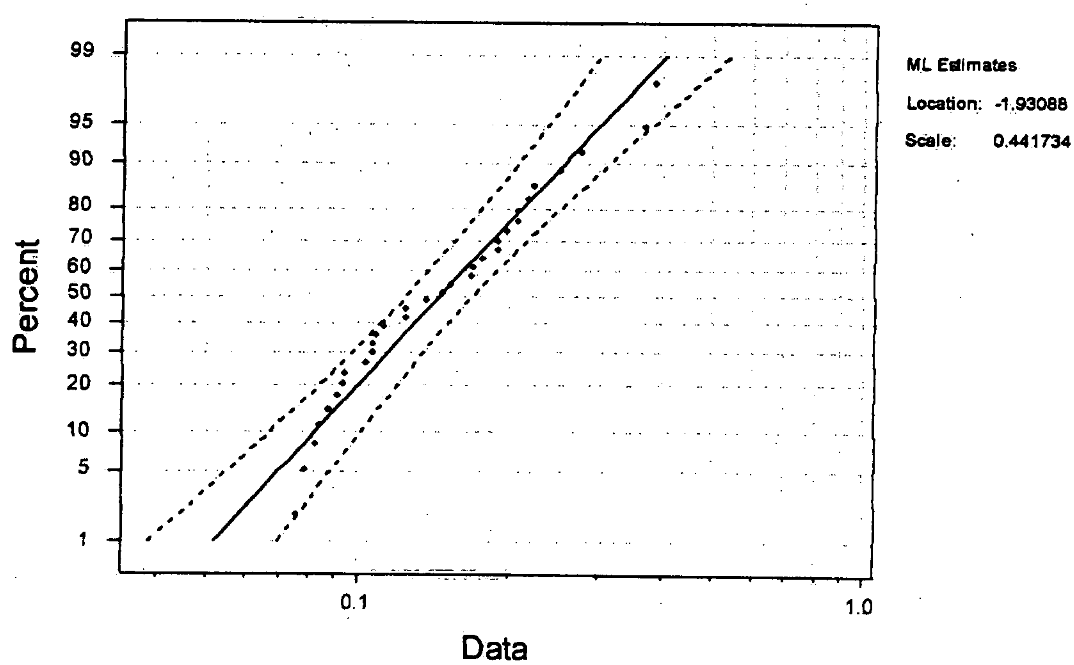

Figure 49

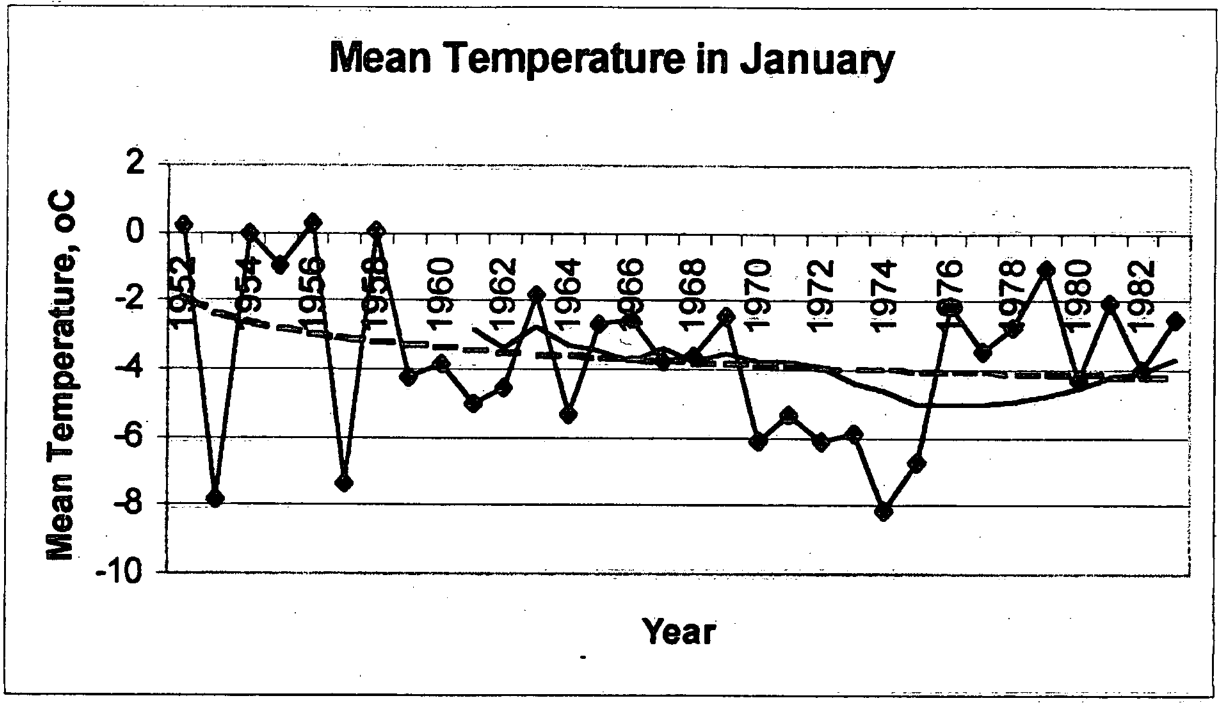

Figure 50

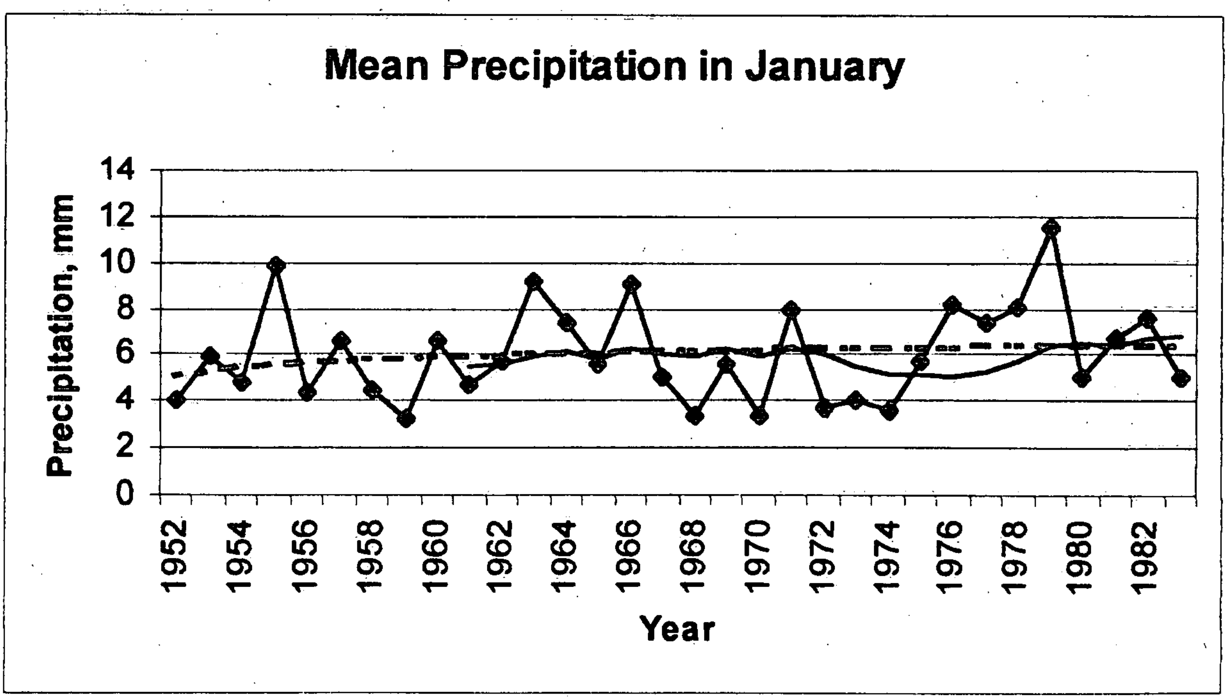

Figure 51

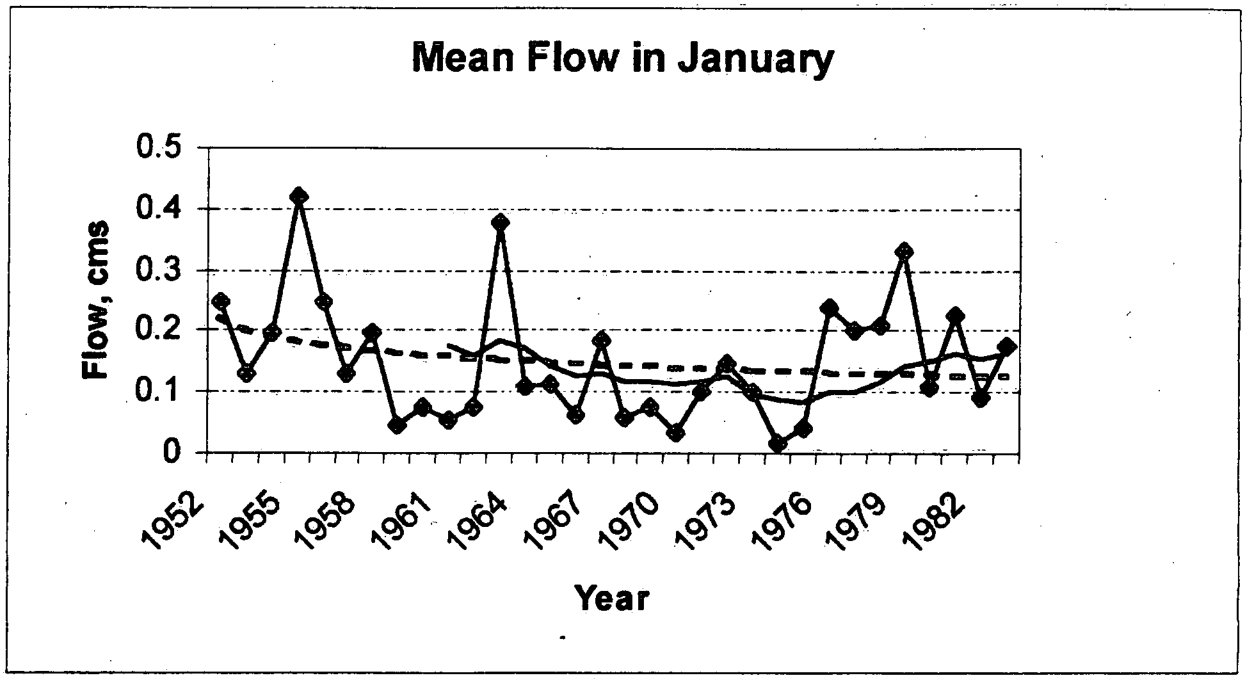

Figure 52

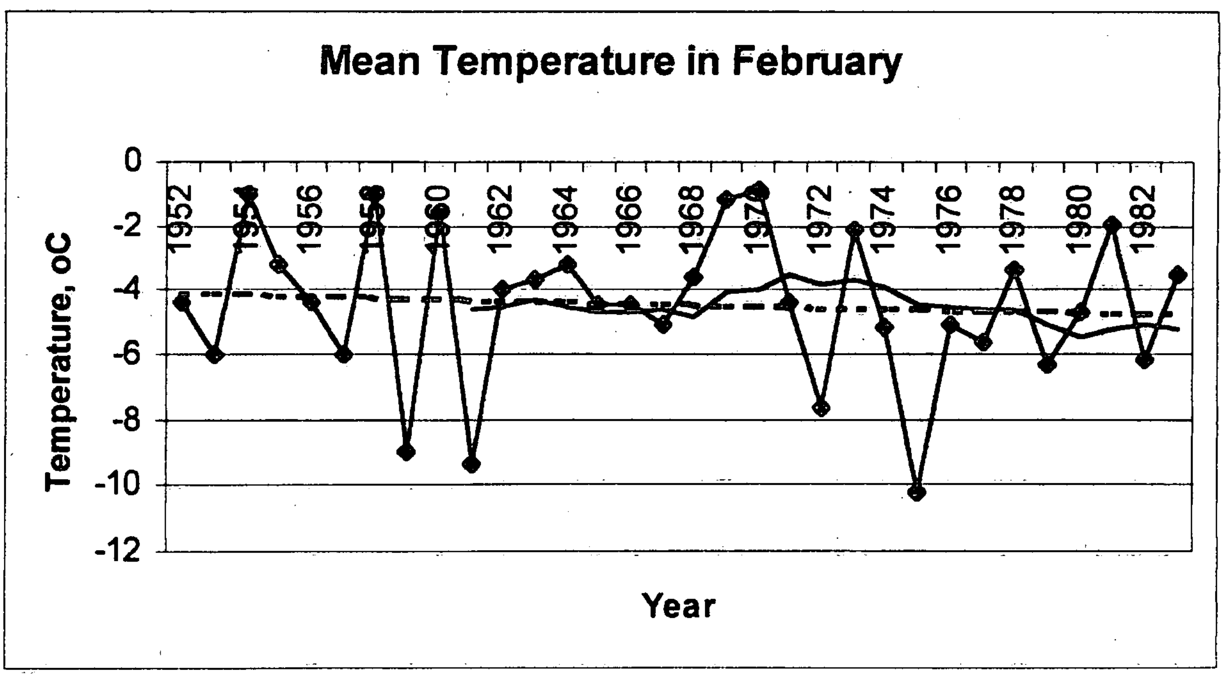

Figure 53

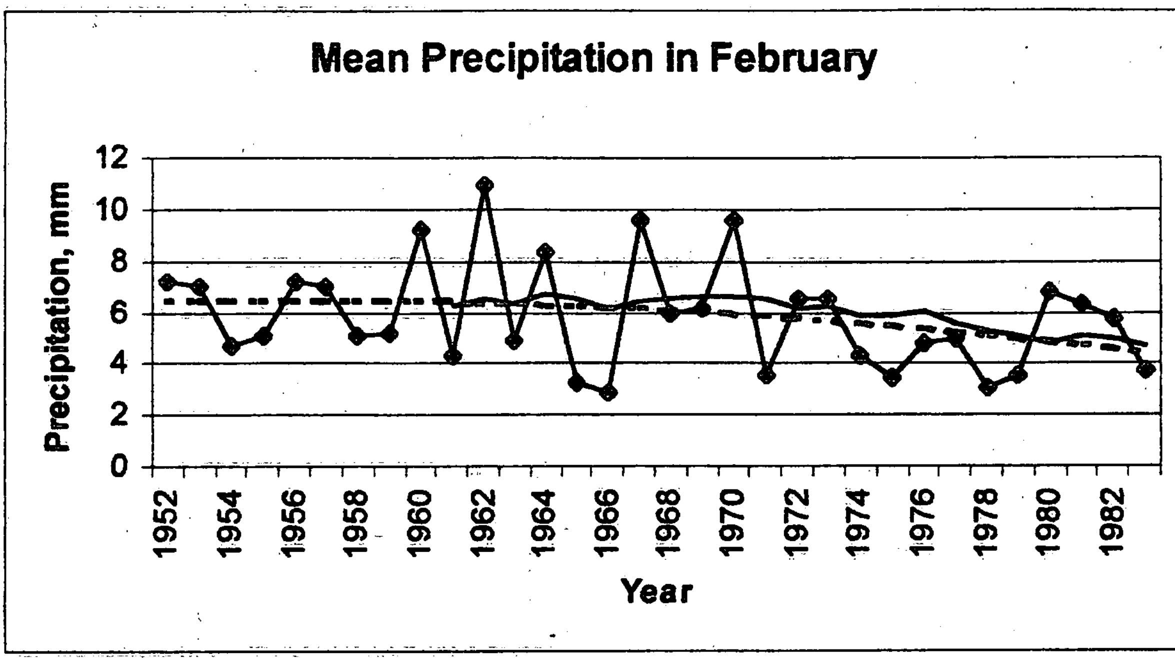

Figure 54

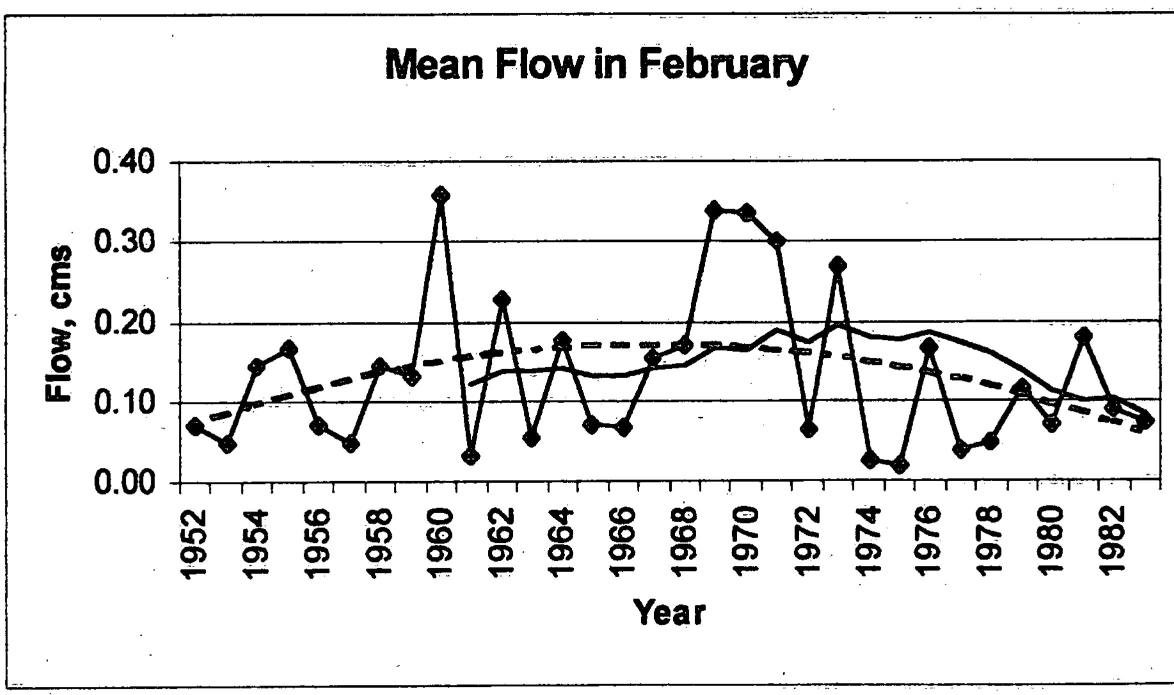

Figure 55

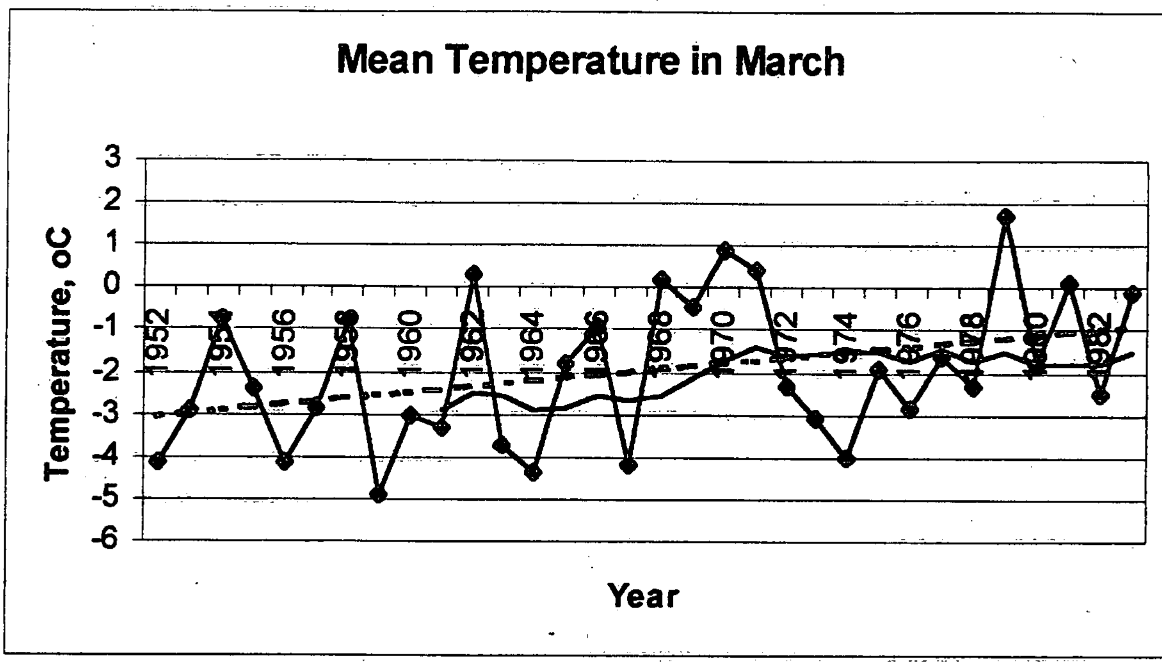

Figure 56

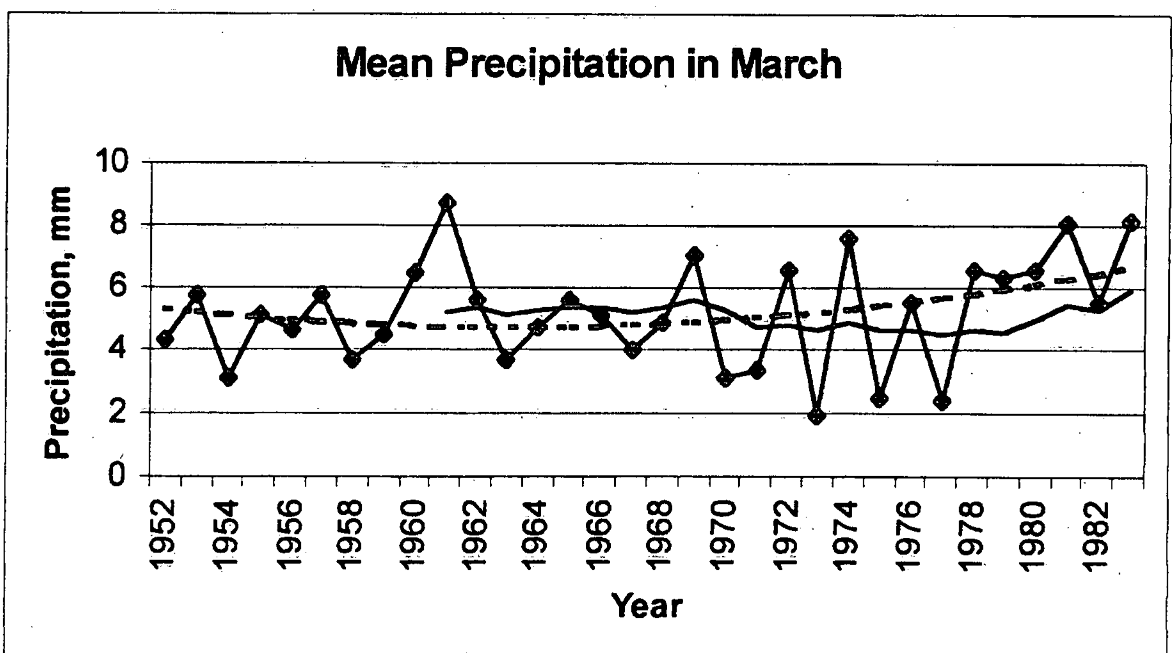

Figure 57

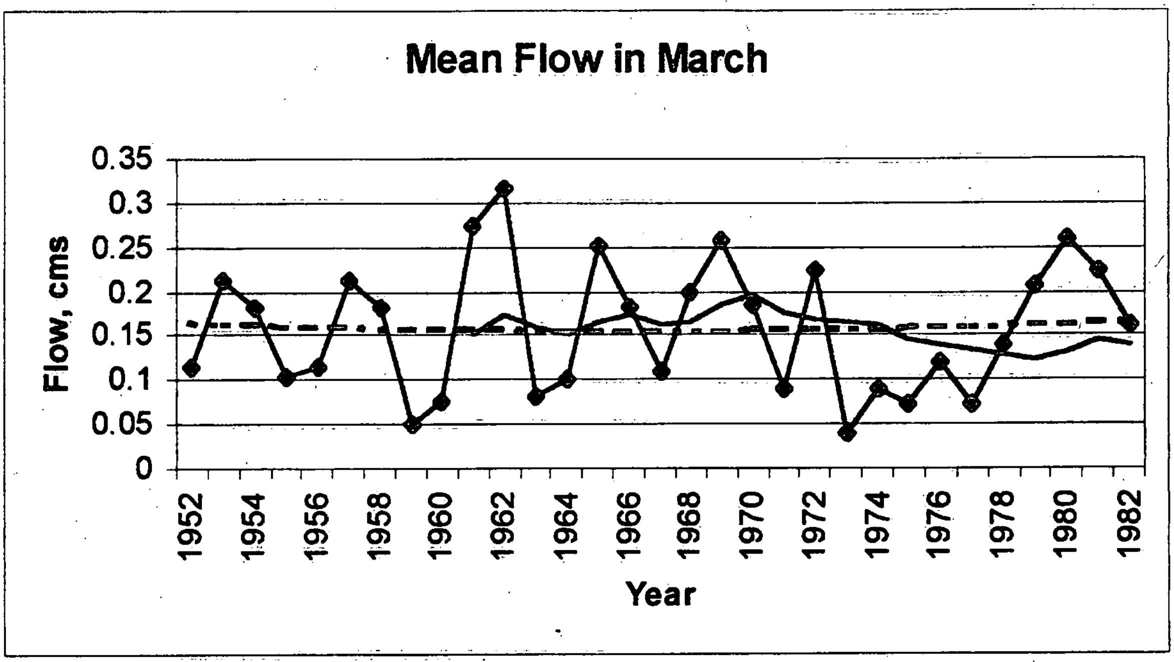

Figure 58

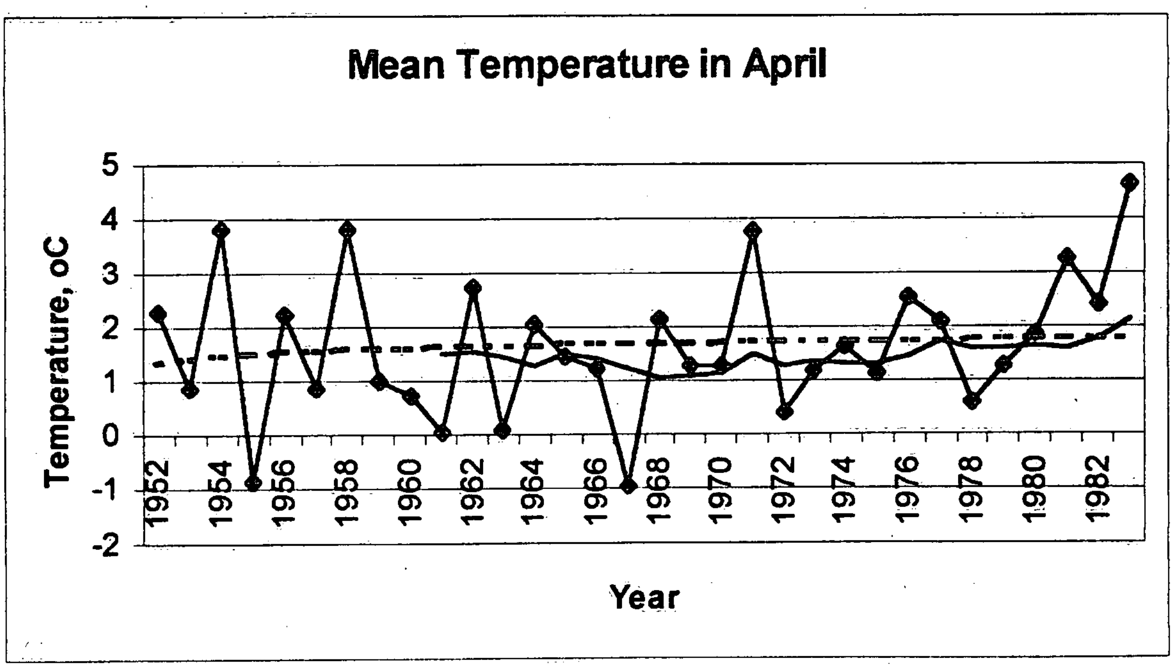

Figure 59

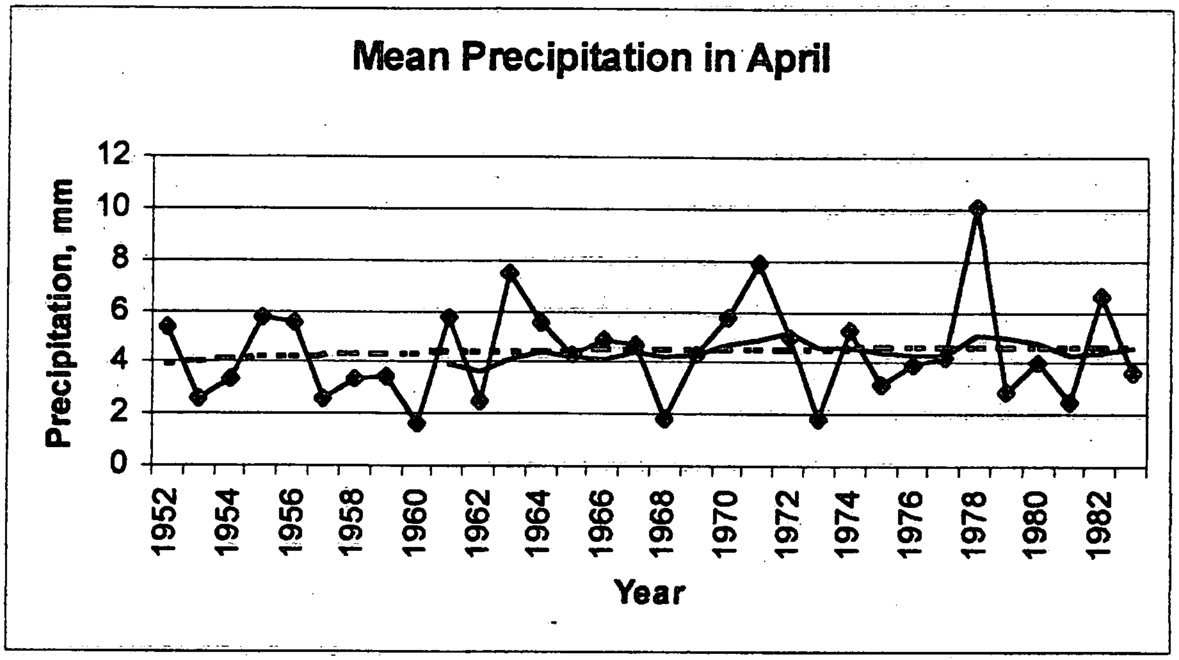

Figure 60

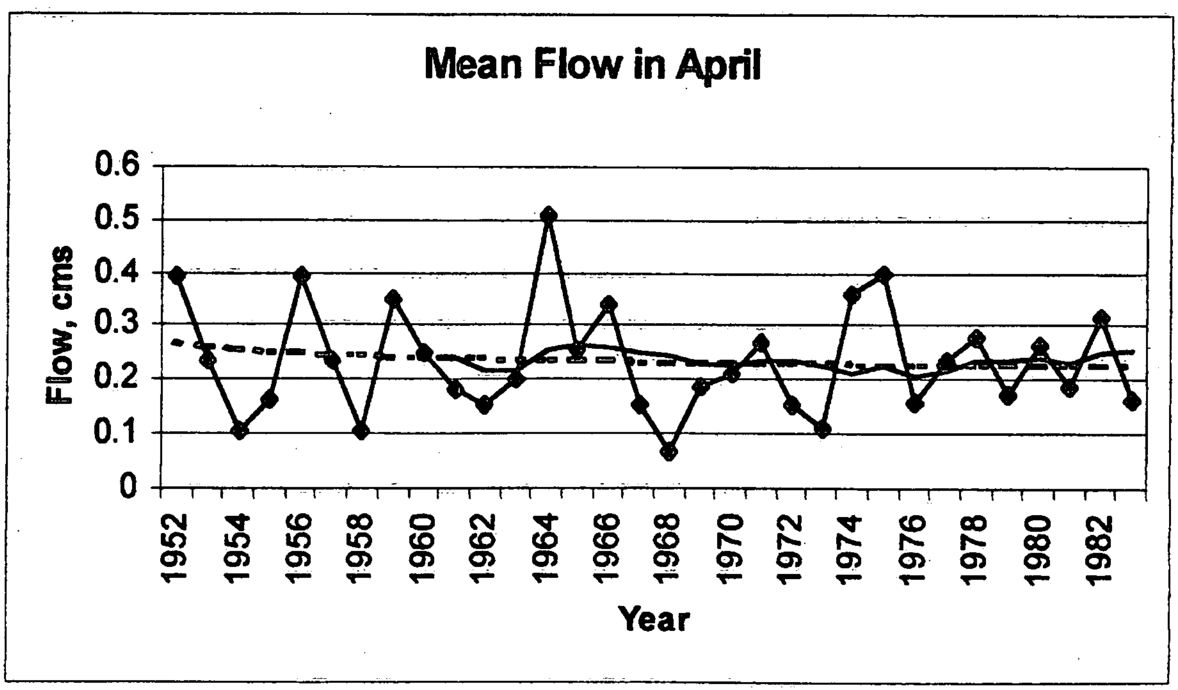

Figure 61

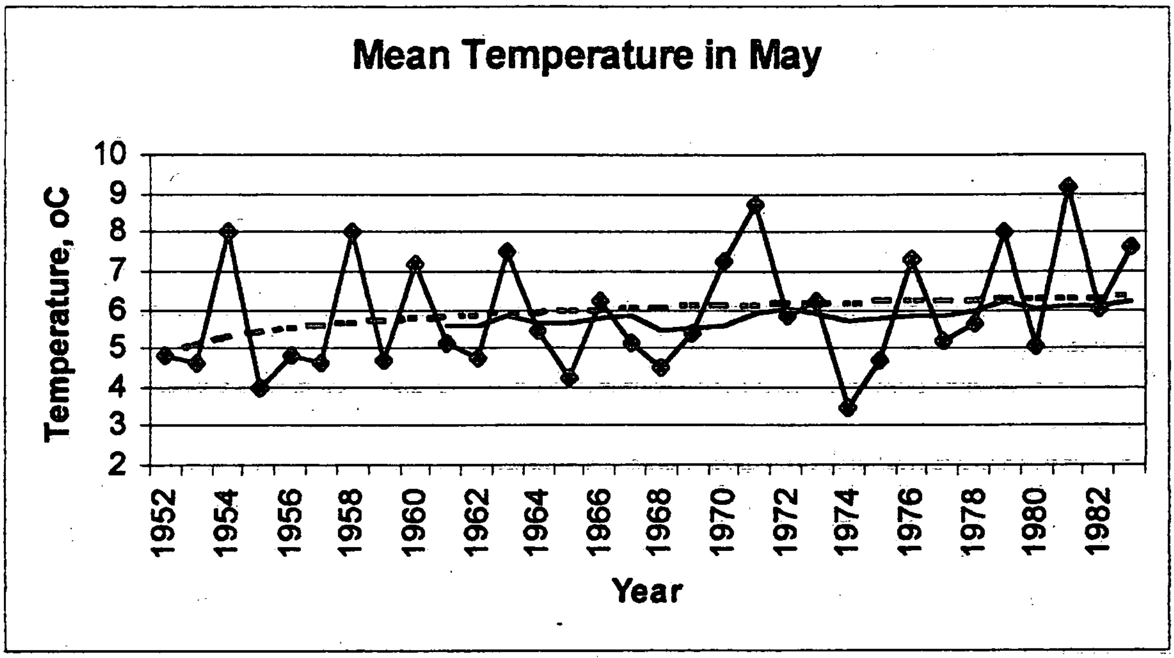

Figure 62

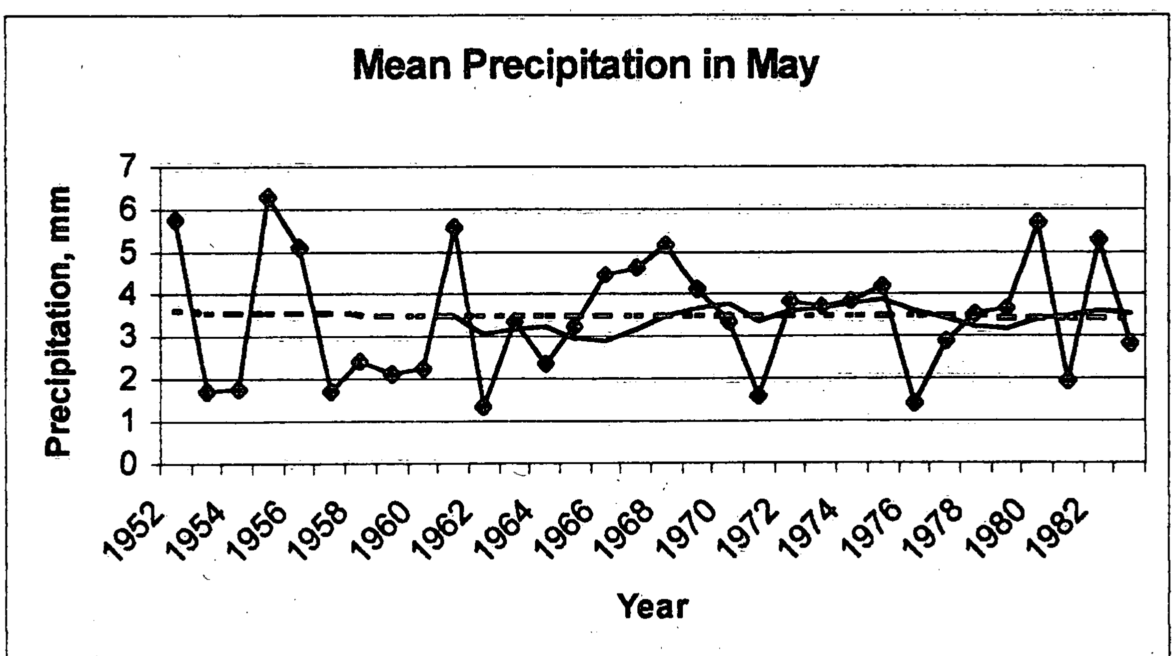

Figure 63

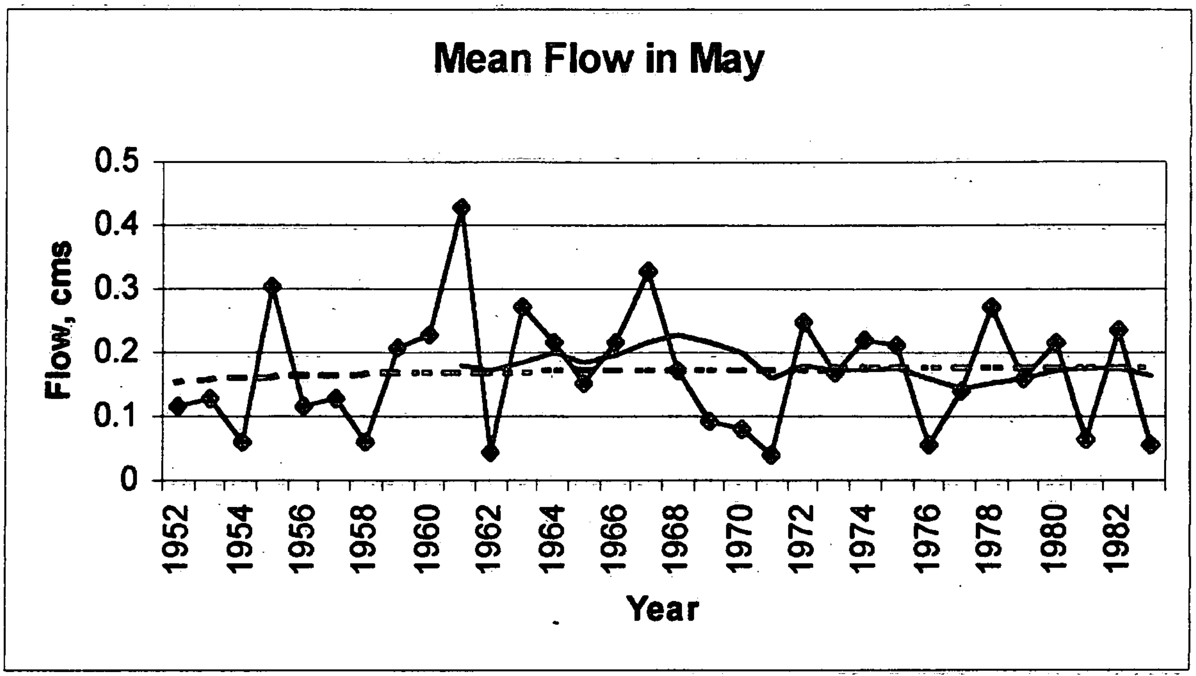

Figure 64

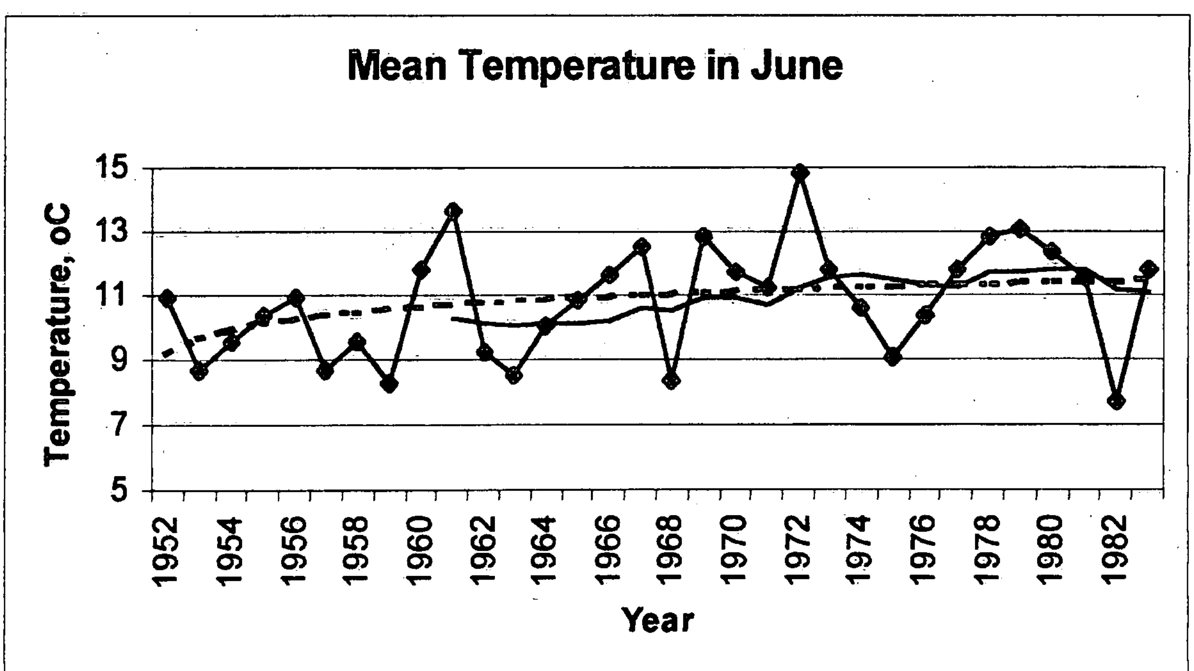

Figure 65

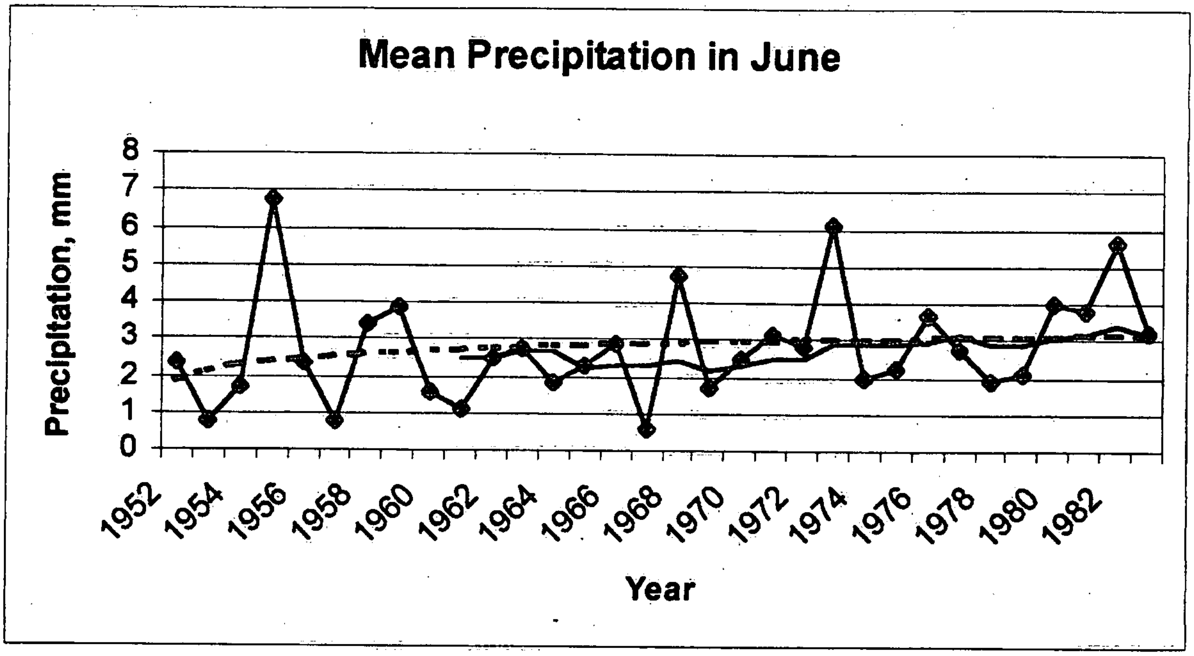

Figure 66

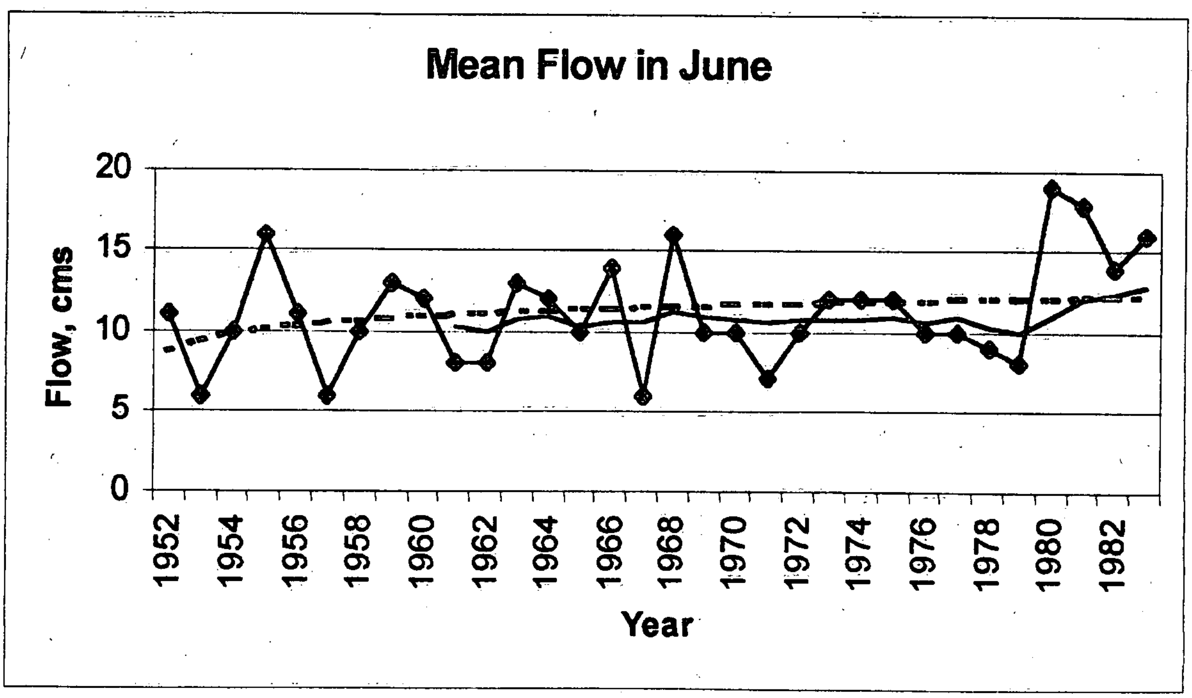

Figure 67

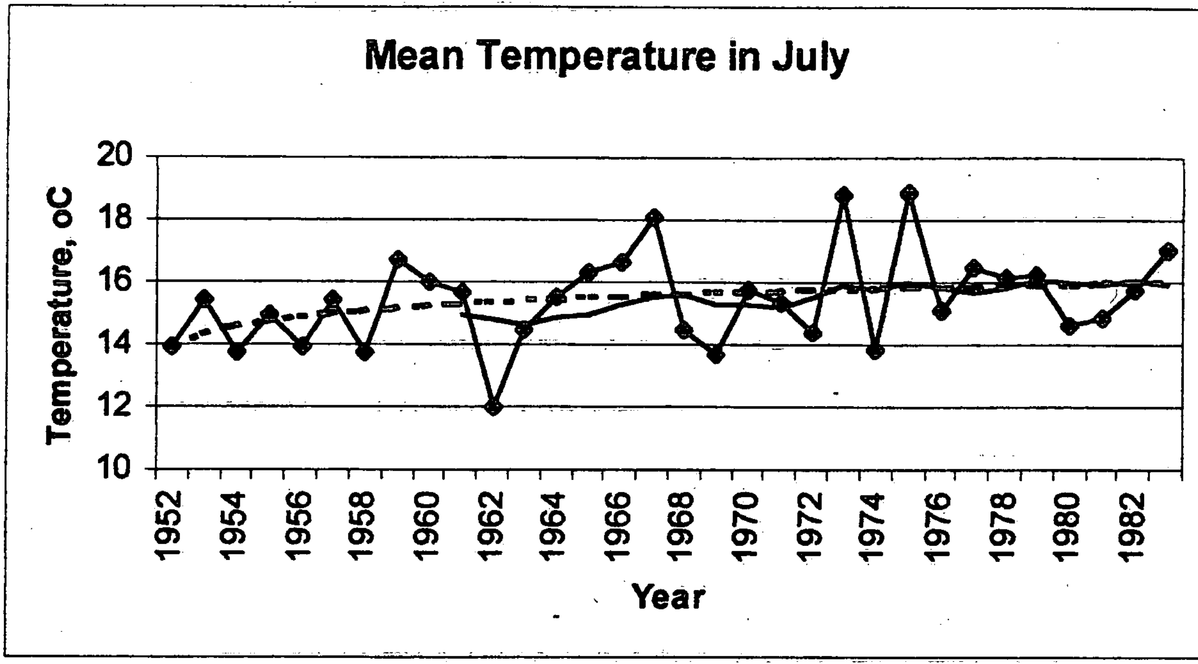

Figure 68

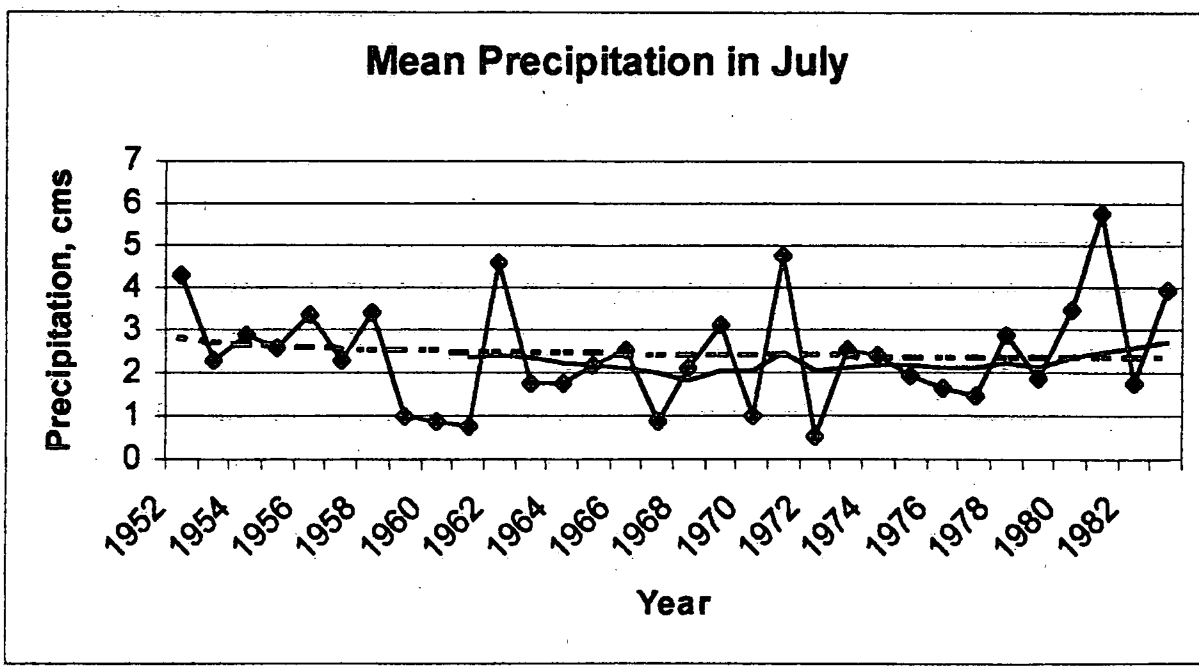

Figure 69

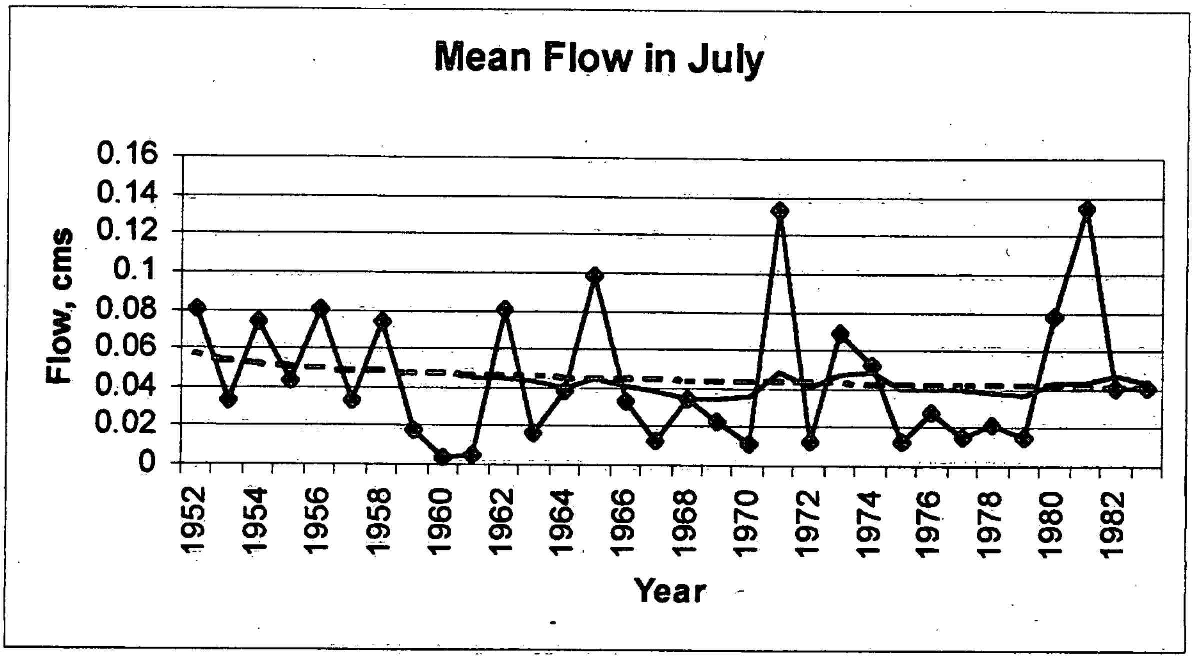

Figure 70

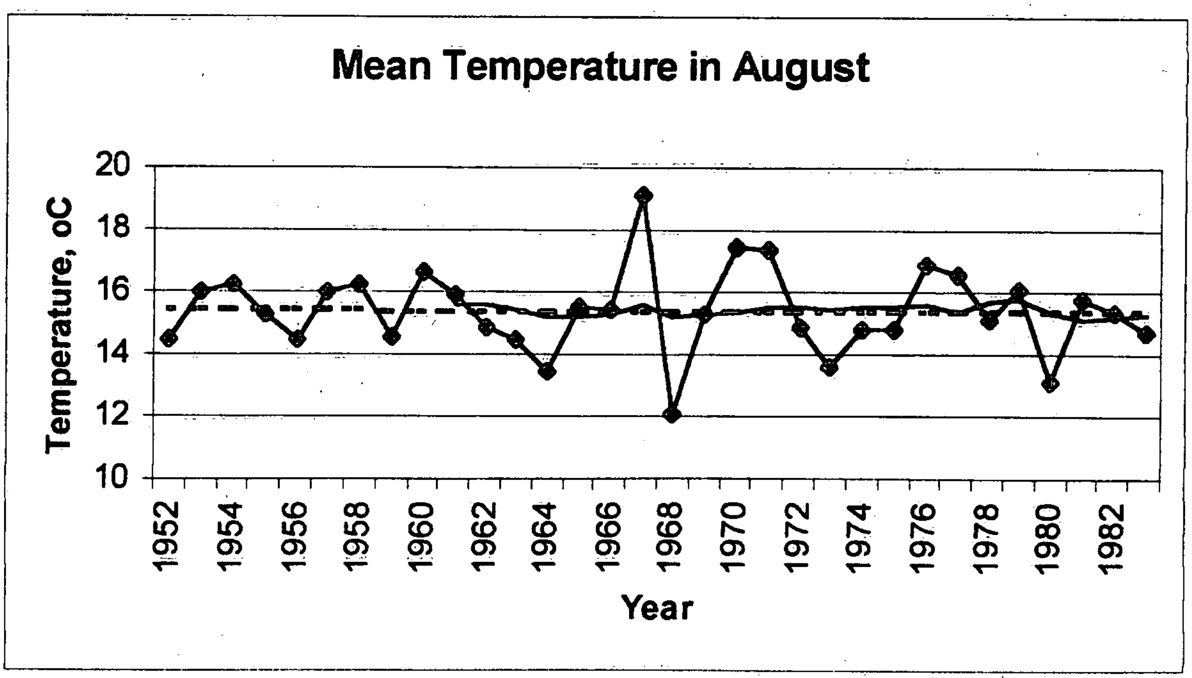

Figure 71

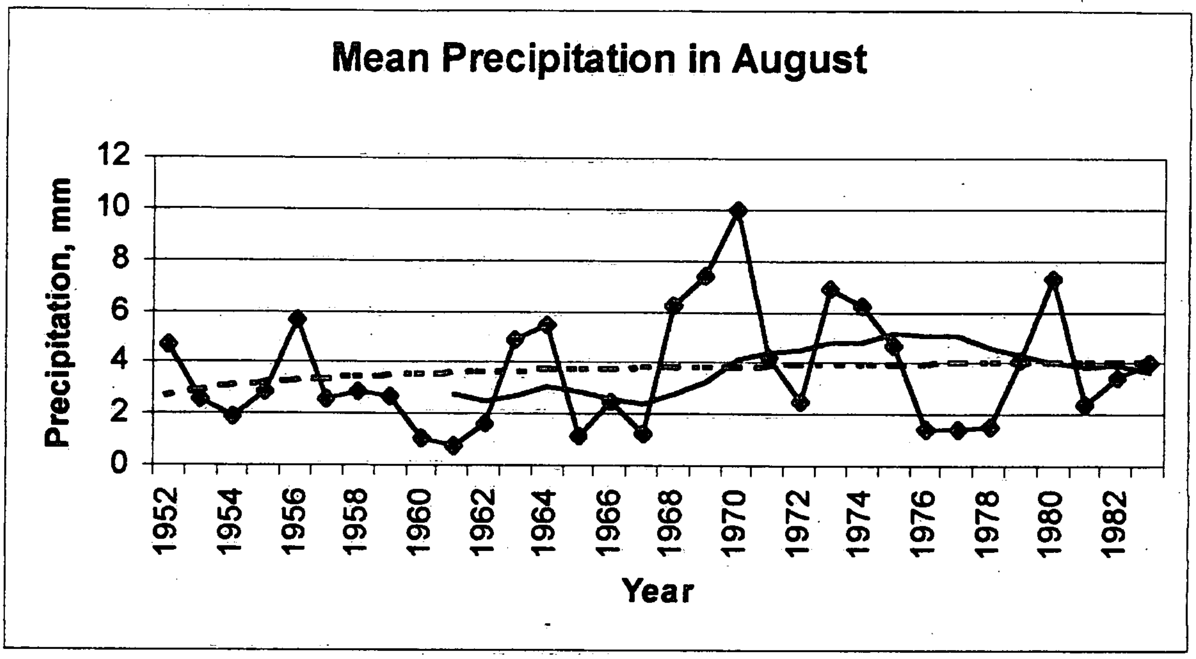

Figure 72

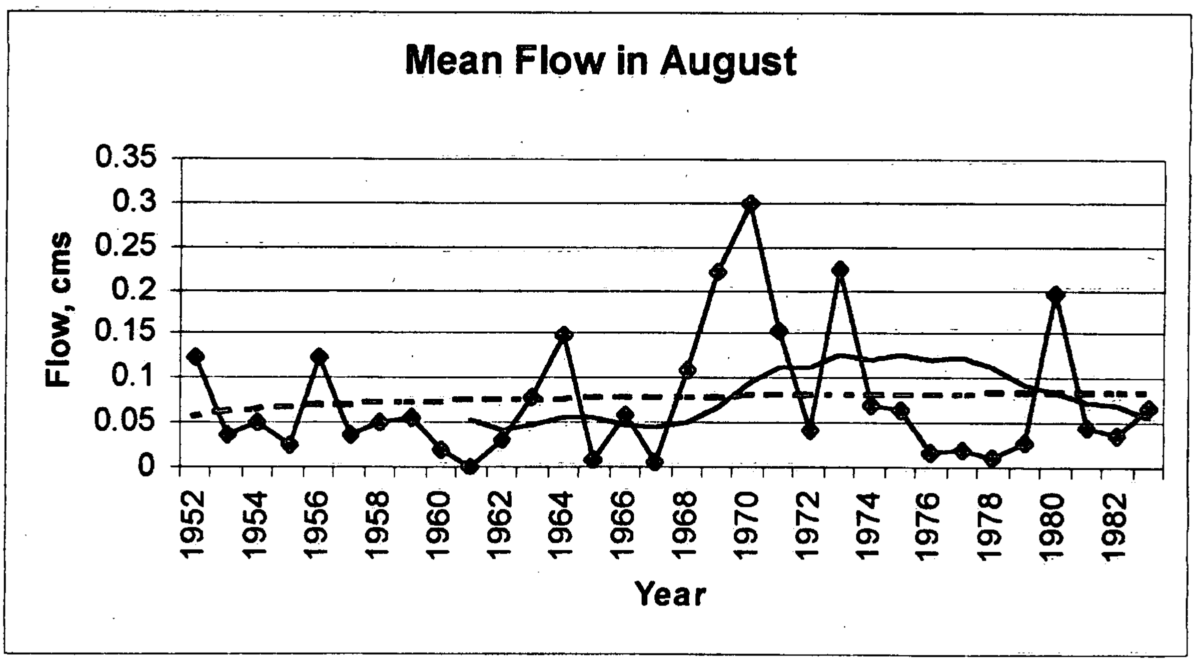

Figure 73

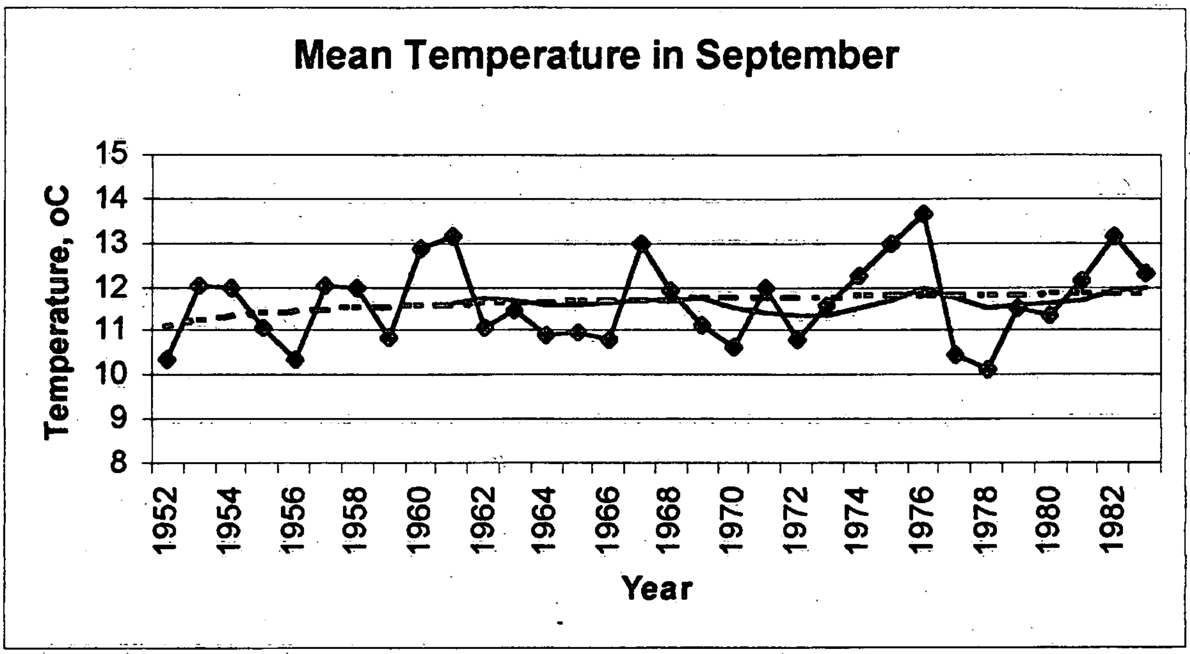

Figure 74

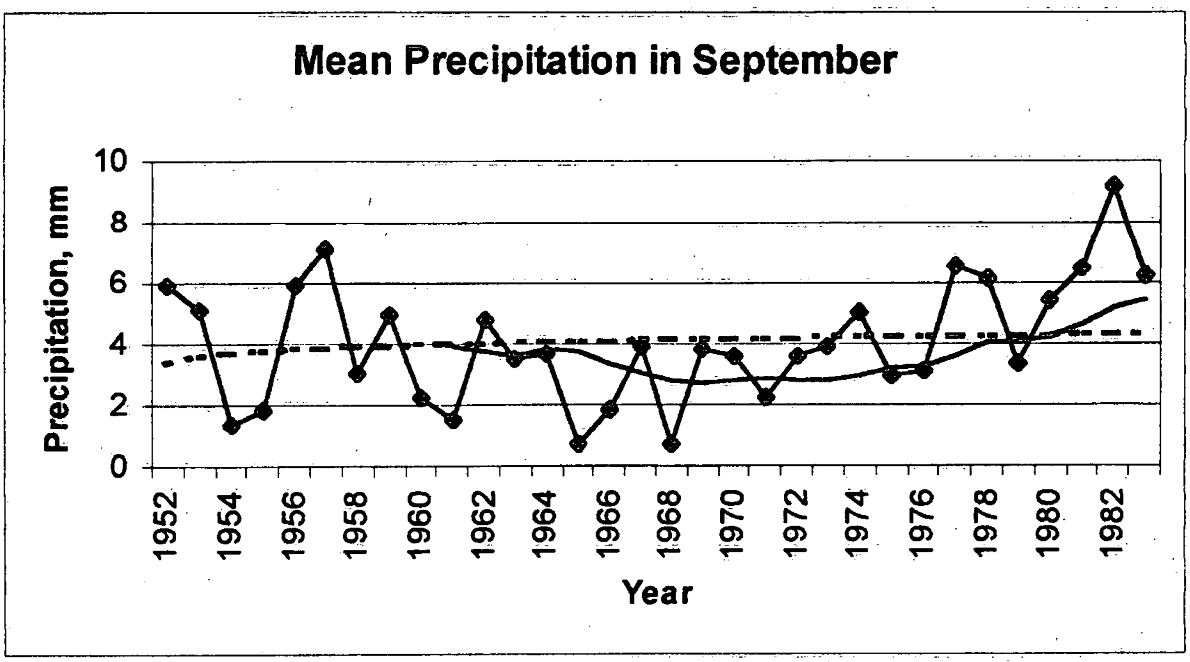

Figure 75

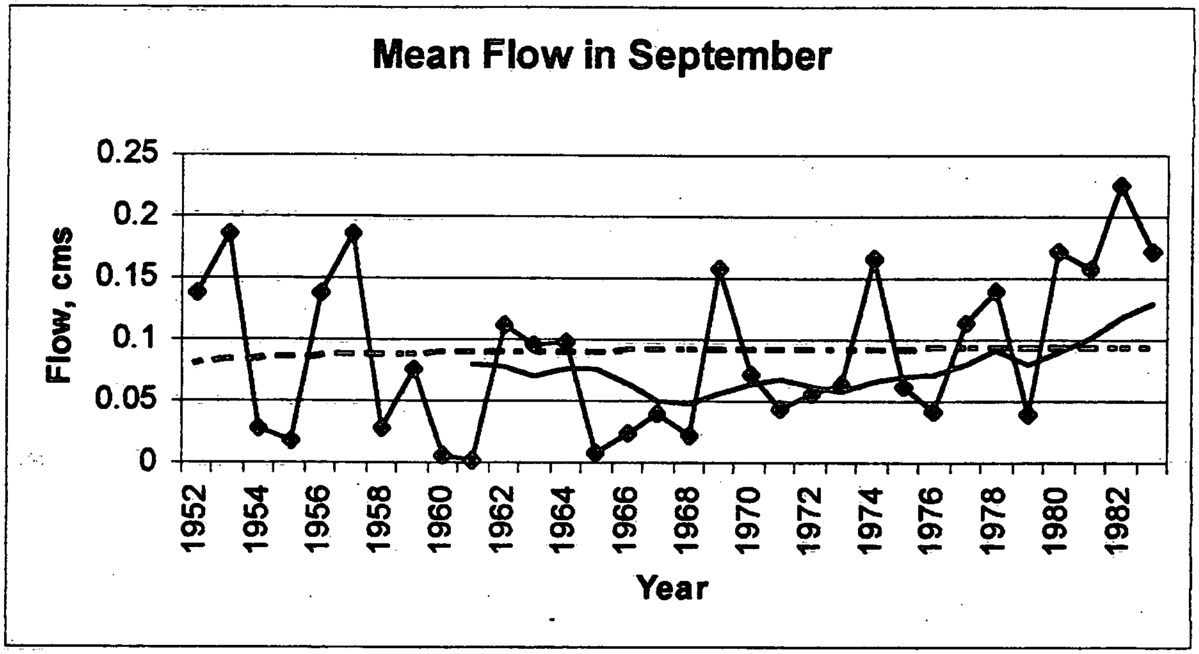

Figure 76

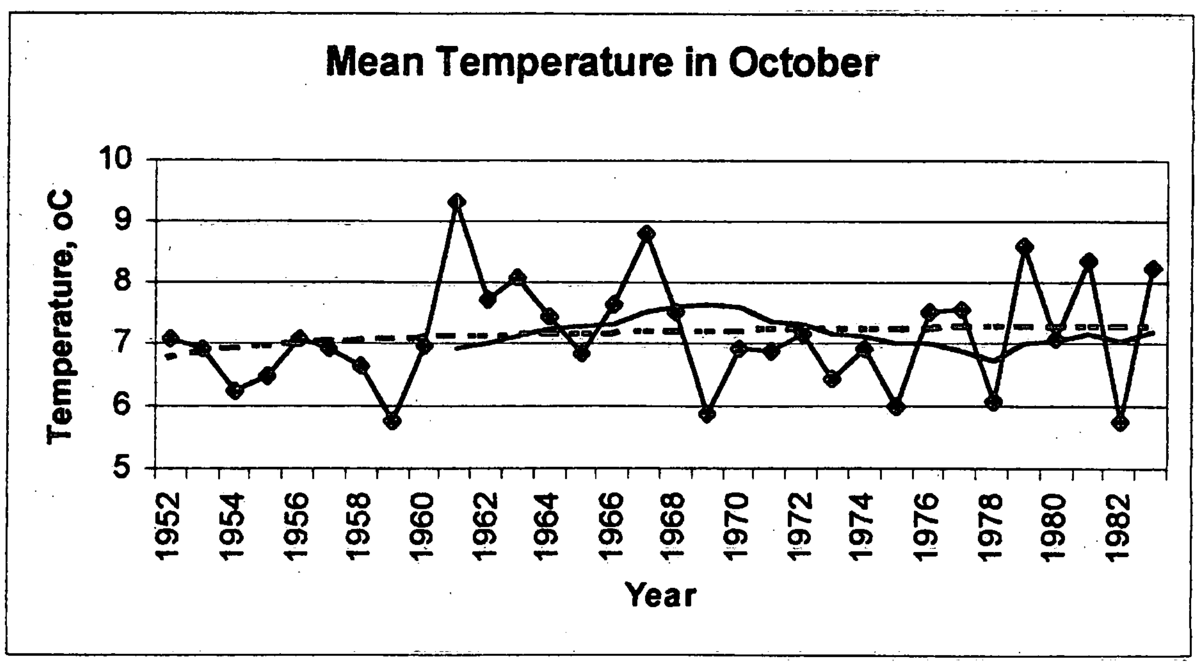

Figure 77

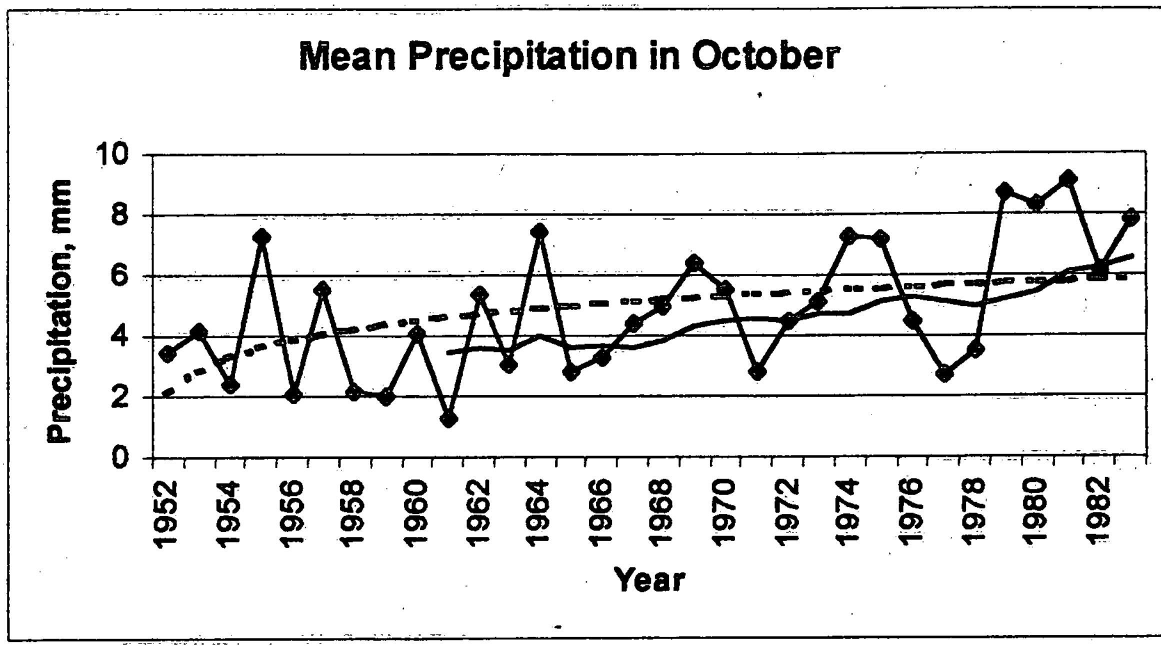

Figure 78

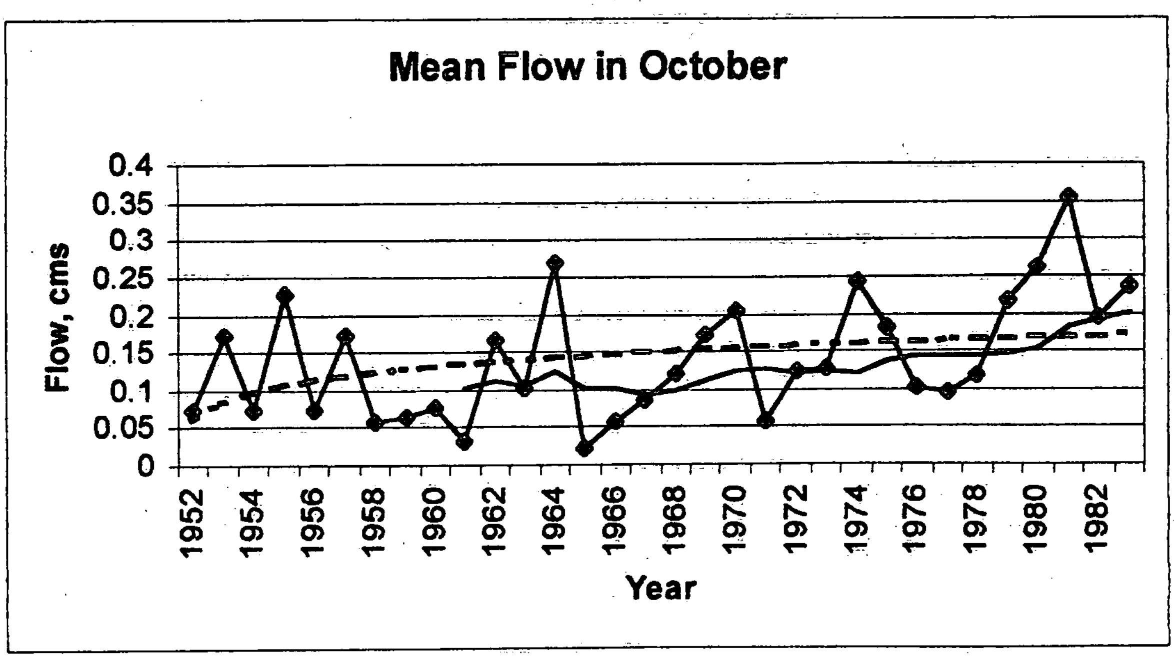

Figure 79

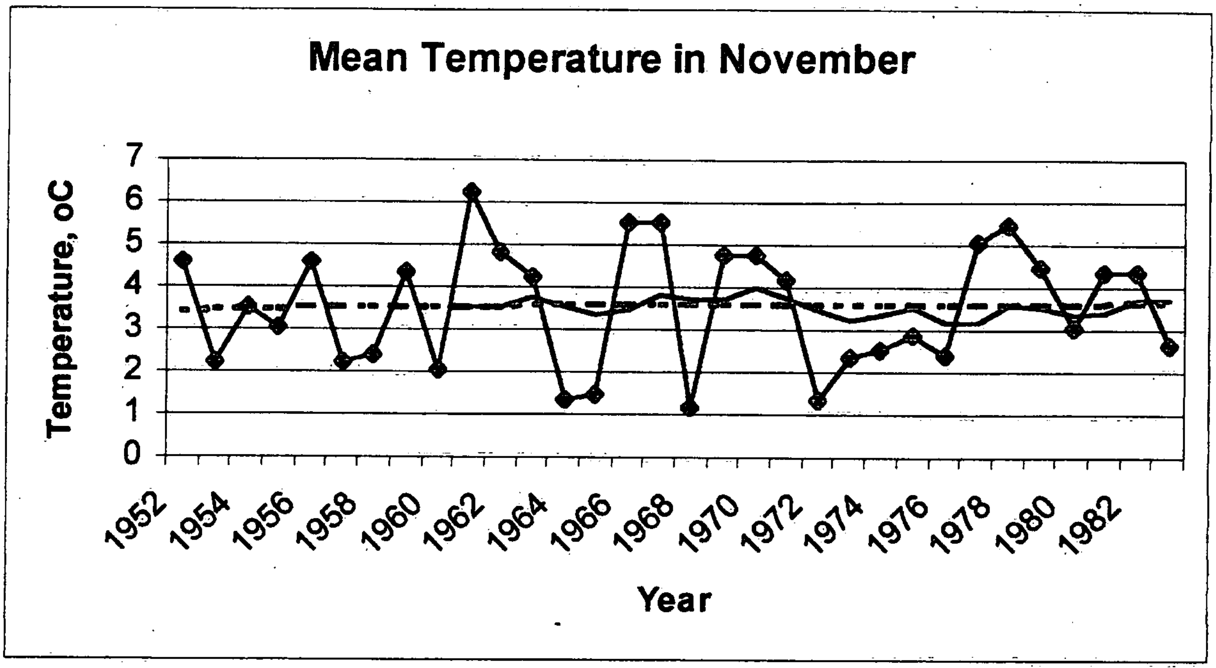

Figure 80

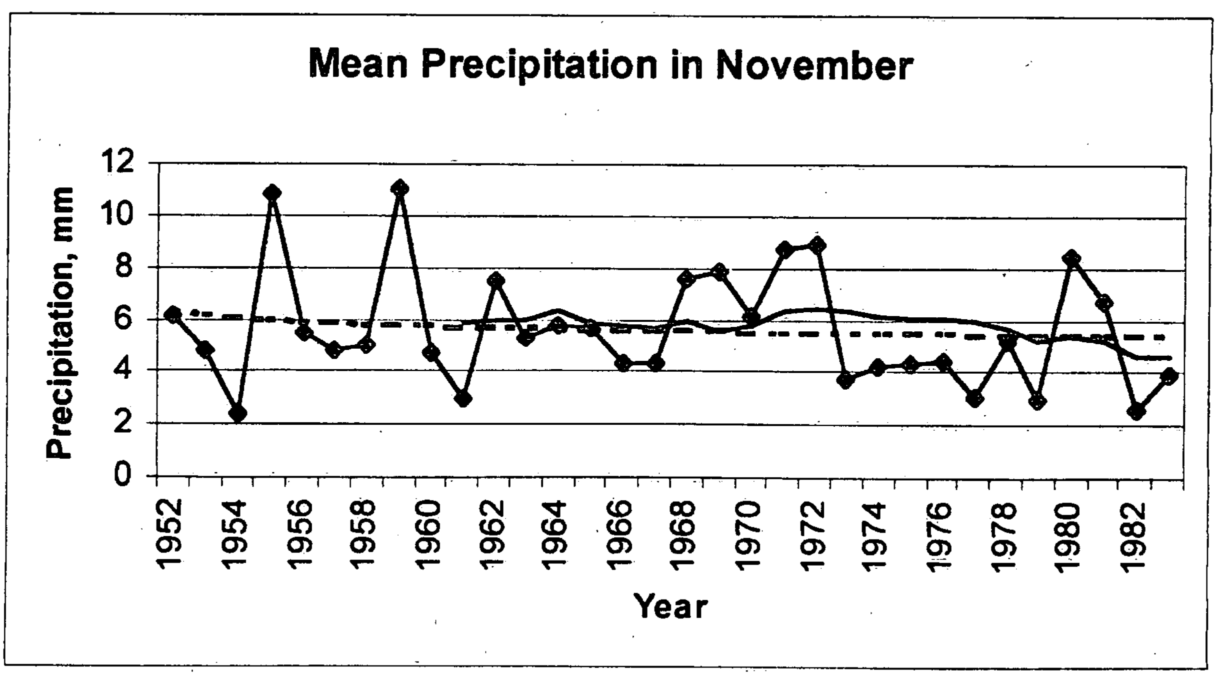

Figure 81

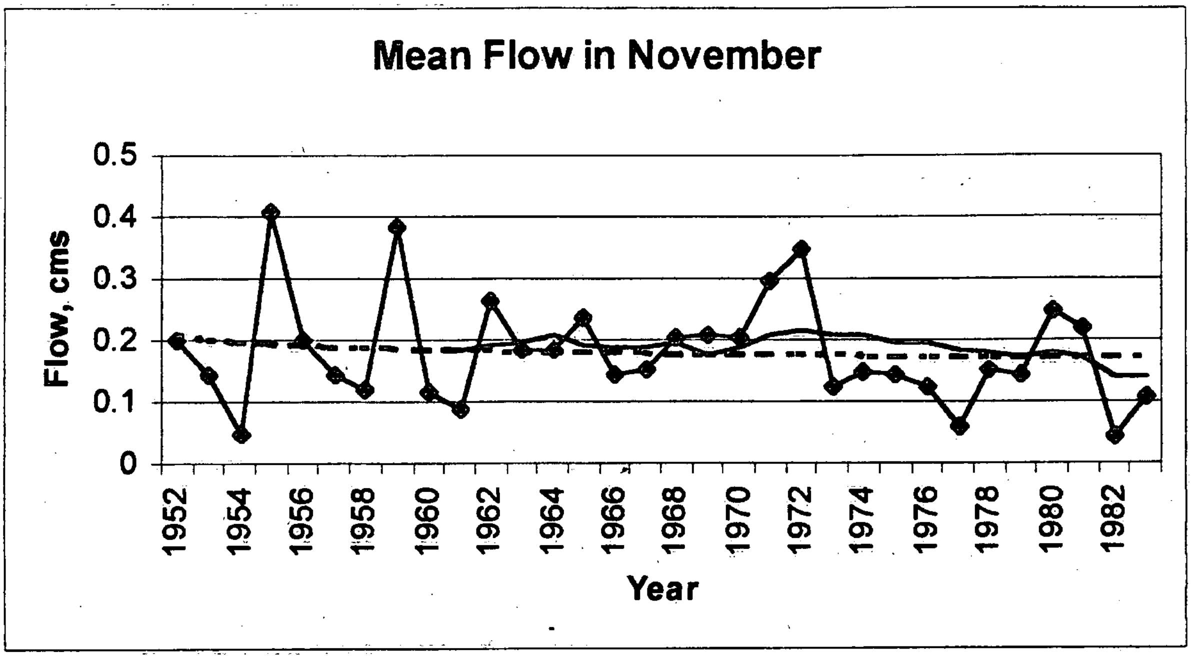

Figure 82

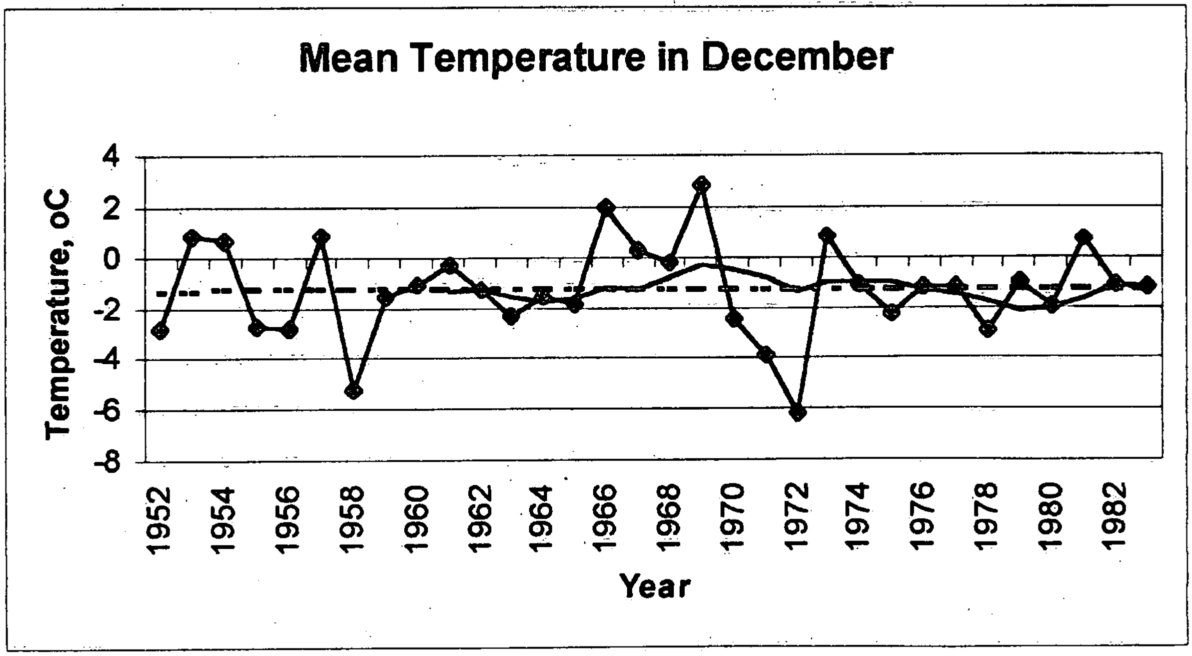

Figure 83

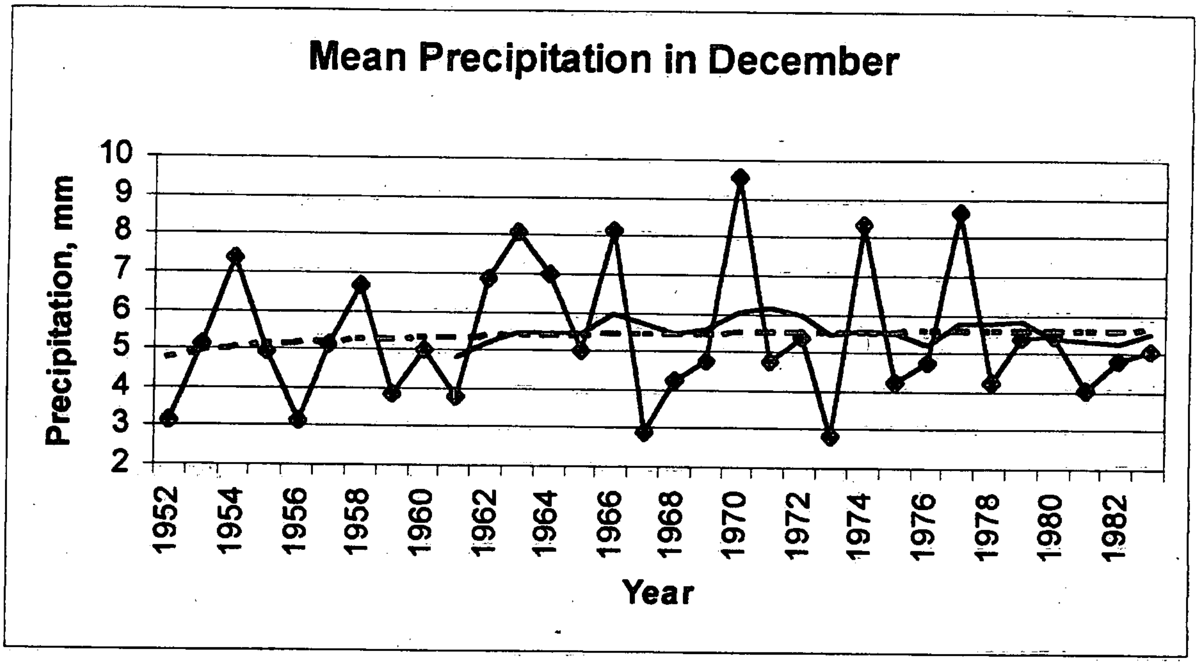

Figure 84

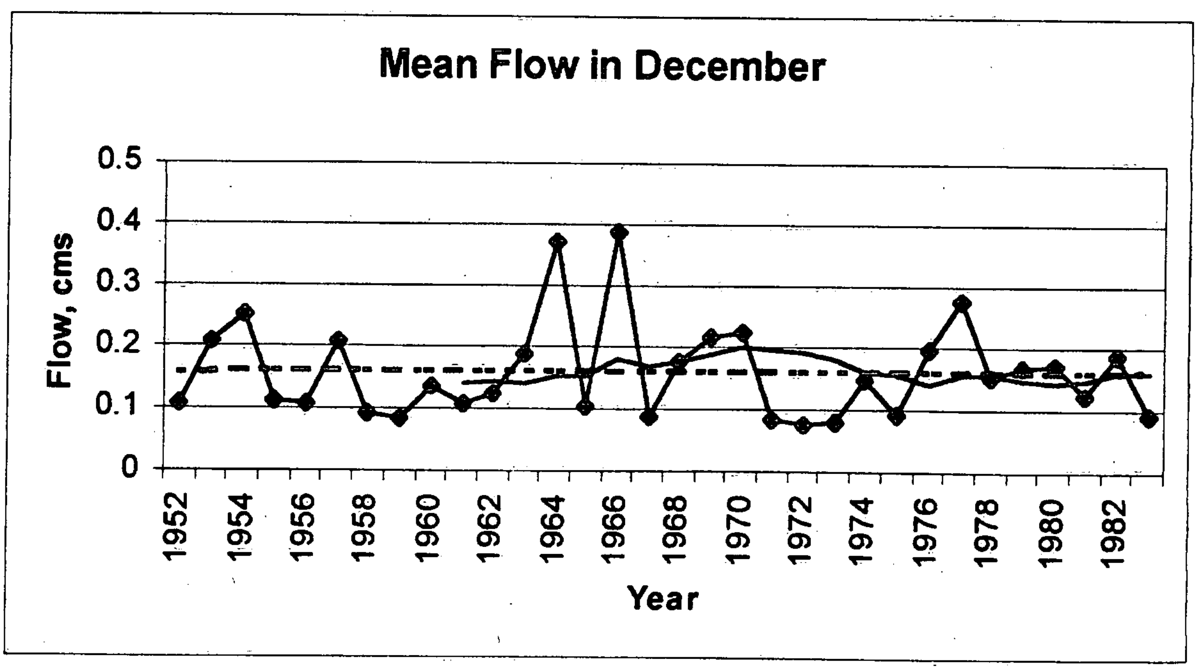

Environment Canada   Environnement Canada

Canada

Canada Centre for Inland Waters
P.O. Box 5050
867 Lakeshore Road
Burlington, Ontario
L7R 4A6 Canada

National Hydrology Research Centre
11 Innovation Boulevard
Saskatoon, Saskatchewan
S7N 3H5 Canada

St. Lawrence Centre
105 McGill Street
Montreal, Quebec
H2Y 2E7 Canada

Place Vincent Massey
351 St. Joseph Boulevard
Gatineau, Quebec
K1A 0H3 Canada

Centre canadien des eaux intérieures
Case postale 5050
867, chemin Lakeshore
Burlington (Ontario)
L7R 4A6 Canada

Centre national de recherche en hydrologie
11, boul. Innovation
Saskatoon (Saskatchewan)
S7N 3H5 Canada

Centre Saint-Laurent
105, rue McGill
Montréal (Québec)
H2Y 2E7 Canada

Place Vincent-Massey
351 boul. St-Joseph
Gatineau (Québec)
K1A 0H3 Canada